Spring 5-16-2020

Spatial Distribution, Sources, and Associated Risks of Toxic Metals In Red Sea Sediments Near Jeddah, Saudi Arabia

Riyadh Halawani
Southern Methodist University, rhalawani@smu.edu

SPATIAL DISTRIBUTION, SOURCES, AND ASSOCIATED RISKS OF TOXIC METALS IN RED SEA SEDIMENTS NEAR JEDDAH, SAUDI ARABIA

Approved by:

Andrew Quicksall, Associate Professor, Chair

Neil Tabor, Professor

Refaat Abohassan, Associate Professor

Wenjie Sun, Assistant Professor

Jaewook Myung, Assistant Professor

SPATIAL DISTRIBUTION, SOURCES, AND ASSOCIATED RISKS OF TOXIC METALS IN RED SEA SEDIMENTS NEAR JEDDAH, SAUDI ARABIA

A Dissertation Presented to the Graduate Faculty of the

Bobby B. Lyle School of Engineering

Southern Methodist University

in

Partial Fulfillment of the Requirements

for the degree of

Doctor of Philosophy

with a

Major in Civil and Environmental Engineering

by

Riyadh Faroq Abbas Halawani

B.S., King Abdulaziz University, 2003
M.S., King Abdulaziz University, 2009

May 16, 2020

ACKNOWLEDGMENTS

The completion of this dissertation would not have been possible without the support and encouragement of several special people. For this reason, I would like to take this opportunity to show my gratitude to those who assisted me.

Foremost, I want to offer this effort to my GOD Almighty for the wisdom he bestowed upon me, the peace of mind, and good health to finish this thesis.

I want to express my most profound respect, gratitude, and appreciation to my academic advisor Dr. Andrew Quicksall. I am very grateful for your support, leadership, and motivation. You have made this work achievable. Thank you for making me a better scholar and researcher. Really, I could not have imagined having a better advisor and mentor for my Ph.D. study.

Besides my advisor, I would like to thank my professors on my supervisory committee, Dr. Refaat Abohassan, Dr. Neil Tabor, Dr. Wenjie Sun, and Dr. Jaewook Myung, not only for their helpful advice and observations but also for their questions which significantly aided me to improve my dissertation.

I would like to express the greatest respect, love, appreciation, and gratitude to my family, especially my father, Faroq Abbas Halawani, and my mother, Azzah Hussein Ammar. Thank you for making me who I am today, and I hope I made you proud of me. I want to thank my sisters, Hend and Senham, and my brothers Abbas, Yasser, Hesham, Hatem, Samer, Ghassan, Niaf, Sultan, and Emad, for their love and for emotional and financial support, for which I am very grateful. I also want to thank my aunts Faigah Halawani and professor Fateen Halawani, for your love and support. Special thanks to my

nephews Ammar and Mohamed Yasser Halawani for their help and effort during the sampling.

Very special thanks to my wife, Rooa Alghamdi, for her love, patience, and unfailing support and continuous encouragement throughout my years of study. Thanks to my daughters ,Taleen and Eleen and my son, Youssef.

Last but not least, I would like to thank my fellow lab mates, Myra Elizabeth Wilson, and Kenneth M. Hamilton, for their help during the preparation and analysis. Thanks to Leal Badakhshanian, Hope Rasmussen, and Uma Lad for being such fantastic lab mates. Special thanks to my friends Abdulrahman Namankani, Dr. Abdulrahman Habib, Dr. Moahd Alghuson, and Dr. Saeed Asiri, for being such wonderful friends and supporters during this journey.

Halawani, Riyadh F. M.S., King Abdulaziz University, 2009
B.S., King Abdulaziz University, 2003

Spatial Distribution, Sources, and Associated Risks of Toxic Metals in Red Sea Sediments near Jeddah, Saudi Arabia

Advisor: Professor Andrew Quicksall

Doctor of Philosophy conferred on May 16, 2020

Dissertation completed on April 28, 2020

Coastal areas are known to be sequestration points for various pollutants generated from industrial and urban activities. Diverse anthropogenic pollutants are typically delivered to coastal sediments via atmospheric or fluvial processes. Heavy metals, such as chromium, copper, manganese, zinc, and lead, are some of the toxic contaminants of greatest concern because of their well-established detrimental effects on the marine environment. In recent years, Saudi Arabia has encouraged activities to bring about economic development, particularly along the Red Sea. Jeddah is located on the Red Sea and is the second largest city in Saudi Arabia, famous for its beautiful coral reef.

In this dissertation, a variety of studies were applied not only to *in situ* sediment samples but also to aerosol particulate matter. The primary goal of the work is to determine the degree of heavy metal pollution in the region and, for key contaminants, identify their sources. The research plan in the dissertation included three phases that are discussed in the first chapter. The first phase included review of the literature, a field survey to design a sampling plan and identify the collection sample points, and meetings with officials, including a Coast Guard representative to obtain the necessary permissions. The second phase involved

collecting sediments and air filter samples and preparing the samples for laboratory analysis. The third phase comprised interpreting the results to obtain valuable relations between measured indices, and to determine the principal sources of pollution.

Chapter 2 of this dissertation investigated the state of pollution in eighty sediments focusing on six heavy metals: chromium (Cr), manganese (Mn), nickel (Ni), copper (Cu), zinc (Zn), and lead (Pb). The study also quantified the degree of pollution in sediments using various risk indices, including Geo-accumulation Indices (Igeo), Enrichment factors (Ef), Contamination factors (Cf), Pollution Load Indices (PLI), Potential Ecological Risk Indices (PERI) and Potential Toxicity Response Indices (RI). Results showed that the majority of the polluted sediments were recorded in the Middle and South locations, and Pb showed the highest concentration of the metals in the study area (77.34 mg/kg). The Igeo values for Pb in the Middle stations showed that 10% of the stations were categorized as moderately polluted, whereas 20% of the South location was classified as moderately polluted. The RI values in the South stations, especially the northern stations within the South location, indicate high Pb pollution in the area. This study recommended that appropriate management strategies should be applied for the Jeddah Coast to control potential pollution sources and prevent permanent hazards to marine ecology currently documented elsewhere. Additionally, the study implicated that the area needs more tracer studies such as isotopic and speciation studies that could be used to investigate the sources of the Pb in sediments, water, and even in airborne aerosols near the shoreline.

The findings of chapter 2 led us to study Pb isotopes in the sediment samples and the results are described in chapter 3. For the first time in the Red Sea area, the Pb isotopic ratios of ^{206}Pb, ^{207}Pb, and ^{208}Pb were examined to evaluate the sources of Pb. A two end-member model and a three component fractional contribution model were both used to identify

possible Pb sources and their percentage contributions in the study area. The isotopic data and modeling show that natural and anthropogenic sources such as gasoline and an identified unknown source contribute to the Pb load of Jeddah's sediments. The most obvious finding to emerge from this study is that different activities were controlling the Pb isotopes for each location. The study concluded that the Middle location was the most effected location by the Pb from different sources, and the Ef outcomes revealed that 80% of the sediment samples were considered extremely severely enriched with Pb. This study has raised many topics of concern in need of further investigation, including the ratio of Pb isotopes in air samples to Pb isotopes in the soil and isotopic variance with time, presumably recorded in sediment cores.

Finally, in chapter 4, the concentration of the heavy metals of particulate matter (PM) with a size less than 2.5 micrometers is determined. The results of this study indicate that the $PM_{2.5}$ concentration was higher in the North location, and the Pb concentration was higher in the Middle location. The results of the backward trajectory analysis help us understand the sudden concentration increase of PM on August 2 and September 13, 2017. On those dates, Jeddah's atmosphere was affected by a massive dust storms originating in the Tokar Desert in northeastern Sudan. According to Principle Component Analysis (PCA) results, the four principal sources of the heavy metals in the Jeddah ambient air were particles originating from the marine aerosol and re-suspension of soil-derived particles, particles originating from the land in addition to the anthropogenic contribution of Fe, particles originating from oil combustion, and particles originating from incineration and fossil fuel combustion.

The outcomes of the dissertation provide the spatial mapping of the distribution of heavy

metals as well as their possible sources. This will help develop pollution control measures and serve as a resource for choosing optimum remediation methods for water and sediments on the Saudi Arabian coast of the Red Sea. Taken together, the findings of each chapter are impactful and have many important implications for future practice.

TABLE OF CONTENTS

LIST OF TABLES

Table Page

LIST OF FIGURES

Figure page

Chapter 1

INTRODUCTION

1.1 Sources and Effects of Heavy Metals

Anthropogenic heavy metal pollution remains one of the main global environmental concerns, notwithstanding the contemporary technological advances in pollution management. Presently, heavy metal contamination has become a severe environmental issue because of the exponential increase in the use of heavy metal compounds in various industrial processes. According to Skaldina et al. (2018), the major sources of heavy metal dispersal into the environment are industry, transport, refuse burning, and power generation. Also, other primary sources of heavy metals are connected to petroleum extraction and use their products and, besides, agricultural manufacture (Ashraf et al., 2018: Mendoza-Carranza et al., 2016; Zhou et al., 2007; Yang et al., 2019; Xie et al., 2020). Fishing industry and tourism and recreation management operations are also considered potential sources of heavy metals (Ruiz-Compean et al., 2017; Jahan and Strezov. 2018; Nazneen et al., 2019; Warnken et al., 2004; Wang et al., 2013; Yang et al., 2019). Heavy metals are major pollutants in marine, ground, industrial and even treated wastewaters (Abu-Zied et al., 2013; Rodgers et al., 2019). Moreover, heavy metals are detected in the waste streams from many industrial processes, and their concentrations are usually higher than municipal wastewaters (Edelstein and Ben-Hur 2018; Wright et al., 2006; Kronvang et al., 2003). Once released, pollutants can transfer to different environmental media. In the coastal environments, heavy metals are absorbed from the water body to the marine

sediments. The adsorption process is affected by the chemistry of the surface particles, salinity, and pH. (Nobi et al., 2010; Sany et al., 2013). Heavy metals tend to accumulate inside the body and some of them cause severe disorders as they typically cannot be metabolized or decomposed naturally (Nemati et al., 2011; Edelstein & Ben-Hur 2018). Coastal areas are obvious targets to study heavy metals in the broader marine environment due to the sensitivity of these areas to industrial and other anthropogenic effects.

Sediment-bound metals are not necessarily stable; changing physio–chemical characteristics of water conditions can yield re-entry to aqueous phases in the environment and, thereby, increase availability to living organisms. Yusof et al. (2004) reported that numerous types of marine biota such as oysters, mussels, and clams were used as the bio-indicator organisms for the accumulation of trace elements from seawater into marine sediments. Thus, sediments often act as both sink and potential source for metals in aquatic environment (Salomons and Stigliani, 2012).

Sediment studies are often used to classify sources of toxins, describe dispersion pathways, and trace contaminant sinks in marine systems (Ruiz-Compean et al., 2017). Sediments can directly interact with industrial materials, the marine animal population, and vegetation across numerous spatial and temporal scales (Liao et al., 2017). Therefore, the evaluation of metal distribution in surface sediments is useful to assess pollution in the marine environment (Yuan et al., 2012).

The increasing impact of anthropogenic activities on sediments of the Red Sea has become a concern. Accordingly, most of the previous studies of the Red Sea surface sediments show them to be contaminated with some heavy metals (Karuppasamy et al., 2017; Idris et al., 2007; Pan et al., 2011; Usman et al., 2013; Mortuza & Al-Misned, 2017).

Moreover, a growing body of studies recognizes the elevation of concentrations of heavy metals and their effects on the Red Sea sediments. A recent report on Red Sea sediments by Karuppasamy et al. (2017) focused on 11 elements (As, Cd, Cr, Cu, Fe, Hg, Mn, Ni, Pb, V, and Zn) and found that Ni and Hg were enriched due to anthropogenic activity. Badr et al. (2009) studied heavy metals in Red Sea core sediments samples near Jeddah, Saudi Arabia. They found that Jeddah has the most contaminated sediments in comparison with the other Red Sea industrial areas. In the same vein, Pan et al. (2011) noted that the fish market site (Middle of Jeddah) was the most polluted site out of the sites sampled in terms of the total metal concentrations of (Cd, Zn, Ag, Cu, and Pb) due to the area's high shipping activities. The highest concentrations of Cu, Zn, Cd, Ni, Cr, and Pb were measured inside the Al-Arbaeen and Al-Shabab inlets, two coastal inlets located near the central Jeddah coast, suggesting their derivation from anthropogenic materials (Abu-Zied et al., 2013). In 2016, Abu-Zied and Hariri reported that the nearshore sediments of the Jeddah Coast showed the regionally highest concentrations of metals as a consequence of urbanization activities. Moreover, Al-Mur et al. (2017), gave similar conclusions when the authors calculated the enrichment factors for Mn, Cr, Pb, Zn, and Cu in Red Sea core sediment samples.

Lead (Pb) is useful in a large number of industrial functions due to its unique physical and chemical features (Wani et al., 2015). Pb is found in many products such as batteries, bullets, paint and fusible alloys (Al-Saleh et al., 1993; Barbosa et al., 2005; Kim and Kang, 2015; Lee et al., 2019). Additionally, Pb can be found naturally from rock weathering or aerosol deposition (Monastra et al., 2004; Choi et al., 2007; Monna et al., 2000). The plethora of Pb's applications make it challenging to indicate its sources in the

environment. For example, Pb pollution can be sourced from exhaust from gasoline vehicles, degrading paint, and pesticides; thus, sourcing lead pollution is often very difficult (Cheng & Hu 2010; Komárek et al. 2008; Chen et al. 2016 b).

Stable Pb isotopes are useful for determining whether Pb in different environments comes from natural or anthropogenic sources. Using isotopic ratios of elements is a more robust tracking method than using elemental concentrations alone to identify sources of contamination (Alyazichi et al 2016; Chen et al 2015). ^{206}Pb, ^{207}Pb, and ^{208}Pb are the typical isotopes of lead used in such environmental studies. Specifically, the ratios ^{208}Pb/^{206}Pb and ^{206}Pb/^{207}Pb are often used as indicators of different pollution sources of Pb. Global examples include Scotland (Bacon et al., 1995), France (Monna et al., 2000), East Antarctica (Townsend & Snapeb, 2002), Czech Republic (Komárek et al., 2008), China (Cheng and Hu 2010; Yu et al 2016; Liu et al. 2019) , Australia (Alyazichi et al., 2016) and Singapore (Chen et al., 2016 a).

There is a strong interest in studying Pb in marine sediments from the countries bordering the Red Sea. Elevated lead concentrations have been found in marine sediment locations near the Jeddah shoreline, (Badr et al., 2009; Pan et al., 2011; Abu-Zied et al., 2013; Al-Mur et al., 2017), along other coastal areas of Saudi Arabia (Ruiz-Compean et al., 2017; Karuppasamy et al., 2017; Kahal et al., 2018), in Egypt (Mansour et al., 2011; Salem et al., 2014; El-Taher et al., 2018; Badawy et al., 2018;), in Sudan (Idris et al., 2007) and in Jordan (Al-Najjar et al., 2011). Despite the many Pb studies conducted, there remains a serious lack of data and doubt concerning Pb, especially in regard to potential sources. Few geological and mineralogical studies where analysis of Pb source via Pb concentrations and isotopic ratios in the Red Sea have been conducted (Laurila et al., 2014; Pierret et al.,

2010; Baumann 1994).

Atmospheric particulates may be discharged directly from a natural source (e.g. volcanoes and dust storms), or form *in situ* in the atmosphere. Anthropogenic sources are mainly due to industrial activities, energy production, construction, urban waste treatment, and vehicle exhaust (Aburas et al., 2011). The major particulate matter fractions ($PM_{2.5}$ and PM_{10}) typically include organic carbon, major anions (such as chloride, nitrate, and sulfate) and cations (such as sodium, potassium, and ammonium), and minor and trace elements (including most toxic metals) (Chow et al., 2015). Fine particulate matter typically has a long atmospheric residence time, which facilitates its transport over thousands of kilometers. The World Health Organization (WHO) collects and publishes a database on the ambient air pollution in global cities every year (Cheng et al., 2016). The emissions of anthropogenic pollutants can be transported through the atmosphere to remote locations. Coastal marine atmosphere close to any urban and industrial area can be highly affected by pollution emissions, which results in an increase in the loading of pollutants in the ambient air (Baker et al., 1997) and potential delivery to the marine system.

Air has been found as a significant carrier of the heavy metals to the sea. According to Zhang et al. (2007), Cd, Pb, Sb, and Zn were associated with suspended particulate matter from a diversity of pollution emission sources in the northern South China Sea. Air to sea precipitation fluxes of trace elements to coastal waters occur when there are high concentrations of elements in aerosol particles. Atmospheric particulate matter analysis has, therefore, routinely been used to understand pollution load in coastal areas (e.g. Cheng et al., 2000).

Few studies were assessing chemical characterization and source apportionment of airborne particulate matter for the city of Jeddah state that the poor air quality might be related to rapid urbanization, industrialization, and vehicular traffic. In 1990, Abulfaraj et al. used fiberglass filters with a high volume air sampler to measure Pb concentrations in Jeddah. The average Pb concentration in the atmosphere of Jeddah was found, in 2011, by Aburas et al. to be 0.07326 $\mu g/m^3$ and they recommended further studies to accurately determine the current sources of atmospheric Pb. Alghamdi et al., (2015) calculated the enrichment factors of atmospheric particles of Jeddah during dust storm and non-dust storm periods, and stated that soil and resuspended dust are the principal sources for the following elements Na, Mg, Si, K, Ca, Ti, Cr, Mn, Fe, Rb and Sr, while anthropogenic sources are prime sources for S, Cl, Co, Cu, Zn, Ga, As, Pb, Cd, Ni and V. Despite this small amount of work on aerosol chemistry, many questions remain regarding exposure and sourcing in Jeddah region.

1.2 The Objectives and Hypotheses of the Study

Most of the prior literature from the study region solely measured total heavy metal concentrations in an effort to document contamination. In the current study, an attempt is made to report the anthropogenic impacts of toxic metals in the Jeddah area of the Red Sea by determining spatial distribution, source and the associated risk. The overall objectives of the study were:

1. To determine the spatial distribution of heavy metals and their risk to the marine environments in surficial Red Sea sediments near Jeddah.

a. To quantify the extent of pollution using geo accumulation indices (Igeo) and enrichment factors (EF).

b. To determine the associated risk using potential ecological risk factor (PER), and potential toxicity response index (RI); and group and categorize locations based on the levels of contamination of the heavy metals.

c. To determine the spatial extent of heavy metals in marine sediments in the near coast environs of Jeddah.

2. To determine the spatial distribution of Pb isotopes.

a. To develop a powerful tool for tracking and evaluating sources of pollution.

b. To set natural Pb background for the study areas.

3. To study the delivery of heavy metals to the marine environment via particulate matter (PM2.5) in a coastal ambient.

a. To determine total delivery of heavy metals to understand the overall impact of this mechanism of marine addition.

b. To determine possible sourcing of aerosols via factor analysis.

The overall hypotheses for the study derived from the objectives are:

1. The study will find high concentrations of selected heavy metals in all sediments, especially in the southern locations, relative to world averages.
2. Lead (Pb) will be the highest normalized sediment concentration element of interest with its highest expression in the Middle location.
3. The study will show spatial trends of selected heavy metals trending from on shore to off shore and from north to south.
4. Pb isotope results will indicate that air pollution could affect and increase the Pb concentration in the sediments.
5. The data will show that a majority of the heavy metal loading in sediments is

derived from airborne particles.

6. Factor analysis will demonstrate that select heavy metals in airborne particulates are anthropogenically derived.

1.3 Study Area

Saudi Arabia is the largest country in the Arabian Peninsula bordered on the west by the Red Sea. The Red Sea (or Bahr al Ahmar in Arabic), is a semi-enclosed warm body of water, surrounded by nine countries, and one of the most environmentally and geopolitically important bodies of water in the Middle East, as it creates the boundary between Asia and Africa while providing a throughway from the Indian Ocean to the Mediterranean Sea (Samman & Gallus, 2018). The Red Sea is a young ocean basin with 3.8% of the world's coral reefs scattered throughout its 2,000 km length and 355 km width. The Red sea area is roughly 458,620 km^2 with volume around 250,000 km^3. Its northern terminus is divided by the Sinai Peninsula into the Gulf of Aqaba and the Gulf of Suez, while the south is bounded by Bab el Mandeb with the Gulf of Aden on the other side (Rasul & Stewart, 2015). The geological history and its location in a dry and hot environment make it remarkable as one of the most saline bodies of water in the world at approximately 35 psu and with two meters of annual evaporation (Tesfamichael & Pauly, 2016).

Historically speaking, the Red Sea has been used as the main route for merchant caravans from Europe to India and Eastern Asia and is considered one of the major transit ways joining several of the world's major oceans. Jeddah (is located in the western region of the Kingdom of Saudi Arabia (the eastern margin of the Red Sea) and west of the Al-Hejaz plateau, in the middle of the eastern shore of the Red Sea south of the Tropic of

Cancer. Jeddah is recognized as one of the most densely populated and industrial areas on the Red Sea (Ruiz- Compean et al., 2017). According to the Saudi Arabia Demographic Profile for 2019 (SADP, 2019), the population of Jeddah is more than 4 million and is located in the municipality area of 5460 km^2 (Nayebare et al., 2019). The Jeddah climate has high temperatures and humidity in the summer with moderate temperatures and little rainfall in winter (Samman, 2014; Basaham et al., 2009). The major airport of Jeddah is located in the northern part of the city, and the main seaport is located in the middle part of the city. In the next five years, the city will have a new comprehensive and integrated public transport service under Jeddah Public Transportation Program. The new programs will include water buses and ferries that comprise 20 marine stations for a fleet of 26 water buses and ferries (Metro Jeddah, 2019).

Numerous industrial activities – such as refineries, food processing industry, paper mill, painting, tanning, chemical and pharmaceutical, and cleaning products – are conducted in the industrial city that has more than 450 factories and is located on the southern side of the city (Al- Farawati 2010; Ramadan & Halawani, 2010). Many of the industrial facilities, such as the oil refineries and the main desalination plant, were originally built outside the population area, but with urban development, are now in the middle of highly populated areas. For example, some of the Jeddah's residential areas are particularly affected by several concrete factories (Khodeir et al., 2012). Jeddah City has around 12 municipal wastewater treatment plants where Al Shabab, Al Arbaeen, and Al Kumrah are the three largest (Ansari et al., 2015; Ziegler et al., 2016). They receive a mixture of organic matter, nutrients, trace elements, petroleum hydrocarbons, polyaromatic hydrocarbons, and chlorinated hydrocarbons. These treatment plants often

run over their suggested capacities and, as a consequence, there is an extensive discharge of untreated or partially treated sewage into the Red Sea (Al-Farawati 2010; Ziegler et al., 2016).

Jeddah, as one of many urban coastal regions, is subject to adverse environmental effects due to rapid industrialization and economic development. The coastline around the city, including coral communities and associated lagoonal habitat, has been dramatically affected and, at some locations, has resulted in enhanced turbidity and sedimentation (Ziegler et al., 2016; Peña- García et al., 2014). Regional anthropogenic influences on the marine environment of the Red Sea area including the pollution by oil spills, wastewater discharge, effluents of desalination plants, building activities along the seashore, and marine traffic. A variety of heavy metals are released, that negatively harm the marine environment and ambient air from these sources.

1.4 Sample Collection

Two different kinds of samples were collected from the city of Jeddah, Kingdom of Saudi Arabia, during the summer of 2017 (May - August). Specified descriptions of the locations of the collected samples from the studied areas are as follows:

- Air filter samples: 44 glass fiber filter samples, size 8″ x 10″ for Total Suspended Particulate (TSP), were collected by using high volume ambient Particulate Matter 2.5 air samplers featuring a mass flow controller during three months over Jeddah for 24 hours for each sample. The air filter samples were collected from three locations in Jeddah near the sea: North, Middle, and South, where the North location was considered as a reference location. (Figure 1.1) The average temperature, Humidity, and wind speed over the city in June 2017 were 31.6 ^{O}C, 55.6%, and 6.6 m/s, respectively, in July were 34.1 ^{O}C, 44.95%, and 6.7 m/s, respectively, in August were 33.6 ^{O}C, 57.7%, and 7.0 m/s, respectively, and in September

were 32.3 ^{O}C, 62.6%, and 5.9 m/s respectively. Each sampling location was determined by using a Global Positioning System. Two filters were collected weekly for three months. Figure 1.3 shows the locations of the high volume air sampler near to the sea. Each filter was massed before and after the sampling. After the sampling, the filters were placed in plastic bags. The North location (Abhour) is at a research center for the faculties of Maritime Studies and Marine Science at King Abdulaziz University. The location has laboratories, classrooms, and a harbor. The location is near the resort are, a closed gulf (Sharm Abhour), and the King Abdulaziz International Airport. The sampler was placed on the roof of the building, around 10 meters above sea level. The middle location (Alhamraa) is located in the city center of Jeddah, near the main fish market, the main desalination plant, and the highest water fountain in the world. The sampler was placed on the roof of a building with around 7 meters above sea level. The south location (Alkhomra) is located south of Jeddah, and near the harbor where fishermen load and unload their boats. The location is also near Jeddah's industrial city and mangroves area. The sampler was placed on the roof of a short building around 5 meters above sea level. All heavy metal analysis of the air filter samples including heavy acid digestion, and the Inductively Coupled Plasma-Mass Spectrometer (ICP-MS) analysis were done at the Faculty of Meteorology, Environment and Arid Land Agriculture at King Abdulaziz University in Jeddah, Saudi Arabia.

- Sediment samples 80 sediment samples were gathered from Jeddah (Figure 1.2). In each station for the North and South sediment samples, three samples were taken, and for the Middle points, only one samples was taken. All the samples were kept in plastic bags and held at 4^{o} C until they were delivered to the laboratory for preparation. Prior to transport to the U.S, the samples were prepared as follows at the Environmental Water Laboratory, Faculty of Meteorology, Environment and Arid Land Agriculture. Each sediment sample was homogeneously mixed and stored in plastic 50 mL vials, labeled, and stored frozen at -20C

until shipping (Figure 1.4). After arrival in the U.S, all the samples were stored at the Civil and Environmental Engineering Laboratory, Southern Methodist University, Dallas, TX, where all further analyses were conducted.

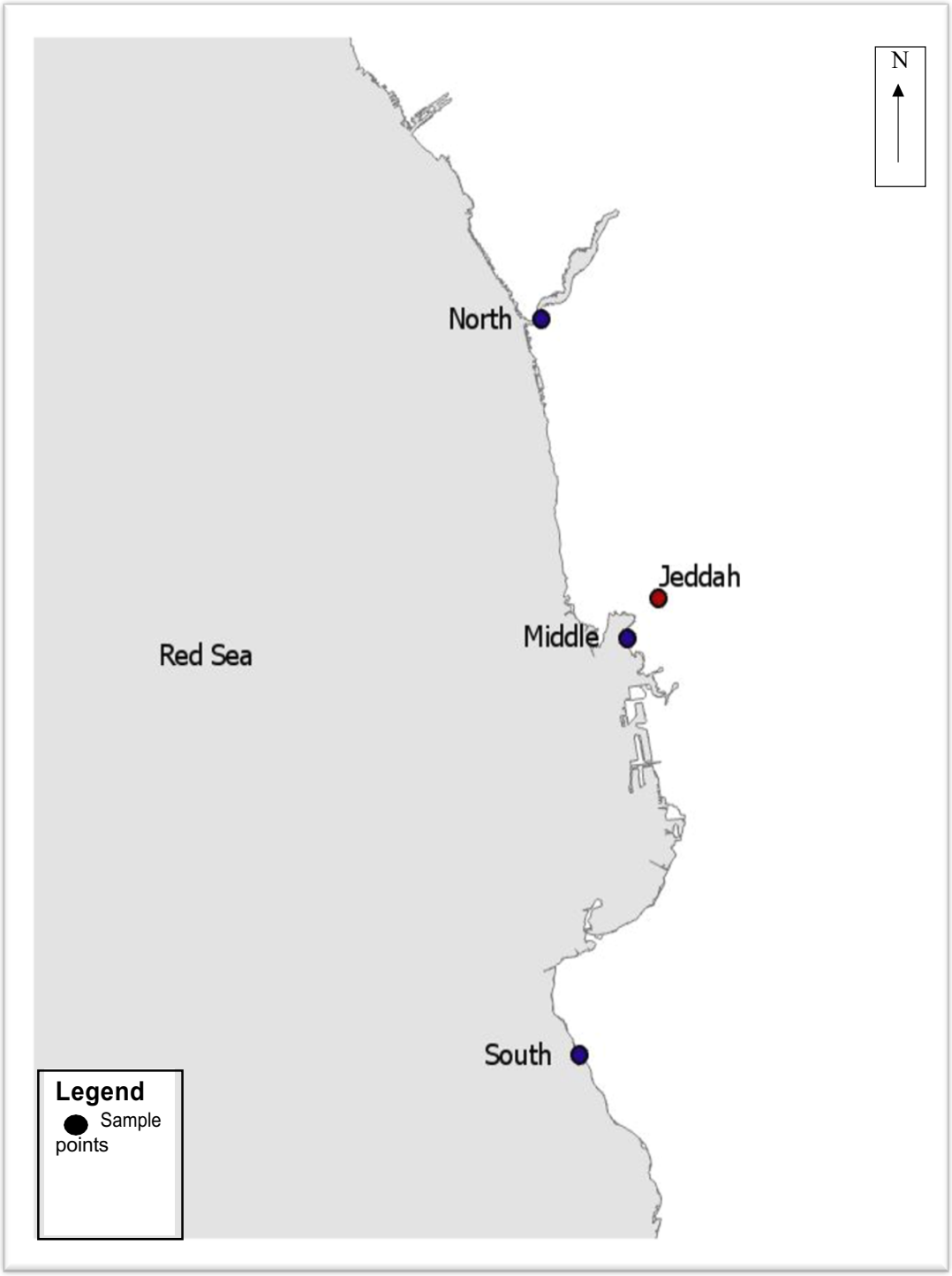

Figure 1. 1 The map shows the location of air samples.

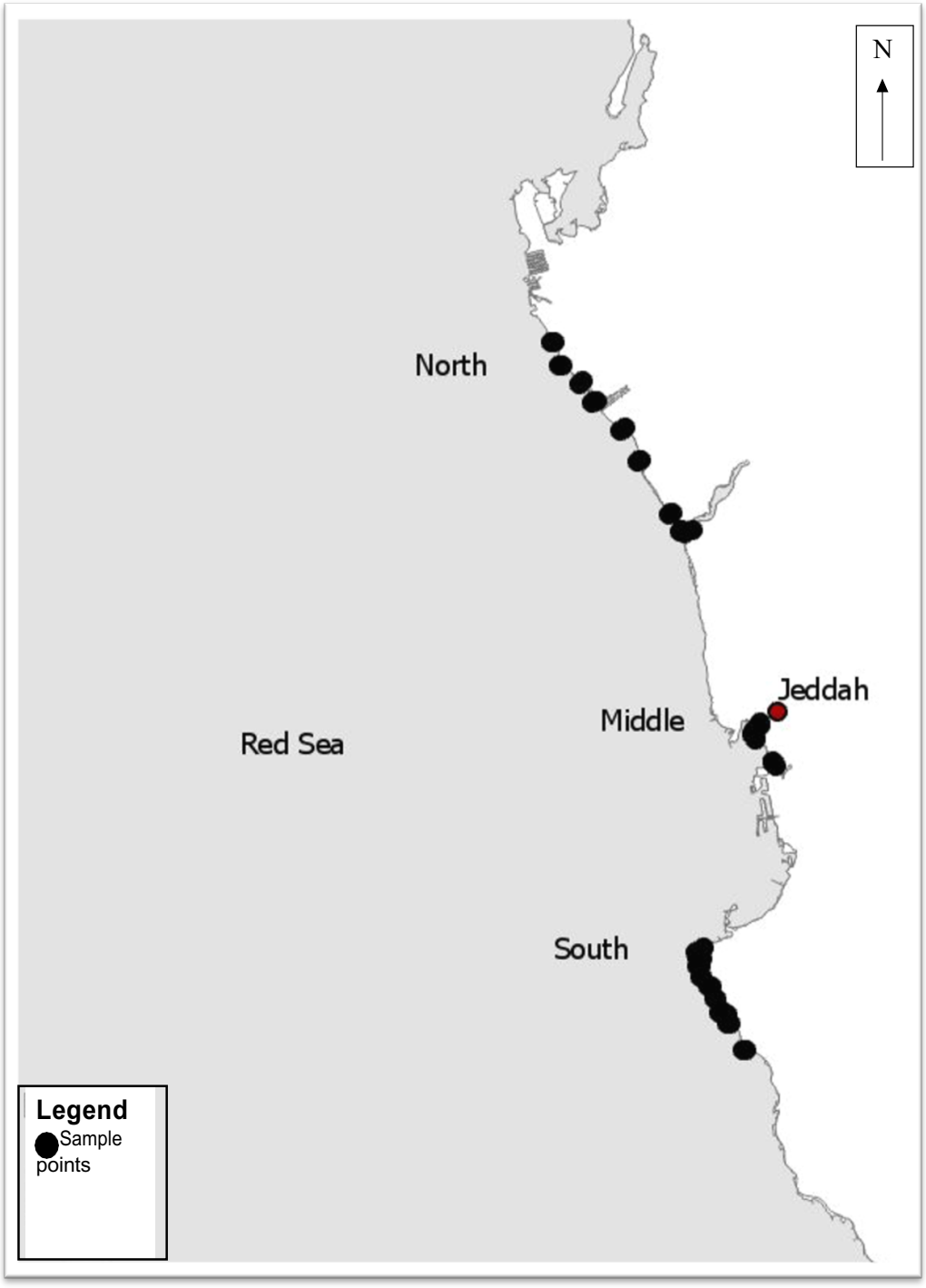

Figure 1. 2 The regional map shows the locations of sediment samples.

Figure 1. 3 Images (A) and (B) show the high volume air sampler near to the sea.

Figure 1. 4 Images (A) and (B) show each sample has been mixed and stored in plastic tubes.

Reference

Abu-Zied, R. H., & Hariri, M. S. (2016). Geochemistry and benthic foraminifera of the nearshore sediments from Yanbu to Al-Lith, eastern Red Sea coast, Saudi Arabia. *Arabian Journal of Geosciences*, 9(4), 245. https://doi.org/10.1007/s12517-015-2274-9

Abu-Zied, R. H., Basaham, A. S., & El Sayed, M. A. (2013). Effect of municipal wastewaters on bottom sediment geochemistry and benthic foraminifera of two Red Sea coastal inlets, Jeddah, Saudi Arabia. *Environmental earth sciences*, 68(2), 451-469. https://doi.org/10.1007/s12665-012-1751-7

Abulfaraj, W. H., Ahmed, M., Mousli, K. M., & Erturk, F. (1990). Measurement of ambient air lead concentrations in the city of Jeddah, Saudi Arabia. *Environment international*, 16(1), 85-88. https://doi.org/10.1016/0160-4120(90)90208-N

Aburas, H. M., Zytoon, M. A., & Abdulsalam, M. I. (2011). Atmospheric Lead in PM2.5 after Leaded Gasoline Phase-out in Jeddah City, Saudi Arabia. *CLEAN–Soil, Air, Water*, 39(8), 711-719. https://doi.org/10.1002/clen.201000510

Al-Farawati, R. (2010). Environmental conditions of the coastal waters of Southern Corinche, Jeddah, Eastern red sea: Physico-chemical approach. Australian Journal of Basic and Applied Sciences, 4(8), 33243337.

Al-Mur, B. A., Quicksall, A. N., & Al-Ansari, A. M. (2017). Spatial and temporal distribution of heavy metals in coastal core sediments from the Red Sea, Saudi Arabia. *Oceanologia*, 59(3), 262-270.

https://doi.org/10.1016/j.oceano.2017.03.003

Al-Najjar, T., Rasheed, M., Ababneh, Z., Ababneh, A., & Al-Omarey, H. (2011). Heavy metals pollution in sediment cores from the Gulf of Aqaba, Red Sea. *Natural science*, 3(09), 775. http://dx.doi.org/10.4236/ns.2011.39102

Alghamdi, M. A., Almazroui, M., Shamy, M., Redal, M. A., Alkhalaf, A. K., Hussein, M. A., & Khoder, M. I. (2015). Characterization and elemental composition of atmospheric aerosol loads during springtime dust storm in western Saudi Arabia. *Aerosol Air Qual. Res*, 15(2), 440-453. doi: 10.4209/aaqr.2014.06.0110

Altherr, R., Henjes-Kunst, F., & Baumann, A. (1990). Asthenosphere versus lithosphere as possible sources for basaltic magmas erupted during formation of the Red Sea: constraints from Sr, Pb and Nd isotopes. *Earth and Planetary Science Letters*, 96(3-4), 269-286. https://doi.org/10.1016/0012-821X(90)90007-K

Alyazichi, Y. M., Jones, B. G., & McLean, E. (2016). Lead isotope fingerprinting used as a tracer of lead pollution in marine sediments from Botany Bay and Port Hacking estuaries, southern Sydney, Australia. *Regional Studies in Marine Science*, 7, 136-141. https://doi.org/10.1016/j.rsma.2016.06.006

Angel, B. M., Apte, S. C., Batley, G. E., & Raven, M. D. (2016). Lead solubility in seawater: an experimental study. *Environmental Chemistry*, 13(3), 489-495.

Ansari, M. I., Harb, M., Jones, B., & Hong, P. Y. (2015). Molecular-based approaches to characterize coastal microbial community and their potential relation to the trophic state of Red Sea. *Scientific reports*, 5, 9001. https://doi.org/10.1038/srep09001

Ashraf, A., Saion, E., Gharibshahi, E., Yap, C. K., Kamari, H. M., Elias, M. S., & Rahman, S. A. (2018). Distribution of Heavy Metals in Core Marine Sediments of Coastal East Malaysia by Instrumental Neutron Activation Analysis and Inductively Coupled Plasma Spectroscopy. Applied Radiation and Isotopes, 132, 222-231. https://10.1016/j.apradiso.2017.11.012.

Bacon, J. R., Beffow, M. L., & Shand, C. A. (1995). The use of isotopic composition in field studies of lead in upland Scottish soils (UK). *Chemical geology*, 124(1-2), 125-134. https://doi.org/10.1016/0009-2541(95)00030-P

Badawy, W. M., El-Taher, A., Frontasyeva, M. V., Madkour, H. A., & Khater, A. E. (2018). Assessment of anthropogenic and geogenic impacts on marine sediments along the coastal areas of Egyptian Red Sea. *Applied Radiation and Isotopes*, 140, 314-326.https://doi.org/10.1016/j.apradiso.2018.07.034

Badr, N. B., El-Fiky, A. A., Mostafa, A. R., & Al-Mur, B. A. (2009). Metal pollution records in core sediments of some Red Sea coastal areas, Kingdom of Saudi Arabia. Environmental monitoring and assessment,155(1-4), 509-526. https://doi.org/10.1007/s10661-008-0452- x

Baker, J.E., Poster, D.L., Clark, C.A., Church, T.M., Scudlark, J.R., Ondov, J.M., Dickau, R.M., Cutter, G., 1997. *Loading of atmospheric trace elements and organic contaminants to the Chesapeake Bay*. In: Baker, J.E. (Ed.), Atmospheric Deposition of Contaminants to the Great Lakes and Coastal Waters. SETAC Press, Pensacola, Florida, pp. 171–194.

Barbosa Jr, F., Tanus-Santos, J. E., Gerlach, R. F., & Parsons, P. J. (2005). A critical review of biomarkers used for monitoring human exposure to lead: advantages,

limitations, and future needs. *Environmental health perspectives*, 113(12), 1669-1674. https://doi.org/10.1289/ehp.7917

Basaham, A. S., Rifaat, A. E., El-Mamoney, M. H., & El Sayed, M. A. (2009). Re-evaluation of the impact of sewage disposal on coastal sediments of the southern Corniche, Jeddah, Saudi Arabia. Journal of King Abdulaziz University, *Marine Sciences*,20,109-126. https://www.kau.edu.sa/Files/320/Researches/54566_24891.pdf

Baumann, A. (1994). Lead and strontium isotopes in metalliferous and calcareous pelitic sediments of the Red Sea axial trough. *Mineralium Deposita*, 29(1), 81-93. https://doi.org/10.1007/BF03326398

Chen, M., Boyle, E. A., Switzer, A. D., & Gouramanis, C. (2016 a). A century long sedimentary record of anthropogenic lead (Pb), Pb isotopes and other trace metals in Singapore. *Environmental pollution*, 213, 446-459. https://doi.org/10.1016/j.envpol.2016.02.040

Chen, M., Goodkin, N. F., Boyle, E. A., Switzer, A. D., & Bolton, A. (2016 b). Lead in the western South China Sea: Evidence of atmospheric deposition and upwelling. *Geophysical Research Letters,* 43(9), 4490-4499. https://doi.org/10.1002/2016GL068697

Chen, M., Lee, J. M., Nurhati, I. S., Switzer, A. D., & Boyle, E. A. (2015). Isotopic record of lead in Singapore Straits during the last 50 years: spatial and temporal variations. *Marine Chemistry,* 168, 49-59. https://doi.org/10.1016/j.marchem.2014.10.007

Cheng, H., & Hu, Y. (2010). Lead (Pb) isotopic fingerprinting and its applications in lead

pollution studies in China: a review. *Environmental Pollution*, 158(5), 1134-1146. https://doi.org/10.1016/j.envpol.2009.12.028

Cheng, Z. L., Lam, K. S., Chan, L. Y., Wang, T., & Cheng, K. K. (2000). Chemical characteristics of aerosols at coastal station in Hong Kong. I. Seasonal variation of major ions, halogens and mineral dusts between 1995 and 1996. *Atmospheric Environment*, 34(17), 2771-2783. https://doi.org/10.1016/S1352-2310(99)00343-X

Cheng, Z., Luo, L., Wang, S., Wang, Y., Sharma, S., Shimadera, H., ... & Zhou, W. (2016). Status and characteristics of ambient PM2.5 pollution in global megacities. *Environment international*, 89, 212-221. https://doi.org/10.1016/j.envint.2016.02.003

Choi, M. S., Yi, H. I., Yang, S. Y., Lee, C. B., & Cha, H. J. (2007). Identification of Pb sources in Yellow Sea sediments using stable Pb isotope ratios. *Marine Chemistry*, 107(2), 255-274. https://doi.org/10.1016/j.marchem.2007.07.008

Chow, J. C., Lowenthal, D. H., Chen, L. W. A., Wang, X., & Watson, J. G. (2015). Mass reconstruction methods for PM2.5: a review. *Air Quality*, *Atmosphere & Health*, 8(3), 243- 263. https://doi.org/10.1007/s11869-015-0338-3

Edelstein, M., & Ben-Hur, M. (2018). Heavy metals and metalloids: Sources, risks and strategies to reduce their accumulation in horticultural crops. *Scientia Horticulturae*, 234, 431-444. https://doi.org/10.1016/j.scienta.2017.12.039

European Food Safety Authority (EFSA). Alexander, J., Benford, D., Boobis, A., Ceccatelli, S., Cravedi, J. P., Di Domenico, A., ... & Filipi9c, M. (2010). Efsa panel on contaminants in the food chain; scientific opinion on marine biotoxins

in shellfish—Emerging toxins: Ciguatoxin group. EFSA J, 1627, 1-38.

Gan, T., Zhao, N., Yin, G., Chen, M., Wang, X., Liu, J., & Liu, W. (2019). Optimal chlorophyll fluorescence parameter selection for rapid and sensitive detection of lead toxicity to marine microalgae Nitzschia closterium based on chlorophyll fluorescence technology.*Journal of Photochemistry andPhotobiology B: Biology*, 111551. https://doi.org/10.1016/j.jphotobiol.2019.111551

Idris, A. M., Eltayeb, M. A. H., Potgieter-Vermaak, S. S., Van Grieken, R., & Potgieter, J. H. (2007). Assessment of heavy metals pollution in Sudanese harbours along the Red Sea Coast. *Microchemical Journal*, 87(2), 104-112. https://doi.org/10.1016/j.microc.2007.06.004

Javed, M. (2012). Effects of zinc and lead toxicity on the growth and their bioaccumulation in fish. Pakistan Veterinary Journal, 32, 357-362. http://www.pvj.com.pk/ /357-362.pdf

Jahan, S., & Strezov, V. (2018). Comparison of pollution indices for the assessment of heavy metals in the sediments of seaports of NSW, Australia. Marine Pollution Bulletin, 128, 295-306. https://10.1016/j.marpolbul.2018.01.036

Kahal, A. Y., El-Sorogy, A. S., Alfaifi, H. J., Almadani, S., & Ghrefat, H. A. (2018). Spatial distribution and ecological risk assessment of the coastal surface sediments from the Red Sea, northwest Saudi Arabia. *Marine pollution bulletin*, 137, 198-208. https://doi.org/10.1016/j.marpolbul.2018.09.053

Karuppasamy, M. P., Qurban, M. A., Krishnakumar, P. K., Mushir, S. A., & Abuzaid, N. (2017). Evaluation of toxic elements As, Cd, Cr, Cu, Ni, Pb and Zn in the surficial sediments of the Red Sea (Saudi Arabia). Marine pollution bulletin,

119(2), 181-190. https://doi.org/10.1016/j.marpolbul.2017.04.019

Khodeir, M., Shamy, M., Alghamdi, M., Zhong, M., Sun, H., Costa, M., Chen, L.C. and Maciejcczyk, P.M. (2012). Source Apportionment and Elemental Composition of PM2.5 and PM10 in Jeddah City, Saudi Arabia. Atmos. *Pollut. Res*. 3: 331–340. https://doi.org/10.5094/APR.2012.037

Kim, J. H., & Kang, J. C. (2015). The lead accumulation and hematological findings in juvenile rock fish Sebastes schlegelii exposed to the dietary lead (II) concentrations. *Ecotoxicology and environmental safety,* 115, 33-39. https://doi.org/10.1016/j.ecoenv.2015.02.009

Komárek, M., Ettler, V., Chrastný, V., & Mihaljevič, M. (2008). Lead isotopes in environmental sciences: A review. *Environment International*, 34(4), 562–577. https://doi.org/10.1016/j.envint.2007.10.005.

Kosnett, M. J. (2007). *Heavy metal intoxication and chelators. Basic and clinical pharmacology*, 10th ed, New York: McGraw-Hill, 945-957.

Kronvang, B., Laubel, A., Larsen, S. E., & Friberg, N. (2003). Pesticides and heavy metals in Danish streambed sediment. Hydrobiologia, 494(1-3), 93-101. https://doi.org/10.1023/A:1025441610434

Lee, J. W., , H., Hwang, U. K., Kang, J. C., Kang, Y. J., Kim, K. I., & Kim, J. H. (2019). Toxic effects of lead exposure on bioaccumulation, oxidative stress, neurotoxicity, and mmune responses in fish: A review. *Environmental toxicology and pharmacology*, 68, 101- 108 https://doi.org/10.1016/j.etap.2019.03.010

Liao, J., Chen, J., Ru, X., Chen, J., Wu, H., & Wei, C. (2017). Heavy metals in river

surface sediments affected with multiple pollution sources, South China: Distribution, enrichment and source apportionment. *Journal of Geochemical Exploration*, 176, 9-19. https://doi.org/10.1016/j.gexplo.2016.08.013

Ligi, M., Bonatti, E., & Rasul, N. M. (2015). Seafloor spreading initiation: geophysical and geochemical constraints from the Thetis and Nereus Deeps, central Red Sea. *The Red Sea* (pp. 79-98). Springer. https://doi.org/10.1007/978-3-662-45201-1_4

Lim, C. C., Thurston, G. D., Shamy, M., Alghamdi, M., Khoder, M., Mohorjy, A. M., ... & Costa, M. (2017). Temporal variation of fine and coarse particulate matter sources in Jeddah, Saudi Arabia. *Journal of the Air & Waste Management Association, 68(2), 123-138* . https://doi.org/10.1080/10962247.2017.1344158

Liu, J., Yin, M., Luo, X., Xiao, T., Wu, Z., Li, N., ... & Feng, Y. (2019). The mobility of thallium in sediments and source apportionment by lead isotopes. *Chemosphere*,219,864-874. ttps://doi.org/10.1016/j.chemosphere.2018.12.041

Mansour, A. M., Nawar, A. H., & Madkour, H. A. (2011). Metal pollution in marine sediments of selected harbours and industrial areas along the Red Sea coast of Egypt. *Ann Naturhist Mus Wien Serie A*, 113, 225-244. https://www.jstor.org/stable/41701739

Mendoza-Carranza, M., Sepúlveda-Lozada, A., Dias-Ferreira, C., & Geissen, V. (2016). Distribution and bioconcentration of heavy metals in a tropical aquatic food web: A case study of a tropical estuarine lagoon in SE Mexico. Environmental Pollution, 210, 155-165. https://10.1016/j.envpol.2015.12.014

Merto Jeddah,2019. The Jeddah Public Transport Program.

http://www.metrojeddah.com.sa/page/JPTP

Monastra, V., Derry, L. A., & Chadwick, O. A. (2004). Multiple sources of lead in soils from a Hawaiian chronosequence. *Chemical Geology*, 209(3-4), 215-231. https://doi.org/10.1016/j.chemgeo.2004.04.027

Monna, F., Clauer, N., Toulkeridis, T., & Lancelot, J. R. (2000). Influence of anthropogenic activity on the lead isotope signature of Thau Lake sediments (southern France): origin and temporal evolution. *Applied Geochemistry*, 15(9), 1291-1305.https://doi.org/10.1016/S0883-2927(99)00117-1

Mortuza, M. G., & Al-Misned, F. A. (2017). Environmental contamination and assessment of heavy metals in water, sediments and shrimp of Red Sea coast of Jizan, Saudi Arabia. J. Aquat. Pollut. Toxicol, 1 (1) (2017)

Nemati, K., Abu Bakar, N. K., Abas, M. R., & Sobhanzadeh, E. (2011). Speciation of heavy metals by modified BCR sequential extraction procedure in different depths of sediments from Sungai Buloh, Selangor, Malaysia. *J Hazard Mater*, 192(1), 402-410. https://doi.org/10.1016/j.jhazmat.2011.05.039

Nobi, E. P., Dilipan, E., Thangaradjou, T., Sivakumar, K., & Kannan, L. (2010). Geochemical and geo-statistical assessment of heavy metal concentration in the sediments of different coastal ecosystems of Andaman Islands, India. Estuarine, Coastal and Shelf Science, 87(2), 253-264. https://10.1016/j.ecss.2009.12.019

Nazneen, S., Singh, S., & Raju, N. J. (2019). Heavy metal fractionation in core sediments and potential biological risk assessment from Chilika lagoon, Odisha state, India. Quaternary International, 507, 370-388. https://10.1016/j.quaint.2018.05.011

Pan , K., Lee, O. O., Qian, P. Y., & Wang, W. X. (2011). Sponges and sediments as monitoring tools of metal contamination in the eastern coast of the Red Sea, Saudi Arabia. *Marine pollution bulletin*, 62(5), 1140-1146. https://doi.org/10.1016/j.marpolbul.2011.02.043

Peng, J. F., Song, Y. H., Yuan, P., Cui, X. Y., & Qiu, G. L. (2009). The remediation of heavy metals contaminated sediment. *Journal of hazardous materials*, 161(2-3), 633-640. https://doi.org/10.1016/j.jhazmat.2008.04.061

Pierret, M. C., Clauer, N., Bosch, D., & Blanc, G. (2010). Formation of Thetis Deep metal-rich sediments in the absence of brines, Red Sea. *Journal of Geochemical Exploration*, 104(1- 2), 12-26. https://doi.org/10.1016/j.gexplo.2009.10.001

Peña-García, D., Ladwig, N., Turki, A. J., & Mudarris, M. S. (2014). Input and dispersion of nutrients from the Jeddah Metropolitan Area, Red Sea. *Marine pollutionbulletin*,80(1-2),41-51. https://doi.org/10.1016/j.marpolbul.2014.01.052

Ramadan, M. H., & Halawani, R. F. (2010). Study on Wastewater in Paper Recycling Plants Case Study. Journal of King Abdulaziz University: Meteorology, Environment & Arid Land Agriculture Sciences, 21(2).

Rasul, N. M., & Stewart, I. C. (Eds.). (2015). *The Red Sea: the formation, morphology, oceanography and environment of a young ocean basin*. Springer. DOI 10.1007/978-3- 662-45201-1

Ruiz-Compean, P., Ellis, J., Curdia, J., Payumo, R., Langner, U., Jones, B., & Carvalho, S. (2017). Baseline evaluation of sediment contamination in the shallow coastal areas of Saudi Arabian Red Sea. *Marine pollution bulletin*, 123(1-2), 205-218.

https://doi.org/10.1016/j.marpolbul.2017.08.059

Rodgers, K., McLellan, I., Peshkur, T., Williams, R., Tonner, R., Hursthouse, A. S., & Henriquez, F. L. (2019). Can the legacy of industrial pollution influence antimicrobial resistance in estuarine sediments?. *Environmental Chemistry Letters*, 17(2), 595-607. https://doi.org/10.1007/s10311-018-0791-y

SADP 2019, Saudi Arabia Demographic Profile 2019, https://www.indexmundi.com/saudi_arabia/demographics_profile.html

Salem, D. M. A., Khaled, A., El Nemr, A., & El-Sikaily, A. (2014). Comprehensive risk assessment of heavy metals in surface sediments along the Egyptian Red Sea coast. *The Egyptian Journal of Aquatic Research*, 40(4), 349-362.

Salomons, W., & Stigliani, W. M. (Eds.). (2012). *Biogeodynamics of pollutants in soils and sediments: risk assessment of delayed and non-linear responses*. Springer Science & Business Media.

Samman, A. (2014). Numerical simulation diagnostics of a flash flood event in Jeddah, Saudi Arabia (Doctoral dissertation, Colorado State University. Libraries). http://hdl.handle.net/10217/82532

Samman, A. E., & Gallus Jr, W. A. (2018) A climatology of the winter low-level jet over the Red Sea. *International Journal of Climatology*. https://doi.org/10.1002/joc.5742

Skaldina, O., Peräniemi, S., & Sorvari, J. (2018). Ants and their nests as indicators for industrial heavymetal contamination. *Environmental Pollution*,240, 574-581. https://doi.org/10.1016/j.envpol.2018.04.134

Sany, S., Sany, S., Salleh, A., Salleh, A., Sulaiman, A., Sulaiman, A., Sasekumar, A.,

Sasekumar, A., Rezayi, M., Rezayi, M., Tehrani, G., & Tehrani, G. (2013). Heavy metal contamination in water and sediment of the Port Klang coastal area, Selangor, Malaysia. Environmental Earth Sciences, 69(6), 2013-2025. https://10.1007/s12665-012-2038-8. https://doi.org/10.1016/j.ejar.2014.11.004

Tesfamichael, D., & Pauly, D. (Eds.). (2016). *The Red Sea ecosystem and fisheries* (Vol. 7).Springer.

Townsend, A. T., & Snape, I. (2002). The use of Pb isotope ratios determined by magnetic sector ICP-MS for tracing Pb pollution in marine sediments near Casey Station, East Antarctica. *Journal of Analytical Atomic Spectrometry*, 17(8), 922-928. https://doi.org/10.1039/B203449M

Usman, A. R., Alkredaa, R. S., & Al-Wabel, M. I. (2013). Heavy metal contamination in sediments and mangroves from the coast of Red Sea: Avicennia marina as potential metal bioaccumulator. *Ecotoxicology and environmental safety*, 97, 263-270. https://doi.org/10.1016/j.ecoenv.2013.08.009

Vinodhini, R., & Narayanan, M. (2008). Bioaccumulation of heavy metals in organs of fresh water fish Cyprinus carpio (Common carp). *International Journal of Environmental Science & Technology*, 5(2), 179-182. https://doi.org/10.1007/BF03326011

Wang, S., Xu, X., Sun, Y., Liu, J., & Li, H. (2013). Heavy metal pollution in coastal areas of South China: A review. Marine Pollution Bulletin, 76(1-2), 7-15. https://10.1016/j.marpolbul.2013.08.025

Wani, A. L., Ara, A., & Usmani, J. A. (2015). Lead toxicity: a review. *Interdisciplinary toxicology*, 8(2), 55-64. https://doi.org/10.1515/intox-2015-0009

Warnken, J., Dunn, R. J. K., & Teasdale, P. R. (2004). Investigation of recreational boats as a source of copper at anchorage sites using time-integrated diffusive gradients in thin film and sediment measurements. Marine Pollution Bulletin, 49(9), 833-843. https://10.1016/j.marpolbul.2004.06.012

World Health Organization. Edition, F. (2011). Guidelines for drinking-water quality. *WHO chronicle*, 38(4), 104-8.

Wright, M. S., Peltier, G. L., Stepanauskas, R., & McArthur, J. V. (2006). Bacterial tolerances to metals and antibiotics in metal-contaminated and reference streams. *FEMS microbiology ecology,* 58(2), 293-302. https://doi.org/10.1111/j.1574-6941.2006.00154.x

Xie, Q., Gui, D., Liu, W., & Wu, Y. (2020). Risk for Indo-Pacific humpback dolphins (Sousa chinensis) and human health related to the heavy metal levels in fish from the Pearl River Estuary, China. Chemosphere, 240, 124844. https://10.1016/j.chemosphere.2019.124844

Yang, T., Cheng, H., Wang, H., Drews, M., Li, S., Huang, W., Zhou, H., Chen, C. M., & Diao, X. (2019). Comparative study of polycyclic aromatic hydrocarbons (PAHs) and heavy metals (HMs) in corals, surrounding sediments and surface water at the Dazhou Island, China. Chemosphere, 218, 157-168. https://10.1016/j.chemosphere.2018.11.06

Yu, R., Hu, G., Yang, Q., He, H., & Lin, C. (2016). Identification of Pb sources using Pb isotopic compositions in the core sediments from Western Xiamen Bay, China. *Marine pollution bulletin*, 113(1-2), 247-252. https://doi.org/10.1016/j.marpolbul.2016.09.027

Yuan, H., Song, J., Li, X., Li, N., & Duan, L. (2012). Distribution and contamination of heavy metals in surface sediments of the South Yellow Sea. *Marine pollution bulletin*, 64(10), 2151-2159. https://doi.org/10.1016/j.marpolbul.2012.07.040

Yusof, A., Yanta, N., & Wood, A. (2004). The use of bivalves as bio-indicators in the assessment of marine pollution along a coastal area. Journal of Radioanalytical and Nuclear Chemistry, 259(1), 119-127. https://10.1023/B:JRNC.0000015816.16869.6f

Zhang, X., Zhuang, G., Guo, J., Yin, K., & Zhang, P. (2007). Characterization of aerosol over the Northern South China Sea during two cruises in 2003. *Atmospheric Environment*, 41(36), 7821-7836. https://doi.org/10.1016/j.atmosenv.2007.06.031

Zhou, F., Guo, H., & Hao, Z. (2007). Spatial distribution of heavy metals in Hong Kong's marine sediments and their human impacts: A GIS-based chemometric approach. Marine Pollution Bulletin, 54(9), 1372-1384. https://10.1016/j.marpolbul.2007.05.017

Ziegler, M., Roik, A., Porter, A., Zubier, K., Mudarris, M. S., Ormond, R., & Voolstra, C. R. (2016). Coral microbial community dynamics in response to anthropogenic impacts near a major city in the central Red Sea. *Marine pollution bulletin*, 105(2), 629-640. https://doi.org/10.1016/j.marpolbul.2015.12.045.

Chapter 2

SPATIAL DISTRIBUTION OF HEAVY METALS IN NEAR-SHORE MARINE SEDIMENTS OF THE JEDDAH, SAUDAI ARABIA REGION: ENRICHMENT AND ASSOCIATED RISK INDICES

2.1 Abstract

Red Sea coastal development has rapidly accelerated in the last decades that lead to a rise in the anthropogenic heavy metals level in sediments. Eighty surficial sediment samples were collected from the shallow waters along the Jeddah coast, eastern Red Sea near Jeddah, Saudi Arabia. These samples were allocated as north, middle and south of the Jeddah coast to assess the concentrations of six heavy metals such as chromium (Cr), manganese (Mn), nickel (Ni), copper (Cu), zinc (Zn), and lead (Pb). The results showed that the concentrations of these metals (mg/kg) in the studied sediments follow this order: Pb (77.34 ± 150.59) > Mn (36.52 ± 37.72) > Zn (18.02± 23.94) > Cr (9.56 ± 5.81) > Cu (9.18 ± 13.67) > Ni (3.68 ±4.54). The majority of the polluted sediments were recorded in the Middle and South locations. It seems that the desalination plant, the outflow tubes for industrial and municipal wastewaters and ships maintenance waste are the possible sources of pollutants in the Middle part of Jeddah coast. Whereas the industrial activities waste from the industrial city is the potential sources pollution in the Southern part of the coast. Pollution and Enrichment indices

such as the geo accumulation indices (Igeo), Enrichment factor (Ef), Contamination factor (Cf), Pollution load index (PLI), Potential ecological risk (PERI) and Potential toxicity response index (RI) were applied on the measured metals to establish baselines and assess their enrichments along the Jeddah coastline. The Igeo values showed that 30% of the Southern location stations are considered moderately to highly polluted. The Ef for all the studied sediments was fallowing this order: Pb (extremely severe enrichment)> Mn > Cu > Zn > Cr (severe enrichment) > Ni (moderate enrichment). In general, this study provides baseline information for future monitoring, and the development of national regulations not only along Jeddah coast, but also in the Red Sea.

2.2 Introduction

The Jeddah coast is a part of the Red Sea, which is a semi enclosed hot water body separating Arabian subcontinent from Africa and surrounded by nine countries (Samman and Gallus, 2018). Historically, the Red Sea has been used as the main route for merchant caravans from Europe toward India and Eastern Asia and is still one of the major transportation routes joining several of the world's major ocean shipping routes. Despite heavy shipping traffic, the Red Sea had been considered relatively unpolluted, apart from localized areas (Hanna and Muir, 1990).

Recently, however, the impact of anthropogenic activities on the sediments of the Red Sea has increased and become a national concern. Different anthropogenic activities could influence the marine environment, including pollution via oil spills, wastewater discharge, effluents of desalination plants, and building activities along the seashore, and marine travel (Al-Mur et al., 2017; Al-Sofyani et al., 2014; Pan et al.,

2011; Louriño-Cabanaet et al., 2011; Badr et al., 2009). According to Skaldina et al. (2018), industry, transport, refuse burning, and power generation are considered significant sources of heavy metals into different environmental media. Direct or indirect wastewater discharge, with its load of heavy metals, leads to increasing environmental contaminants in marine environments (Cui et al., 2014; Fu & Wang, 2011). Many of the industrial facilities, such as the oil refineries and the main desalination plant, were originally been built outside the population area. With ensuing urban development, they are now in the middle of highly populated areas and some of the Jeddah's residential areas are particularly affected by several concrete factories (Khodeir et al., 2012). More than 450 factories and various industrial activities are located on the southern side of the city. Prior work showed that anthropogenic activities are clearly affecting sediments according to the rapid industrial transformation in the coastal area of Saudi Arabia (Karuppasamy et al 2019, Ghandour et al., 2014). Indeed, coastal sediments of Jeddah are attractive objectives for scholars to study heavy metal enrichment due to the sensitivity of these sediments to industrial and anthropogenic activities (Amin et al., 2009; Pan et al., 2011) coastal area of Saudi Arabia (Karuppasamy et al 2019, Ghandour et al., 2014).

Sediments can directly interact with other media across numerous spatial and temporal scales (Liao et al. 2017). The concentration of heavy metals in sediment, therefore, is a vital indicator for identifying and classifying the degree of pollution for any area of concern (Yaun et al., 2012). The concentrations of heavy metals in seawater are often governed by suspended particulate matter and sediment type (Amin et al., 2009; Karuppasamy et al., 2019). Usually, metals bind to particulate matter once

discharged into aquatic systems; they settle and are sorbed by sediments (Khodami et al., 2017). Heavy metal concentrations in sediments are also influenced by factors such as pH, conductivity, salinity, and the availability of organic matter (Chakraborty et al., 2014). Distribution and expression of concentrations in sediments is, therefore, a complex issue containing a variety of information relating to the current environmental conditions, diagenetic conditions, and transport processes. Most of this information is vital in understanding sourcing and availability of the metals in question. Some heavy metals — such as lead, cadmium, mercury, chromium, and arsenic — are identified as toxic for living organisms, whereas copper, manganese, sodium, iron, and zinc are essential metals, which can be toxic when reaching above permissible levels (Ahmed et al., 2015; Canli and Atli, 2003). For either case, identifying bioavailability, remobilization and source is of interest to investigators for long-term management and possible remediation.

A number of studies have investigated the surface sediments of the Red Sea and shown that sediments are contaminated with some heavy metals. Badr et al., (2009), studied heavy metals in Red Sea sediments near Jeddah and reported that Jeddah has the most contaminated sediments in comparison with the other industrial areas along the Red Sea coast. The peak concentrations of Pb, Ni, Zn, Cd, Cr, and Cu were recorded in the Al-Shabab and Al-Arbaeen inlets (central Jeddah coast), indicating their association with anthropogenic materials (Abu-Zied et al., 2013). Pan et al. (2011) reported that Pb, Cu, and Zn were high in sediment samples collected from near the Jeddah fish market. Moreover, Al-Mur et al., (2017) reported the same conclusions for sediments near Jeddah, where the highest enrichment was found for metals such as Cu,

Cr, Pb, Zn, and Mn.

Here, the study area, including North, Middle, and South Jeddah (Figure 2.1), is highly urbanized with many potential anthropogenic sources, especially the industrial activities of the Industrial City located in the southern part of Jeddah. Jeddah industrial and sewage treatment plants, which may add more sources of contaminants, discharge directly to the Red Sea within the study area (Basaham et al., 2009; Ramadan and Halawani, 2010). Al-Sofyani et al. (2014) reported the sewage discharge to Jeddah's coast at over 100,000 m^3 daily. Therefore, a comprehensive evaluation of heavy metals contamination in sediments of the entire Jeddah coastal region needs to be covered. While prior work exists, a more complete spatial analysis is wanted. The specific aims of this work are to i) investigate the state of heavy metal pollution along the Jeddah's Coast by measuring the total metal concentrations in the sediments; ii) quantify the extent of pollution in sediments using the Geo-accumulation Indices (Igeo), Enrichment factor (Ef) and Contamination factor (Cf); iii) determine the associated risk by using Pollution Load Index (PLI), Potential Ecological Risk Index (PERI), and Potential Toxicity Response Index (RI).

2.3 Materials and Methods

2.3.1 Sample collection and preparation

Eighty surficial nearshore sediment samples were recovered from the North, Middle and South locations of the Jeddah coast, during the summer of 2017 (Figure 2.1). The sample location was recorded using GPS and the study area occurs between ($21^0$52'56"N $38^0$58'12"E) and ($21^0$14'0" N $39^0$8'38"E). The North location is located in the northern region of Jeddah near resort areas. The Middle location is the downtown

area and near the main fish market, the main desalination plant, and the highest water fountain in the world. The South location is located south of Jeddah near the harbor, Jeddah's industrial city, a mangrove area, and a petrol refinery. These locations were chosen to cover the study area. The Northern and Southern samples were collected at ten stations, where at each station, three sample points were collected in transects perpendicular to the shoreline with a distance between points of approximately 50 m. Only one sediment sample was collected of the Middle location for 20 stations. All samples were collected by stainless steel soil scoop, stored in polyethylene clear flat zipper bags, and held in at 4ºC until they were transported to the laboratory.

At the laboratory, the sediment samples were placed in an oven overnight at 105ºC. The dried sediment samples were split to carry out the analysis of soil organic matter, carbonate, sediment grain size, and heavy metal analysis.

2.3.2 Analytical procedure and analysis

The percentages of soil organic matter (SOM) and carbonate in sediment samples were measured by the sequential loss on ignition (LOI) technique following Heiri et al. (2001). Approximately 1 g of the dried sediment at 105 °C was placed in a pre-weighed ceramic crucible (D1). Samples were placed in a Thermo Scientific muffle furnace and heated to 550 °C for two hours to remove the soil organic matter (SOM). Once crucibles were cooled, they were to obtain the loss on ignition at 550°C (D2). Samples were placed again in the furnace and heated to 950°C for two hours to calculate the carbonate. Crucibles were allowed to cool, and samples were weighed over (D3). Loss on ignition for the determination of soil organic matter (SOM) and soil carbonate was calculated using the following equations:

$$\mathrm{LOI_{SOM}} = \frac{(D1-D2)}{D1} \times 100 \quad (2.1)$$

$$\mathrm{LOI_{Carb}} = \frac{(D2-D3)}{D1} \times 100 \quad (2.2)$$

$$\text{Carbonate \%} = \mathrm{LOI_{Carb}} \times 1.36 \quad (2.3)$$

Where LOI_{SOM} is the loss on ignition of soil organic matter and LOI_{Carb} is the loss on ignition for the carbon dioxide lost, both as weight percentages. The Carbonate % (equation 2.3) is then calculated by multiplying the LOI_{Carb} by 1.36, the ratio between the molecular weights of CO_3 (60.01g/mol) and CO_2 (44.01 g/mol) (Heiri et al.,2001). D1 is the sediment dry weigh at 105 °C in gram, D2 is the sediment dry weight after heating at 550°C in gram, and D3 is the sediment dry weight after heating at 950°C in gram.

For sediment grain size, samples were sieved individually in an 8 inches stainless steel set of U.S.A Standard Testing Sieves, E-11 Specification, produced by VWR International. The fractions were No. 4 (4.25 mm) No. 10 (2.0 mm), No. 20 (0.850 mm), No. 40 (0.425 mm), No. 60 (0.250 mm), No. 200 (0.075 mm), and the residual fraction (< 0.075 mm). The sediment types were identified following Kroetsch and Wang (2008).

For the heavy metal analysis, the dried sediment was ground into a powder using a mortar and pestle and sieved through a 0.075 mm sieve. Heavy metal concentrations of the sediment samples were determined according to a modified US EPA Method 3050B (USEPA 1996). Approximately 0.20g of the powdered sediment sample was used as explained by Badr et al. (2009). Samples were placed in 50 mL tubes, and 5 mL 5% HNO_3 was added to remove carbonate. Then, 20 mL of 70% HNO_3 was added and they were digested at 85ºC on a hot block until dryness. Samples were

resuspended in 10 mL of 5% HNO_3 after dryness.

The concentrations of heavy metals of interest (Cr, Mn, Ni, Cu, Zn ,and Pb) in the digested sediment samples were measured by a Thermo Scientific X-Series 2 Inductively Coupled Plasma- Mass Spectrometer (ICP-MS). In order to calculate the enrichment factor, rubidium (Rb) was analyzed as a normalizing element in this study. Samples were run in collision cell technology with kinetic energy discrimination (CCT-KED) mode. Multi-element standards (CLMS-2A, from SPEX Certi Prep, Metuchen, NJ, USA) were prepared with a range from 0.1 to75 ppb to establish calibration curves. To ensure quality control, replicate of blanks (5% HNO_3) were analyzed every 12 samples. The uncorrected values as counts were converted to concentration (mg/kg) by establishing calibration curves with r^2 values of 0.999 or higher. For quality assurance, the ICP- MS tubes used in the analysis were cleaned in an acid bath (5% HCL) for 24 hours and washed with distilled deionized water before use. During the sediment digestion procedure, all dilutions were made using 5% HNO_3 prepared from trace metal grade concentrated 70% HNO_3 and 18.2 mΩ nanopure water.

2.3.3 Assessing pollution impact

A number of factors were applied in the study to evaluate the contamination risk assessment, metal contamination levels, and potential toxicity in the study area, which follow.

2.3.3.1 Contamination Factor (C_f)

A contamination factor is one of the easiest and the most common methods for determining contamination of the heavy metals by expressing the ratios among the metal concentration in the sample of the area being studied and the concentration of the

same metal in a background value. The C_f values where calculated using the equation proposed by Hakanson (1980):

$$C_f^i = C_s^i / C_b^i \quad (2.4)$$

where C_f^i is the contamination factor for a specific metal, C_s^i is the concentration of the specific metal in a sediment sample and C_b^i is value of the given heavy metal in the natural background (Turekian and Wedepohl 1961) (Appendix A1). Badr et al (2009), and Alharbi et al. (2018) used this same background for this region. Using this metric, if the $C_f < 1$ means to the low contamination, $1 \leq C_f < 3$ means to the moderate contamination, $3 \leq C_f < 6$ means to the considerable contamination, and $C_f \geq 6$ means to the very high contamination (Hakanson, 1980).

2.3.3.2 Enrichment factor (Ef)

Different authors have measured the Ef values by using several normalizing elements, such as aluminum, rubidium, iron, lithium and scandium (Grant and Middleton 1990; Amin et al., 2009; Dou et al., 2013; Chakraborty et al., 2014; El Nemr et al., 2016; Alyazichi et al., 2016 ;Al-Mur et al., 2017; Badawy et al., 2018; Alharbi et al., 2019). However, in this study, the Ef was calculated using rubidium as the reference element. The Ef is analyzed using the following equation:

$$E_f^i = (C_i/C_{Rb})_S / (C_i/C_{Rb})_B \quad (2.5)$$

where E_f^i is an enrichment factor for the metal of interest, $(C_i/C_{Rb})_S$ is the metal concentration (mg/kg) in relation to rubidium Rb in the studied sediment samples (Table 2.2), and $(C_i/C_{Rb})_B$ is the average background shale value from Turekian and Wedepohl, 1961. Enrichment factors values and associated sediment quality are as

proposed by Amin et al. (2009) showed in Table 2.3.

2.3.3.3 Pollution Load Index (PLI)

Pollution Load Index is utilized to contrast the total concentration of elements at different sampling locations. The PLI was calculated according to the equation used via Tomlinson et al. (1980).

$$PLI = \left(C_f^1 \times C_f^2 \times \ldots \times C_f^n\right)^{\frac{1}{n}} \quad (2.6)$$

Where C_f, is the contamination factor and n is the number of metals.

2.3.3.4 Potential Ecological Risk Index (PERI)

PERI is one of the most common methods for determining the environmental sensitivity to heavy metal pollution in a specific location. It combines total concentrations and toxicities to yield a weighted metric per metal. In the current study, the PERI equation of Hakanson (1980) was used as follows:

$$PERI = C_f^i * T_f^i \quad (2.7)$$

Where PERI is Potential Ecological Risk, C_f^i is the contamination factor, and T_f^i is the coefficient for the toxicity of a single metal. The corresponding T_f^i listed values are Zn=Mn= 1, Cr= 2 and Cu= Ni = Pb =5 (Hakanson 1980). The categories of Potential Ecological Risk Index (PERI) are displayed in table (2.4).

2.3.3.5 Potential Toxicity Response index (RI)

The RI is the total of the all of the metals of interest that were used in the (PERI). The RI value was calculated as follows (Hakanson,1980):

$$RI = \sum PERI \quad (2.8)$$

where RI is the summation of the PERI values for every metal of interest. Table (2.4) provides the categories of Risk Index (RI).

2.3.3.6 The Geo-accumulation Index (Igeo)

The Igeo was used to define and categorize the pollution status of sediments by comparing the sediment metal concentrations with the natural background concentrations of the same metal. Müller (1979) described the calculation of the (Igeo) with the following equation:

$$\mathrm{Igeo} = \ln(C_n/1.5B_n) \quad (2.9)$$

C_n is the measured concentration of elements in the sediments sample, B_n is the geochemical background value of the element (Turekian and Wedepohl 1961), and 1.5 is the correction factor for lithogenic effects. Müller (1981) proposed seven descriptive classes of Igeo displayed in Table 2.5.

2.4 Results

2.4.1 Distribution of soil organic matter, soil carbonate, and grain size

The averages of the soil organic matter, carbonate, and sediment grain size per location are illustrated in Table 2.6. The percentage of SOM ranged in the study area from 3.24% to 5.90%, 2.31% to 14.81%, and 2.86% to 12.58% for the North, Middle, and South, respectively. On the other hand, carbonate in the sediment samples ranged from 24.46% to 57.11%, 10.89% to 55.37%, and 43.01% to 55.71% for the North, Middle, and South, respectively (Table 2.6). The geographical setting, the sedimentary condition, and various level of the anthropogenic sources are the most recognized factors affecting marine sediments and their grain size (Magno et al., 2018). The distribution of sand and silt-clay in the in the studied locations were 82.12%–99.90% for sand and 0.10%–17.88% for silt-clay for the North location, 94.16%–99.46% for sand and 0.54%–5.84% for silt-clay for the Middle location, and 89.13%–99.93% for

sand and 0.07%– 10.87% for silt clay for the South location (Table 2.6). The study area stations show two dominant grain size distributions including fine sand in the Middle location, and a mix of medium sand and fine sand in the North and South locations.

2.4.2 Heavy metal concentrations

The average metal concentrations (mg/kg) in the surface sediment of the study area were Pb (77.34) > Mn (36.52) > Zn (18.02) > Cr (9.56) > Cu (9.18) > Ni (3.68) (Table 2.7). These results show the average Pb concentration measured in the sediments of the Jeddah coastal region (77.34 mg/kg) is consistent with prior studies near Jeddah (Table 2.7) falling between those found by Pan et al. (2011) (69.38 mg/kg) and those of Badr et al., (2009) (98.77 mg/kg). The Pb concentration in the present study is higher than that in Yanbu (an industrial coastal city north of Jeddah,) and Jizan sediments (an urban coastal city located south of Jeddah) 23.33 and 3.86 mg/kg, respectively (Alharbi et al. 2018; Mortuza and Al-Misned, 2017). Moreover, Pb concentrations found along the Jeddah coastline were higher than those of the northern Red Sea near Egypt (4.68 mg/kg) (Badawy et al., 2018).

The average Mn concentration in the present study was 36.52 mg/kg, which is lower than those from prior work near Jeddah (205.06 mg/kg) and near Shuaiba (an urban coastal city located south of Jeddah) (61.33 mg/kg) (Badr et al., 2009; Abohassan, 2013). In addition, it was lower than those of the Red Sea samples that were reviewed via Ruiz-Compean et al. (2017) (213.78 mg/kg) and by Badawy et al. (2018) (291.94 mg/kg) representing the east and west sides of the basin respectively. The Zn concentration from the present study (18.02 mg/kg) was lower than those from the Jizan sediments (24.74 mg/kg) (Mortuza and Al-Misned 2017) and the northern

Red Sea (38.77 mg/kg) (Karuppasamy et al., 2019). Further, it was greater than those from Shuaiba (2.76 mg/kg) (Abohassan, 2013).

The copper concentration showed an average of 9.18 mg/kg, which is minor than those stated for Jeddah by Pan, et al., (2011) and Badr, et al.(2009) (82.99 and 23.77 mg/kg, respectively), for Yanbu by Alharbi, et al. (2018) (73 mg/kg), for Jizan by Mortuza and Al-Misned (2017) (16.39 mg/kg), for the northern Red Sea by Karuppasamy et al. (2019) (15.51 mg/kg), and for the eastern side of the Red Sea by Ruiz-Compean, et al. (2017) (9.33 mg/kg) (Table 2.7). However, copper concentrations in the current study were greater than those reported previously for sites near Shuaiba and Egypt (4.13 and 7.70 mg/kg) (Abohassan 2013; Badawy et al., 2018).

The average chromium concentration in the present study (9.56 mg/kg) was higher than the average concentration reported by Abohassan (2013) in Shuaiba (8.75 mg/kg) and Mortuza & Al- Misned (2017) in Jizan (5.64 mg/kg). However, it was minor than the value that was recorded in Jeddah (22.81 mg/kg) by Badr, et al. (2009), in the eastern side of the Red Sea (24.79 mg/kg) by Ruiz-Compean, et al. (2017), in the northern Red Sea (14.6 mg/kg) by Karuppasamy, et al (2019) and in the Red Sea Egyptian side (53.84 mg/kg) by Badawy, et al. (2018).

The average concentration of nickel in the sediments of Jeddah from this study (3.68 mg/kg) was lower than that reported in Jeddah (85.50 mg/kg) by Badr, et al. (2009), in Jizan (14.32 mg/kg) by Mortuza and Al-Misned (2017), in the northern of Red Sea (15.92 mg/kg) by Karuppasamy et al (2019), and from the eastern side of the Red Sea (14.24 mg/kg) by Ruiz- Compean, et al. (2017).

2.4.3 Risk assessment

Risk assessments and degree of pollution were calculated using various

established methods. The Contamination factor C_f, Enrichment factor E_f, Pollution Load Index PLI, Potential Ecological Risk Index PERI, Potential Toxicity Response Index (RI), and the Geo-accumulation Index (Igeo) are all presented per location to identify areas of concern within the study area.

Zhuang & Gao (2014) interpreted any E_f values for a metal > 1.5 to be anthropogenic in source. In general, the order of enrichment of the surficial sediments of the Jeddah coast was Pb (extremely severe enrichment)> Mn > Cu > Zn > Cr (severe enrichment) > Ni (moderate enrichment). The E_f of Pb, Cu, and Cr were the highest in the southern stations (2397.99, 46.60, 42.79, respectively), while the E_f of Pb, Zn and Cr were also high in the North location (71.50, 36.73, and 26.80) (Table 2.8). The Igeo was used to assess the concentration of metals compared to average continental crust concentrations as reference values. The average Igeo values are summarized in Table 2.8. The Igeo values in the studied sediments of all locations were low and categorized as not polluted, except the Igeo values of Pb in the Middle and Southern locations. In the Middle, 30% of the stations were categorized as unpolluted to moderately polluted and 10% of the stations were categorized as moderately polluted. Similarly, 20% of the South stations were classified as unpolluted to moderately polluted and 20% as moderately polluted.

The C_f values of the recorded heavy metals showed that sediments of the Jeddah

coast have, in general, a low degree of contamination. Pb is an exception which showed a considerable contamination (4.02) and very high contamination (7.39) in the Middle and South locations, respectively (Table 2.9). The average PERI values (< 40) showed a low risk for all the studied stations of the Jeddah coast (Table 2.9). However, the PERI values of Pb demonstrate that some stations of the Middle location of the Jeddah coast, such as stations M18 and M14, should be given special attention due to the existence of high PERI values (93.17 and 71.71, respectively) that categorize the Middle location as under moderate risk. The same was recorded for the S1, S2, S3 and S7 of Southern location where the PERI values were 144.62, 63.16, 76.68 and 46.65, respectively, suggesting an occurrence of considerable risk.

The Potential Toxicity Response index (RI) showed a value of < 150 for all the studied stations, suggesting a low risk for the study area. The PLI of most of the studied stations was < 1.0 and the average PLI values were 0.06, 0.30, and 0.11 for North, Middle and South locations of the Jeddah coast, respectively (Table 2.10). All of these values are well below reported PLI values of contaminated sediments from the literature (e.g. Amin, et al., 2009).

2.4.4Statistical analysis

The statistical and correlation examination in this study were performed using SAS 9.4. As shown in Table 2.11, there are strong and statistically significant positive correlations betweenCr and Mn (r = 0.73), Ni (r = 0.81), Cu (r = 0.51), and Zn (r =0.67), where, Mn is shown to have strong positive correlations with Ni (r=0.96), Cu

(r=0.69), Zn (r=0.80). Also, Ni is shown a correlation with Cu, and Zn (r=0.69, 0.80), and Cu shown moderate correlation with Zn (r=0.65). On the other hand, Pb is poorly correlated with other metals. The results suggest that Cr, Mn, Ni Cu, and Zn are likely to have come from the same source, while Pb is likely derived from another contaminant source. Moreover, as determined in Table 2.11, PLI is strongly correlated with Ni, Mn, Cr, Zn, and Cu ($r > 0.7$), however it is weakly correlated with Pb (r=0.46).

2.5 Discussion

The Northern location of the Jeddah coast showed higher average concentrations of Mn and Zn (31.08 and 11.02 mg/kg, respectively) especially for samples N32, N72, N101 (Figure 2.2). These points are near resorts, a boat station, workshops for general maintenance and body shops for marine transportation such as boats and jet skis. As Additionally, wastewater discharge and boat painting/repair waste around these stations and may cause the observed elevations in sediment metals concentrations (Bryan & Langston 1992; Usman et al. 2013; Ghandour et al. 2014; Karuppasamy et al 2019). Moreover, most of the resorts and beach houses in the North location are not connected to the municipal drainage network and, therefore, discharge wastewater directly to the sea. Some authors (Abu-Zied et al., 2013; Prego et al., 1999) report that discharge of wastewater may lead to rise in the concentration of Mn in surface sediments. Zinc in the Northern stations may be due to the usage of pesticides as well as antifouling paints where Zn-containing compounds are mainly used as detergents and dispersant improvers for lubricating oil and antioxidants (Ungureanu et al., 2017; Youssef, 2015). Most of the resorts use pesticides which have been shown elsewhere to yield elevated Zn levels (Kronvang et al., 2003; Ghrefat & Yusuf 2006).

Also, batteries and wear of automobile tires could be substantial anthropogenic source of zinc near marine environments (Badr et al., 2009; Youssef, 2015). Indeed, most of the marinas use old tire products as anti-scratch material between the body of ships and the base of the marina.

Most of the metals were higher in the Middle locations of the Jeddah coast (Figure 2.3) than the other locations especially Pb, Mn, Zn and Cu (80.44, 76.94, 41.04, 21.92 mg/kg, respectively) (Table 2.7). According to Abu-Zied and Orif (2019), the marine environment in the vicinity of the northern stations of the Middle location (Stations M1to M10) is used as a dumping zone for sewage and industrial wastewaters via sewage outflow pipe. This is supported by the high SOM found in the Middle location (Table 2.6) and has been cited as a possible consequence of the direct outflow of domestic and industrial wastes in this area (Abu-Zied & Orif 2019). This elevation in organic matter could act as a significant carrier phase for heavy metals and has been repeatedly shown to play a key role in the bioavailability, reactivity, and mobility of metals in sediments (Filgueiras et al., 2004). In the present study, the prominent high concentration of Zn in the Middle location (Stations M6-M14) (Figure 2.3) could be due to the outflow of organic matter from sewage sludge, industrial discharge, and antifouling paints (Alharbi et al 2018; Abu-Zied et al., 2013).

The Middle location is near the biggest desalination plant on the Jeddah Coast. This plant is a major consumer of gasoline for onsite power production. The use of gasoline may be a possible source for the Pb in sediment especially at stations M14, M15, M16, and M18 (Usman et al., 2013) (Figure 2.3). Elevated Mn concentrations recorded at stations M17- M20 occur near the main seaport of Jeddah; here, body shops

for small fishing ships operate and residual ship wastes and antifouling paints are prevalent. According to Abu-Zied, et al. (2013), domestic sewage from the municipal drainage network of Jeddah City could be one of the reasons of rising Mn concentrations. The high Cu concentrations in the sediments of the Middle stations may be attributed to the availability of high amounts of organic matter in the sediments. (Bryan and Langston 1992). Also, a public park that was renovated and expanded between station M6 and station M15 may add a new source of organic matter to the location (Figure 2.3).

The contamination factor Cf analysis showed that about 40% of the Middle stations were classified as being contaminated and very highly contaminated with Pb (Table 2.9). Multiple sources of pollution at the Middle location of the Jeddah Coast—such as the desalination plant, industrial and sewage wastewater outflow pipes, the seaport, the fish market, and extensive shipping activities –explain the north to south trends of PLI and RI values (Figure 2.5 ML and MT). There is strong correlation between Pb concentrations and RI ($r = 1.00$); however, the correlation between Pb concentrations and PLI was the weakest of all metals ($r = 0.46$) (Table 2.11). These trends taken together suggest that while Pb is not controlling the total metal contamination it is responsible for the location's toxicity risk.

Low concentrations of metals are commonly connected with high carbonate percentage (Pan et al., 2011). The average carbonate was the highest in the South location (Table 2.6), and the average concentrations of the measured heavy metals were the lowest except for the Pb. Pb was the most elevated heavy metal in the South location up to 147.91 mg/kg (Table 2.7). Most of the industrial activities of Jeddah City are

located in the south yielding a potential source for pollutants for the studied southern stations. Industrial contamination, therefore, is expected in the South location near the Industrial City. This complex is located near the northern end of the South location. As an example, a major petrol refinery is located near the northern stations of the South location. As expected, the most affected stations of the South location of the Jeddah coast are located in the northern part of this location (Figure 2.4). Additionally, station 7 is one of the most impacted stations by Pb due possibly to its proximity to the boat station and small local fish market (Figure 2.6).

The concentration of Pb is known to increase offshore in the region (Youssef, 2015). The current study shows a similar trend as seen in Table 2.12. The concentrations of Cr, Mn, Ni, Cu, and Zn were high for all the nearshore stations, however Pb concentration were higher for the offshore, deepest stations in the northern stations as well as in the central stations of transects of the southern part of Jeddah Coast. About 36% of the South location stations were classified as very high contaminated with Pb via contamination factor calculations. Also, Pb was the most enriched metal in approximately 88% of these stations, which may indicate that the source of Pb is anthropogenic (Badr et al., 2009). Figure 2.5 SL shows that the PLI values for the stations S1 – S4 were low; however, RI values (ST) were higher which indicates the high toxicity at these stations. The strong correlation of Pb with RI in (r= 1.00) again shows Pb is governing the toxicity exposure for the location (Table 2.11).

2.6 Conclusion

Eighty stations were chosen for collection of surficial marine sediments from the North, Middle and South locations of the nearshore Jeddah Coast. The

concentrations of six heavy metals (Cr, Mn, Ni, Cu, Zn, and Pb) in the collected sediments were determined. The average concentrations of these metals in surface sediments showed that Pb > Mn > Zn > Cr > Cu > Ni. The Enrichment factors clearly show Pb was the most abundant heavy metal relative to background values in the study area. The Igeo values of the Pb in the Middle stations showed that 10% of the stations were categorized as moderately polluted, whereas 20% of the South location were classified as moderately polluted. This is further supported by the contamination factor values as seen in Table 2.9. Furthermore, Pb was the most enriched metal in about 88% of the South stations, withal suggesting an anthropogenic source of Pb. The RI values in the South stations, especially the northern stations within the South location, indicate high Pb toxicity exposure in the area.

The study results suggest the potential sources of pollutants in the Middle stations of the Jeddah Coast could be anthropogenically released from the desalination plant, the outflow tubes of industrial and municipal wastewaters and waste of ship maintenance. The South location of the Jeddah Coast, however, is interpreted to be polluted by the industrial activity from the Industrial City. This study recommends that appropriate management strategies should be applied for the North location of the Jeddah Coast to control potential pollution sources and prevent permanent hazards to marine ecology currently documented elsewhere. This study indicates that the Middle location is impacted by various sources due to the highest activity in the region. Stringent management practices are suggested to limit further metals contamination to the area. The Southern location of the Jeddah coast is the most toxic location; it, therefore, needs more effort and stronger regulations to treat and remediate the marine

environment. The area needs more research towards exact sourcing of contaminants, specifically Pb. A further study of metals speciation in marine sediments of the Jeddah Coast should be carried out to yield more information about the bioavailability and mechanism of deposition of these metals and their sourcing. Also, tracer studies, such as isotopic studies paired with Pb speciation, could be used to investigate the sources of the lead in sediments, water, and even in airborne aerosols near to the shoreline.

Table 2. 1 The natural background values for heavy metals of interest in mg/kg (Turekian and Wedepohl 1961).

Metals	Natural Background Values
Cr	90
Mn	850
Ni	68
Cu	45
Zn	95
Pb	20

.

Table 2. 2 The concentration of rubidium (Rb)(mg/kg) in the study area.

North	Rb	South	Rb	Middle	Rb
N11	0.259	S11	0.373	M1	1.132
N12	0.241	S12	0.428	M2	2.716
N13	0.155	S13	0.438	M3	2.640
N21	0.357	S21	1.503	M4	2.914
N22	0.149	S22	0.609	M5	6.222
N23	0.316	S23	0.451	M6	4.709
N31	1.125	S31	0.859	M7	1.694
N32	2.331	S32	0.478	M8	2.031
N33	0.202	S33	0.315	M9	2.601
N41	0.813	S41	0.846	M10	1.362
N42	0.390	S42	0.402	M11	0.747
N43	0.342	S43	0.172	M12	1.817
N51	1.248	S51	0.214	M13	3.657
N52	1.063	S52	0.147	M14	4.279
N53	0.564	S53	0.115	M15	4.524
N61	0.784	S61	0.369	M16	1.665
N62	0.446	S62	0.203	M17	1.588
N63	0.396	S63	0.164	M18	2.757
N71	0.526	S71	0.370	M19	1.644
N72	0.245	S72	0.241	M20	2.407
N73	0.228	S73	0.167		
N81	0.748	S81	0.404		
N82	0.696	S82	0.110		
N83	0.819	S83	0.202		
N91	2.299	S91	0.578		
N92	0.826	S92	0.416		
N93	0.900	S93	0.302		
N101	0.377	S101	0.394		
N102	0.733	S102	0.353		
N103	0.640	S103	0.579		

Table 2. 3 Enrichment Factor (Ef) and sediment quality. (Amin et al.,2009).

Ef	Sediment quality
< 1	No enrichment
< 3	Minor enrichment
3–5	Moderate enrichment
5–10	Moderately severe enrichment
10–25	Severe enrichment
25–50	Extremely severe enrichment

Table 2. 4 The categories of Potential Ecological Risk (PERI) and Potential Toxicity Response Index (RI) (Hakanson 1980).

Potential Ecological Risk Index		Potential toxicity response index	
Value	Category	Value	Category
PERI< 40	Low	RI ≤ 150	Low
40 ≤ PERI < 80	Moderate	150 ≤ RI < 300	Moderate
80 ≤ PERI < 160	Considerable	300 ≤ RI < 600	Considerable
160 ≤ PERI < 320	High	600 ≤ RI	Very high
PERI ≥ 320	Very high		

Table 2. 5 Classification scheme for the Geo-accumulation index (Igeo) by Müller, 1981.

I geo	Igeo class	Sediment Pollution Status
≤ 0	0	Unpolluted
0–1	1	Unpolluted to moderately polluted
1–2	2	Moderately polluted
2–3	3	Moderately to highly polluted
3–4	4	Highly polluted
>5	5	Highly to very highly polluted

Table 2. 6 The sediment grain sizes (%), soil organic matter (SOM) (%), and soil carbonate (%) of the studied stations along Jeddah shoreline.

		North	Middle	South
Sand	Average	95.90	98.07	97.46
	Max	99.90	99.46	99.93
	Min	82.12	94.16	89.13
Silt - Clay	Average	4.10	1.93	2.54
	Max	17.88	5.84	10.87
	Min	0.10	0.54	0.07
SOM	Average	4.58	6.68	4.73
	Max	5.90	14.81	12.58
	Min	3.24	2.31	2.86
Carbonate	Average	51.66	35.05	52.76
	Max	57.11	55.37	55.71
	Min	24.46	10.89	43.01

Table 2. 7 Concentrations, average, and standard deviation of heavy metals in the study area compared to other studies fromthe broader region. All concentrations are expressed in mg/kg. M= Mean. N= North. M= Middle. S=South.

Location	Cr	Mn	Ni	Cu	Zn	Pb	Reference
Red Sea, Jeddah North	8.12 ± 2.04	31.08 ± 19.11	2.74 ± 2.15	2.44 ± 2.23	11.02 ± 17.92	4.72 ± 2.17	This study
Red Sea, Jeddah Middle	12.08 ± 8.46	76.94 ± 51.29	8.14 ± 6.58	21.92 ± 14.18	41.04 ± 30.02	80.44 ± 99.25	
Red Sea, Jeddah South	9.32 ± 5.62	15.01 ± 9.67	1.59 ± 1.57	7.36 ± 14.25	8.73 ± 8.80	147.91 ± 208.91	
Averages	9.56	36.52	3.68	9.18	18.02	77.34	
Red Sea, Jeddah, Saudi Arabia	-	-	-	0.45 - 82.99	5.3 - 179	0.46 - 69.38	Pan et al., (2011)
Red Sea, Jeddah, Saudi Arabia	12.98 - 22.81	33.71 - 205.06	67.78 - 85.50	17.47 - 23.77	52.74 - 76.36	80.30 - 98.77	Badr et al., (2009)
Red Sea, Jeddah, Saudi Arabia	M= 245.96	M=478.45	-	M=251.82	M=623.09	M= 362.75	Al-Mur et al.,(2017)
Red Sea, Shuaiba, Saudi Arabia	8.75	61.33	-	4.13	2.76	0.53	Abohassan (2013)
Red Sea, Yanbu coast, Saudi Arabia	4.8 -201	-	1.37 - 94	1.35 -73	5.88- 241	0.08 - 23	Alharbi et al. (2018)
Red Sea, Jizan, Saudi Arabia	M = 5.64	M = 9.58	M = 14.32	M = 16.39	M = 24.74	M = 3.86	Mortuza and Al-Misned. (2017)
Red Sea, North side, Saudi Arabia	M = 14.6	-	M =15.92	M = 15.51	M = 38.77	-	Karuppasamy et al., (2019)
Red Sea, Saudi Arabia	M = 24.79	M = 213.78	M =14.23	M = 9.33	M = 26.79	M = 5.55	Ruiz-Compean et al., (2017)
Red Sea, Egypt	M = 53.84	M = 291.94	M = 15.37	M = 7.70	M = 27.55	M = 4.68	Badawy et al., (2018)
Average Chemical Composition in sediments	74	680	40	40	65	17	Taylor and McLennan. (2008)

Table 2. 8 The Enrichment factor and the Geo-accumulation Index of the sediment samples from different locations.

Elements	Location	Enrichment Factor normalized by Rb			The Geo-accumulation index		
		Average ± SD	Maximum	Minimum	Average ± SD	Maximum	Minimum
Cr	N	26.8 ± 14.73	66.43	8.21	- 2.48 ± 0.25	-2.39	-3.31
	M	6.97 ± 2.68	11.17	2.64	- 2.64 ± 0.69	-1.42	-3.96
	S	42.79 ± 25.68	103.93	8.78	- 2.87 ± 0.64	-1.89	-4.01
Mn	N	8.95 ± 4.27	20.63	3.78	- 3.91 ± 0.64	-2.78	-5.37
	M	4.60 ± 1.90	9.18	1.54	- 3.06 ± 0.77	-1.94	-4.80
	S	6.76 ± 3.25	17.51	2.53	- 4.63 ± 0.60	-3.41	-5.90
Ni	N	8.27 ± 2.21	14.85	5.12	- 3.91 ± 0.79	-2.34	-5.23
	M	5.72 ± 2.50	10.89	1.12	- 2.88 ± 0.89	-1.45	-5.11
	S	7.23 ± 5.16	28.16	0.57	- 4.66 ± 1.05	-2.84	-7.34
Cu	N	10.71 ± 5.46	30.56	3.66	-3.73 ± 0.97	-1.79	-5.42
	M	24.68 ± 9.32	44.31	10.24	-1.36 ± 0.75	-0.12	-3.10
	S	46.60 ± 75.50	410.99	4.52	-3.21 ± 1.37	0.12	-5.63
Zn	N	36.73 ± 98.70	557.97	3.58	-3.24 ± 1.14	-0.37	-5.34
	M	21.06 ± 9.01	42.69	8.45	-1.55 ± 0.83	-0.11	-3.35
	S	29.76 ± 20.60	71.18	0.64	-3.45± 1.39	-1.32	-7.58
Pb	N	71.50 ± 49.65	238.96	13.10	-1.95 ± 0.44	-0.93	-2.88
	M	243.99 ± 284.44	946.31	10.18	0.04 ± 1.57	2.52	-2.87
	S	2397.99 ± 3357.43	14458.22	31.16	0.14 ± 1.97	3.38	-3.04

N= North. M= Middle. S=South.

Table 2. 9 Contamination factor and the Potential Ecological Risk Index for metals of interest from different locations in the Jeddah region.

Elements	Location	Contamination Factor			Potential Ecological Risk Index		
		Average ± SD	Maximum	Minimum	Average ± SD	Maximum	Minimum
Cr	N	0.09 ± 0.02	0.138	0.055	0.180 ± 0.05	0.28	0.11
	M	0.13 ± 0.09	0.361	0.029	0.27 ± 0.19	0.72	0.06
	S	0.10 ± 0.06	0.226	0.027	0.21 ± 0.12	0.45	0.05
Mn	N	0.04 ± 0.02	0.090	0.007	0.04 ± 0.02	0.09	0.007
	M	0.09± 0.06	0.220	0.010	0.09 ± 0.060	0.22	0.01
	S	0.02 ± 0.01	0.050	0.004	0.018 ± 0.011	0.05	0.004
Ni	N	0.04 ± 0.03	0.145	0.008	0.20 ± 0.16	0.72	0.04
	M	0.11 ± 0.10	0.352	0.009	0.59 ± 0.48	1.76	0.05
	S	0.02 ± 0.02	0.088	0.001	0.11 ± 0.11	0.44	0.01
Cu	N	0.054 ± 0.05	0.250	0.007	0.27 ± 0.25	1.25	0.03
	M	0.48 ± 0.32	1.326	0.068	2.43 ± 1.58	6.63	0.34
	S	0.16 ± 0.31	1.700	0.005	0.82 ± 1.58	8.49	0.03
Zn	N	0.12 ± 0.19	1.033	0.007	0.12 ± 0.19	1.03	0.007
	M	0.43 ± 0.32	1.338	0.053	0.43 ± 0.32	1.34	0.05
	S	0.092 ± 0.093	0.401	0.001	0.09 ± 0.093	0.40	0.001
Pb	N	0.23 ± 0.11	0.592	0.084	1.180 ± 0.54	2.96	0.42
	M	4.02 ± 4.96	18.636	0.085	20.11 ± 24.81	93.18	0.42
	S	7.395 ± 10 45	44.157	0.072	36.97 ± 52.23	220.78	0.36

N= North. M= Middle. S=South.

Table 2. 10 Pollution Load Index and the Potential Toxicity Response Index for the North, Middle and South locations in the study area.

	Pollution Load Index			Potential Toxicity Response Index		
	Average ± SD	Maximum	Minimum	Average ± SD	Maximum	Minimum
N	0.067 ± 0.04	0.181	0.020	1.98 ± 0.80	3.98	0.71
M	0.30 ± 0.21	0.780	0.030	23.94 ± 25.96	99.38	1.03
S	0.11 ± 0.10	0.340	0.008	38.19 ± 52.72	223.10	0.45

N= North. M= Middle. S=South.

Table 2. 11 Correlation coefficients for heavy metals in marine sediment samples from each location near Jeddah, Pollution Load Index (PLI), Potential Toxicity Response Index (RI), Sand (%), soil organic matter (SOM) (%), and carbonate (%).

All	Cr	Mn	Ni	Cu	Zn	Pb	PLI	RI	Sand	SOM	CO_3
Cr	1										
Mn	0.73**	1									
Ni	0.81**	0.96**	1								
Cu	0.51**	0.69**	0.69**	1							
Zn	0.67**	0.80**	0.80**	0.65**	1						
Pb	0.45**	0.11	0.19	0.23*	0.12	1					
PLI	0.87**	0.88**	0.92**	0.72**	0.78**	0.46**	1				
RI	0.48**	0.15	0.23*	0.28*	0.16	1**	0.50**	1			
Sand	0.08	0.06	0.08	0.07	0.14	0.25*	0.16	0.25*	1		
SOM	0.02	0.14	0.09	0.23*	0.25*	-0.10	0.10	-0.09	-0.05	1	
CO_3	-0.41**	-0.70**	-0.72**	-0.55**	-0.61**	0.04	-0.61**	0.01	-0.06	-0.49**	1

* Significance at the 0.05 level
** Significance at the 0.01 level

Table 2. 12 The average concentrations (mg/kg) of heavy metals in the North and South locations with different distances from shoreline.

	Cr	Mn	Ni	Cu	Zn	Pb
	North					
Near	9.33	32.72	3.49	3.25	21.23	5.09
Middle	8.08	32.46	2.89	2.32	5.8	3.93
Far	6.96	28.08	1.85	1.75	6.03	5.14
	South					
Near	10.53	19.18	2.15	13.74	11.39	133.31
Middle	8.5	12.54	1.15	4.38	5.76	206.28
Far	8.93	13.3	1.3	3.23	6.42	104.13

*Red= High concentration. Yellow= Moderate concentration. Green =Low concentration

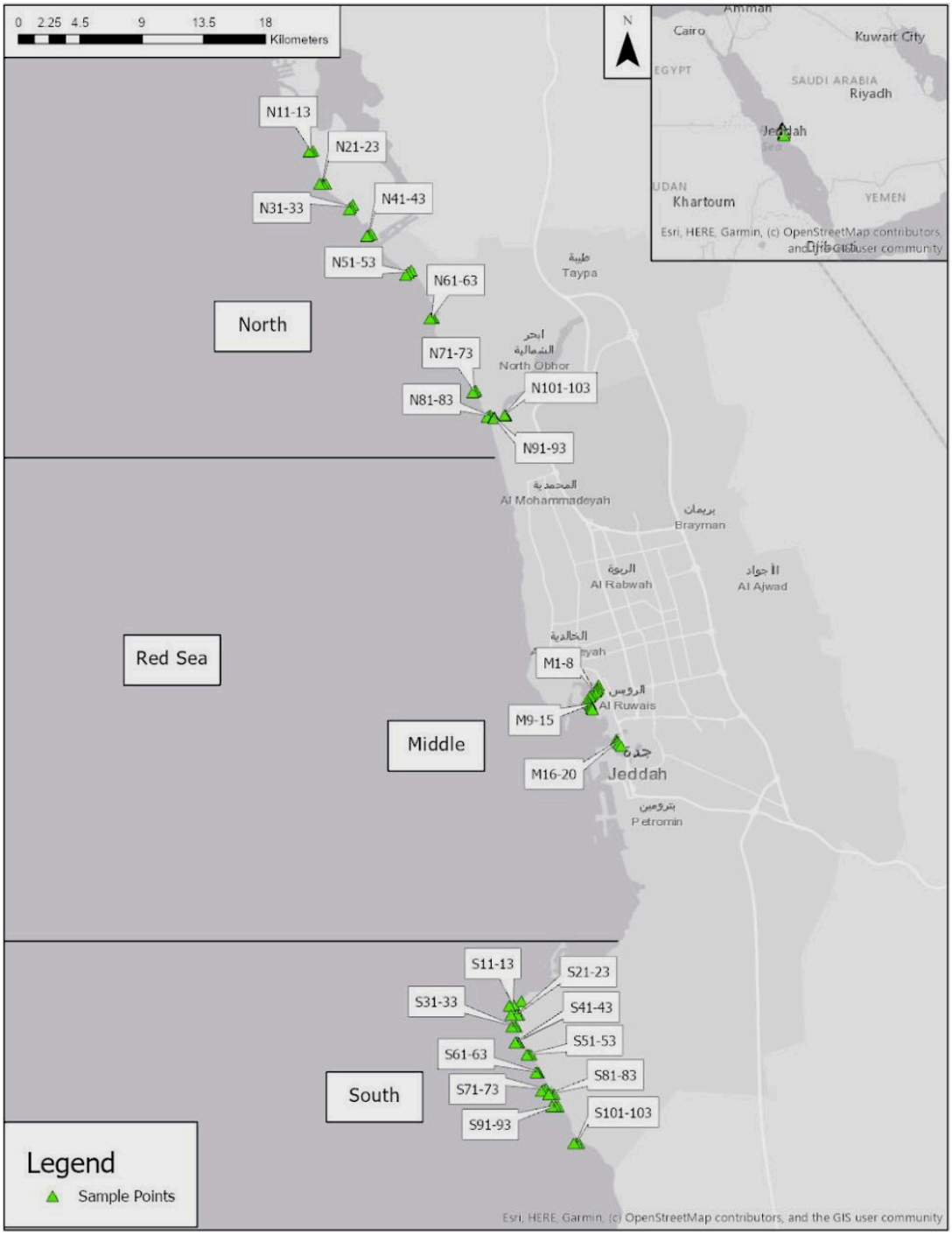

Figure 2. 1 Station locations for sediment sampling.

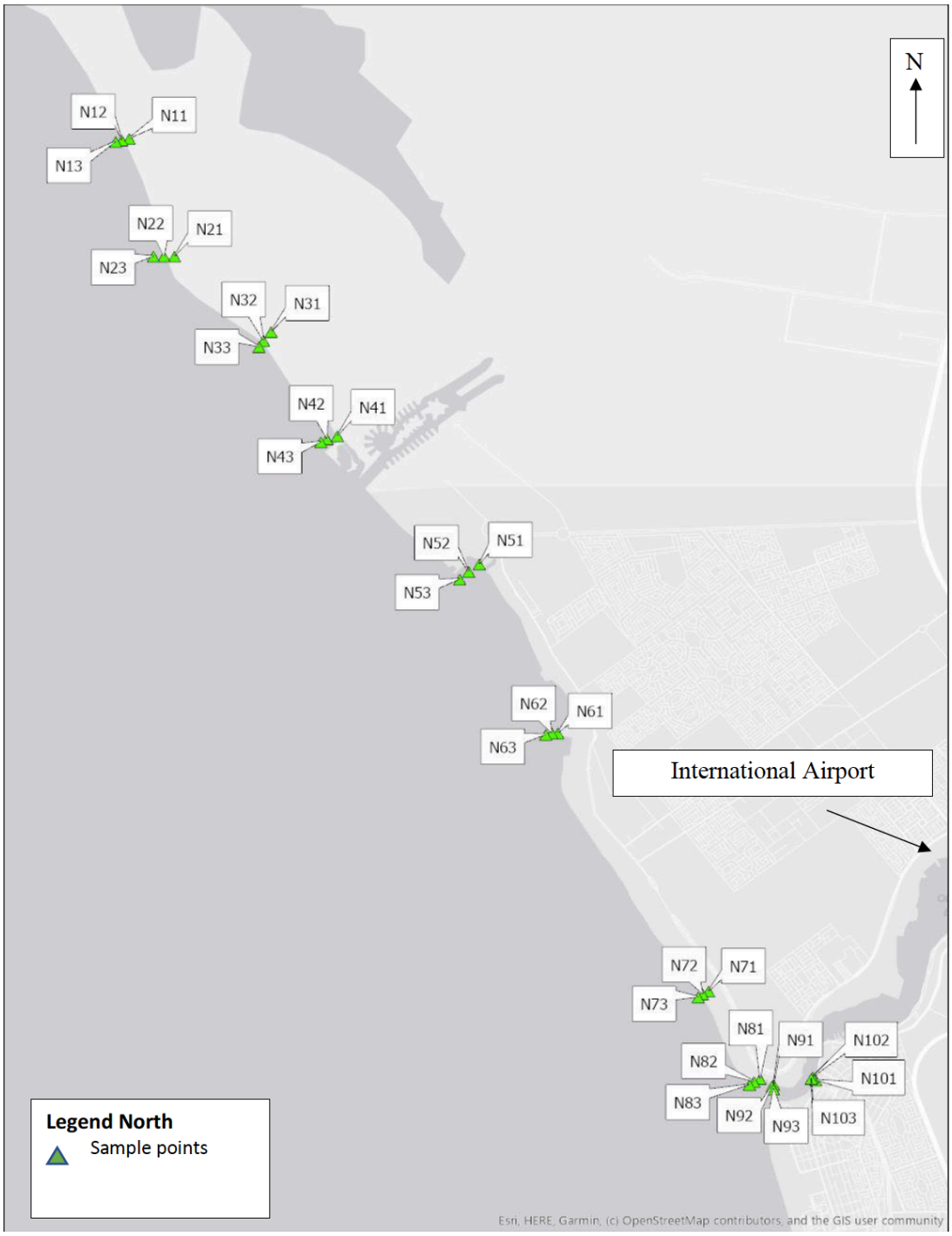

Figure 2. 2 Map showing the stations and point samples in the North location

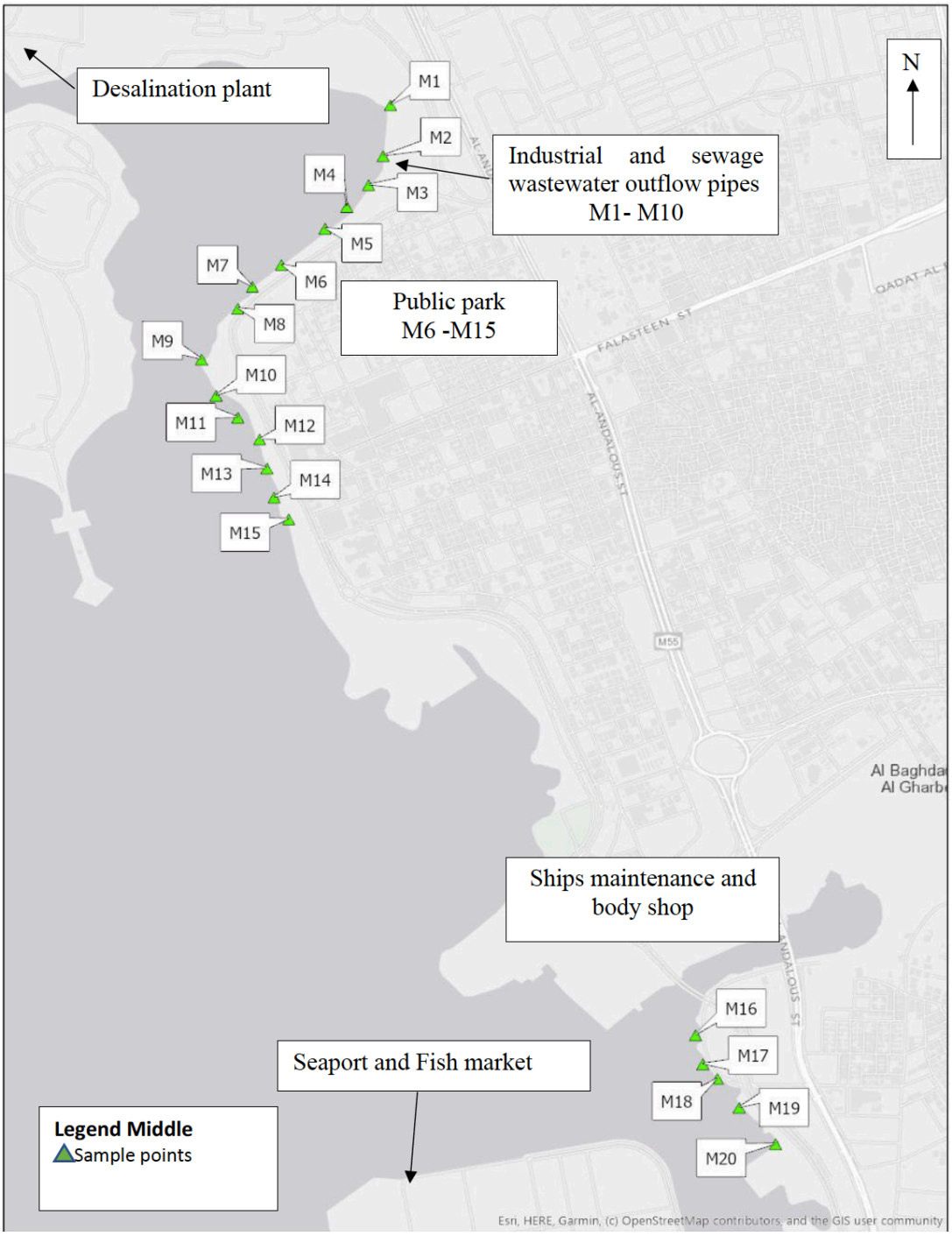

Figure 2. 3 Map showing the stations in the Middle location.

Figure 2. 4 Map shows the stations and point samples in the South location.

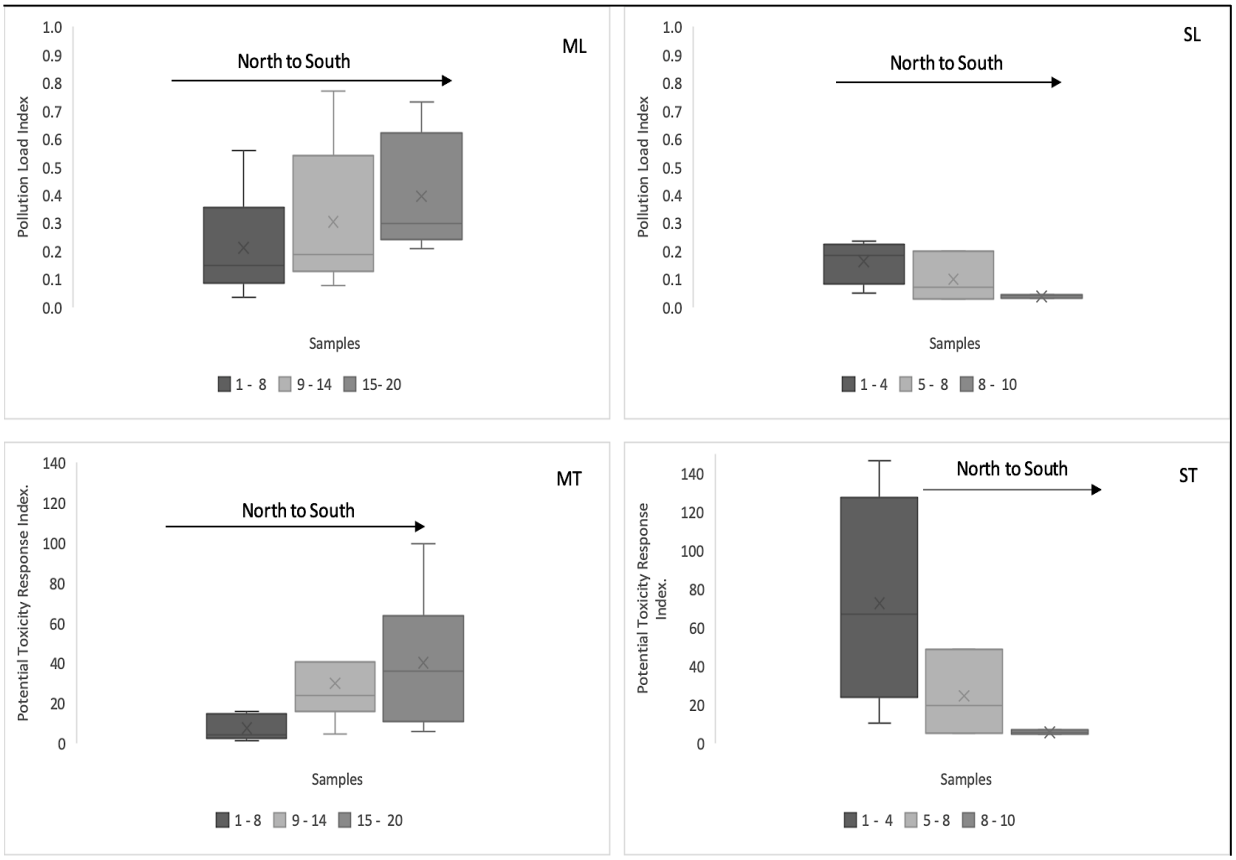

Figure 2. 5 5 Pollution Load Index for Middle (ML) and South (SL) locations, and Potential Toxicity Response Index for Middle (MT) and South locations (ST)

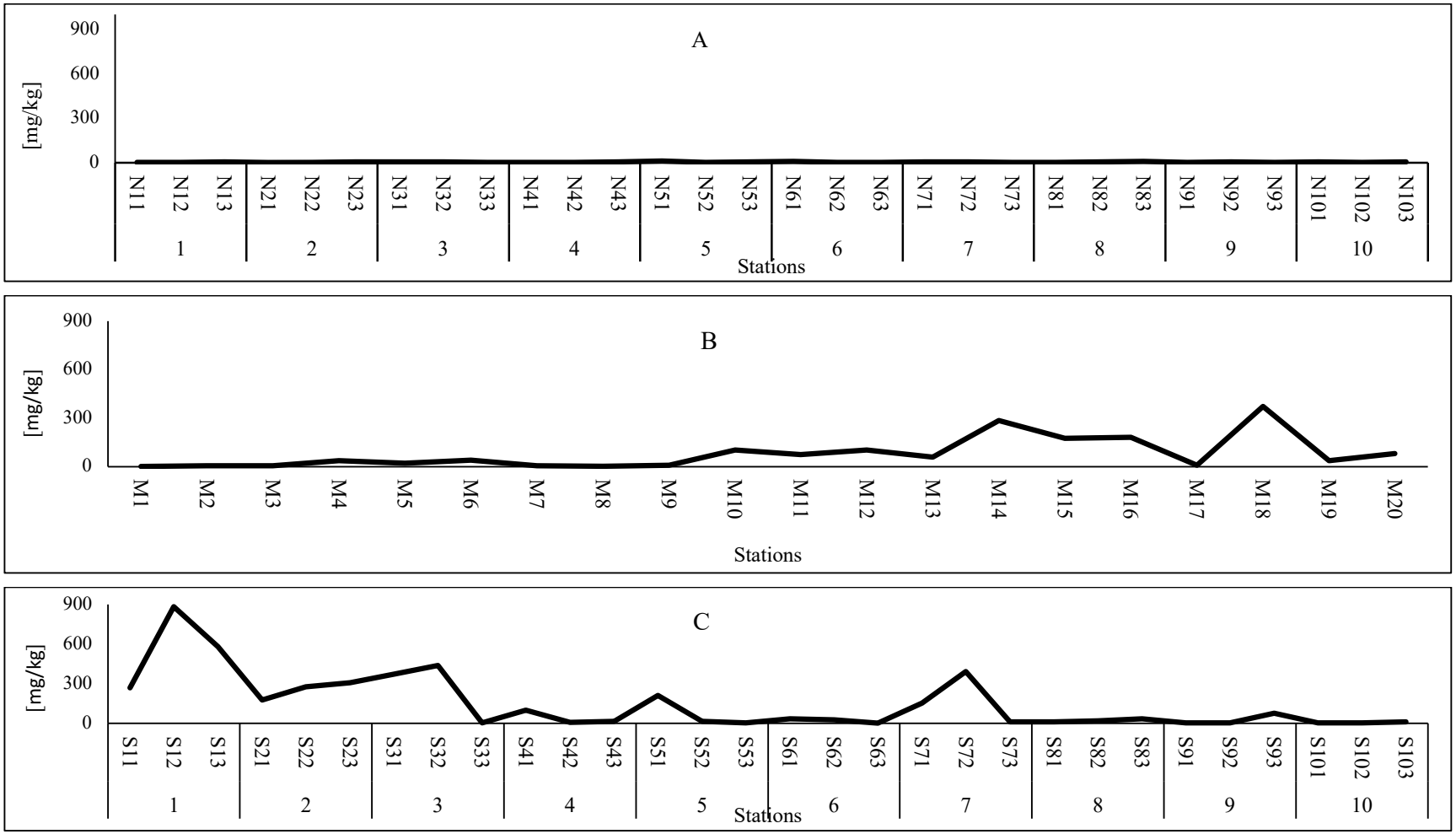

Figure 2. 6 Pb concentrations in the all locations, where (A) North, (B) Middle and (C) for South.

References

Abohassan, R. A. (2013). Heavy metal pollution in Avicennia marina mangrove systems on the Red Sea coast of Saudi Arabia. Journal of King Abdulaziz University: Metrology, Environment and Arid Land Agricultural Sciences, 142(579), 1-38. doi:10.4197/Met.24-1.3

Abu-Zied, R. H., Basaham, A. S., & El Sayed, M. A. (2013). Effect of municipal wastewaters on bottom sediment geochemistry and benthic foraminifera of two Red Sea coastal inlets, Jeddah, Saudi Arabia. *Environmental earth sciences*, *68*(2), 451-469. doi:10.1007/s12665-012-1751-7

Abu-Zied, R. H., & Orif, M. I. (2019). Recent environmental changes of Al-Salam Lagoon as inferred from core sediment geochemistry and benthic foraminifera, Jeddah City, Saudi Arabia. *Environmental Earth Sciences*, *78*(3), 60. doi:10.1007/s12665-019-8057-y

Ahmed, M. K., Baki, M. A., Islam, M. S., Kundu, G. K., Habibullah-Al-Mamun, M., Sarkar,S. K., & Hossain, M. M. (2015). Human health risk assessment of heavy metals in tropical fish and shellfish collected from the river Buriganga, Bangladesh. Environmental science and pollution research, 22(20), 15880-15890. doi:10.1007/s11356-015-4813-z

Al-Mur, B. A., Quicksall, A. N., & Al-Ansari, A. M. (2017). Spatial and temporal distribution of heavy metals in coastal core sediments from the Red Sea, Saudi Arabia. Oceanologia, 59(3), 262-270. doi:10.1016/j.oceano.2017.03.003

Al-Sofyani, A. A., Marimuthu, N., & Wilson, J. J. (2014). A rapid assessment of Scleractinian and non-Scleractinian coral growth forms along the Saudi Arabian coast, Red Sea. Journal of Ocean University of China, 13(2), 243-248.

Alharbi, B. H., Pasha, M. J., & Al-Shamsi, M. A. S. (2019). Influence of Different Urban Structures on Metal Contamination in Two Metropolitan Cities. Scientific reports, 9(1), 4920. doi:10.1038/s41598-019-40180-x

Alharbi, O. M., Khattab, R. A., Ali, I., Binnaser, Y. S., & Aqeel, A. (2018). Evaluation of the heavy metals threat to the Yanbu shoreline, Red Sea, Saudi Arabia. Marine and Freshwater Research, 69(10), 1557-1568. doi:10.1071/MF18079

Amin, B., Ismail, A., Arshad, A., Yap, C. K., & Kamarudin, M. S. (2009). Anthropogenic impacts on heavy metal concentrations in the coastal sediments of Dumai, Indonesia. *Environmental Monitoring and Assessment*, *148*(1-4), 291-305. doi:10.1007/s10661-008-0159-z

Badawy, W. M., El-Taher, A., Frontasyeva, M. V., Madkour, H. A., & Khater, A. E. (2018). Assessment of anthropogenic and geogenic impacts on marine sediments along the coastal areas of Egyptian Red Sea. Applied Radiation and Isotopes, 140, 314-326. doi:10.1016/j.apradiso.2018.07.034

Badr, N. B., El-Fiky, A. A., Mostafa, A. R., & Al-Mur, B. A. (2009). Metal pollution records in core sediments of some Red Sea coastal areas, Kingdom of Saudi Arabia. Environmental monitoring and assessment, 155(1-4), 509-526. doi:10.1007/s10661-008-0452-x

Basaham, A.S., Rifaat, A.E., El-Mamoney, M.H., El Sayed, M.A., (2009). Re-evaluation of the impact of sewage disposal on coastal sediments of the southern Corniche,

Jeddah, Saudi Arabia. JKAU: Mar. Sci. 20, 109–126. doi:10.4197/Mar.20-1.8

Bryan, G. W., & Langston, W. J. (1992). Bioavailability, accumulation and effects of heavy metals in sediments with special reference to United Kingdom estuaries: a review. Environmental pollution, 76(2), 89-131. doi:10.1016/0269-7491(92)90099-V

Canli, M., & Atli, G. (2003). The relationships between heavy metal (Cd, Cr, Cu, Fe, Pb, Zn) levels and the size of six Mediterranean fish species. Environmental pollution, 121(1), 129-136. doi.org/10.1016/S0269-7491(02)00194-X

Chakraborty, S., Bhattacharya, T., Singh, G., & Maity, J. P. (2014). Benthic macroalgae as biological indicators of heavy metal pollution in the marine environments: A biomonitoring approach for pollution assessment. Ecotoxicology and Environmental Safety, 100, 61-68. doi:10.1016/j.ecoenv.2013.12.003

Cui, Y., Ge, Q., Liu, X. Y., & Chung, T. S. (2014). Novel forward osmosis process to effectively remove heavy metal ions. Journal of Membrane Science, 467, 188-194. doi.org/10.1016/j.memsci.2014.05.034

Dou, Y., Li, J., Zhao, J., Hu, B., & Yang, S. (2013). Distribution, enrichment and source of heavy metals in surface sediments of the eastern Beibu Bay, South China Sea. Marine pollution bulletin, 67(1-2), 137-145. doi:10.1016/j.marpolbul.2012.11.022

El Nemr, A., El-Said, G. F., Khaled, A., & Ragab, S. (2016). Distribution and ecological risk assessment of some heavy metals in coastal surface sediments along the Red Sea, Egypt. International Journal of Sediment Research, 31(2), 164-172. doi:10.1016/j.ijsrc.2014.10.001

Filgueiras, A. V., Lavilla, I., & Bendicho, C. (2004). Evaluation of distribution, mobility

and binding behaviour of heavy metals in surficial sediments of Louro River (Galicia, Spain) using chemometric analysis: a case study. Science of the Total Environment, 330(1-3), 115-129. doi:10.1016/j.scitotenv.2004.03.038

Fu, F., & Wang, Q. (2011). Removal of heavy metal ions from wastewaters: a review. Journal of environmental management, 92(3), 407-418. doi:10.1016/j.jenvman.2010.11.011

Ghandour, I. M., Basaham, S., Al-Washmi, A., & Masuda, H. (2014). Natural and anthropogenic controls on sediment composition of an arid coastal environment: Sharm Obhur, Red Sea, Saudi Arabia. Environmental monitoring and assessment, 186(3), 1465-1484.doi:10.1007/s10661-013-3467-x.

Ghrefat, H., & Yusuf, N. (2006). Assessing Mn, Fe, Cu, Zn, and Cd pollution in bottom sediments of Wadi Al-Arab Dam, Jordan. Chemosphere, 65(11), 2114-2121.

Grant, A., & Middleton, R. (1990). An assessment of metal contamination of sediments in the Humber Estuary, UK. Estuarine, Coastal and Shelf Science, 31(1), 71-85.

Hakanson, L. (1980). An ecological risk index for aquatic pollution control. A sedimentological approach. Water research, 14(8), 975-1001.

Hanna, R. G., & Muir, G. L. (1990). Red Sea corals as biomonitors of trace metal pollution. Environmental Monitoring and Assessment, 14(2-3), 211-222. doi:10.1007/BF00677917.

Heiri, O., Lotter, A. F., & Lemcke, G. (2001). Loss on ignition as a method for estimating organic and carbonate content in sediments: reproducibility and comparability of results. Journal of paleolimnology, 25(1), 101-110.

Karuppasamy, M., Qurban, M. A. B., & Krishnakumar, P. K. (2019). Metal Contamination

Assessment in the Sediments of the Red Sea Coast of Saudi Arabia. In Oceanographic and Biological Aspects of the Red Sea (pp. 147-170). Springer, Cham. doi.org/10.1007/978-3-319-99417-8_9

Khodami, S., Surif, M., WO, W. M., & Daryanabard, R. (2017). Assessment of heavy metal pollution in surface sediments of the Bayan Lepas area, Penang, Malaysia. Marine pollution bulletin, 114(1), 615-622. doi:10.1016/j.marpolbul.2016.09.038

Khodeir, M., Shamy, M., Alghamdi, M., Zhong, M., Sun, H., Costa, M., Chen, L.C. and Maciejcczyk, P.M. (2012). Source Apportionment and Elemental Composition of PM2.5 and PM10 in Jeddah City, Saudi Arabia. Atmos. Pollut. Res. 3: 331–340.

Kroetsch, D., & Wang, C. (2008). Particle size distribution. Soil sampling and methods of analysis, 2, 713-725.

Kronvang, B., Laubel, A., Larsen, S. E., & Friberg, N. (2003). Pesticides and heavy metals in Danish streambed sediment. Hydrobiologia, 494(1-3), 93-101.

Liao, J., Chen, J., Ru, X., Chen, J., Wu, H., & Wei, C. (2017). Heavy metals in river surface sediments affected with multiple pollution sources, South China: Distribution, enrichment and source apportionment. Journal of Geochemical Exploration, 176, 9-19. doi:10.1016/j.gexplo.2016.08.013

Louriño-Cabana, B., Lesven, L., Charriau, A., Billon, G., Ouddane, B., & Boughriet, A. (2011). Potential risks of metal toxicity in contaminated sediments of Deûle river in Northern France. Journal of hazardous materials, 186(2-3), 2129-2137. doi:10.1016/j.jhazmat.2010.12.124.

Magno, M. C., Venti, F., Bergamin, L., Gaglianone, G., Pierfranceschi, G., & Romano, E. (2018). A comparison between Laser Granulometer and Sedigraph in grain size

analysis of marine sediments. Measurement, 128, 231-236.

Mortuza, M. G., & Al-Misned, F. A. (2017). Environmental contamination and assessment of heavy metals in water, sediments and shrimp of Red Sea coast of Jizan, Saudi Arabia. J. Aquat. Pollut. Toxicol, 1(1).

Müller, G. (1981). Schwermetallbelastung der sedimente des Neckars und seiner Nebenflusse: eine Estandsaufnahmedie. Chemiker Zeitung 105,157–163.

Müller, G., 1979. Schwermetalle in den Sedimenten des Rheins-Veränderungen seit 1971. Umschau 79, 778–783.

Pan, K., Lee, O. O., Qian, P. Y., & Wang, W. X. (2011). Sponges and sediments as monitoring tools of metal contamination in the eastern coast of the Red Sea, Saudi Arabia. *Marine pollution bulletin*, *62*(5), 1140-1146. doi:10.1016/j.marpolbul.2011.02.043

Prego, R., Belzunce Segarra, M. J., Helios-Rybicka, E., & Barciela, M. (1999). Cadmium, manganese, nickel and lead contents in surface sediments of the lower Ulla River and its estuary (northwest Spain). doi:10.1016/j.aca.2004.03.032

Ramadan, M. H., & Halawani, R. F. (2010). Study on Wastewater in Paper Recycling Plants Case Study. Journal of King Abdulaziz University: Meteorology, Environment & Arid Land Agriculture Sciences, 21(2). doi:10.4197/Met. 21-2.15.

Ruiz-Compean, P., Ellis, J., Cúrdia, J., Payumo, R., Langner, U., Jones, B., & Carvalho, S. (2017). Baseline evaluation of sediment contamination in the shallow coastal areas of Saudi Arabian Red Sea. Marine pollution bulletin, 123(1-2), 205-218. doi:10.1016/j.marpolbul.2017.08.059

Samman, A. E., & Gallus Jr, W. A. (2018) A climatology of the winter low-level jet over

the Red Sea. International Journal of Climatology. doi:10.1002/joc.5742

Skaldina, O., Peräniemi, S., & Sorvari, J. (2018). Ants and their nests as indicators for industrial heavy metal contamination. Environmental pollution, 240, 574-581. doi.org/10.1016/j.envpol.2018.04.134

Taylor, S. R., & McLennan, S. M. (2001). Chemical composition and element distribution in the Earth's crust. Encyclopedia of Physical Science and Technology. https://doi.org/10.1016/B0-12-227410-5/00097-1

Tomlinson, D. L., Wilson, J. G., Harris, C. R., & Jeffrey, D. W. (1980). Problems in the assessment of heavy-metal levels in estuaries and the formation of a pollution index. Helgoländer meeresuntersuchungen, 33(1), 566.

Turekian, K. K., & Wedepohl, K. H. (1961). Distribution of the elements in some major units of the earth's crust. Geological Society of America Bulletin, 72(2), 175-192.

Ungureanu, T., Iancu, G. O., Pintilei, M., & Chicoș, M. M. (2017). Spatial distribution and geochemistry of heavy metals in soils: A case study from the NE area of Vaslui county, Romania. Journal of Geochemical Exploration, 176, 20-32. doi:10.1016/j.gexplo.2016.08.012

US Environmental Protection Agency. (1996). Method 3050B: Acid digestion of sediments, sludges, and soils. Test methods for evaluating solid waste, physical/chemical methods.

Usman, A. R., Alkredaa, R. S., & Al-Wabel, M. I. (2013). Heavy metal contamination in sediments and mangroves from the coast of Red Sea: Avicennia marina as potential metal bioaccumulator. Ecotoxicology and environmental safety, 97, 263-270. doi:10.1016/j.ecoenv.2013.08.009

Youssef, M. (2015). Heavy metals contamination and distribution of benthic foraminifera from the Red Sea coastal area, Jeddah, Saudi Arabia. Oceanologia, 57(3), 236-250. doi:10.1016/j.oceano.2015.04.002

Yuan, H., Song, J., Li, X., Li, N., & Duan, L. (2012). Distribution and contamination of heavy metals in surface sediments of the South Yellow Sea. Marine pollution bulletin, 64(10), 2151-2159. doi:10.1016/j.marpolbul.2012.07.040

Zhuang, W., & Gao, X. (2014). Integrated assessment of heavy metal pollution in the surface sediments of the Laizhou Bay and the coastal waters of the Zhangzi Island, China: comparison among typical marine sediment quality indices. PLoS One, 9(4), e94145. doi.org/10.1371/journal.pone.0094145

Chapter 3

A LEAD ISOTOPE STUDY TRACING POLLUTION IN NEAR-SHORE SEDIMENTS NEAR JEDDAH, SAUDI ARABIA

3.1 Abstract

This study evaluates Red Sea, near-shore sourcing of Pb from the Jeddah, Saudi Arabia region by examining ratios of ^{206}Pb, ^{207}Pb, and ^{208}Pb in marine sediment samples. The study region was divided into three locations: North, Middle, and South. Inductively Coupled Plasma-Mass Spectrometry (ICP-MS) was used to determine $^{208}Pb/^{206}Pb$ and $^{206}Pb/^{207}Pb$ values from forty sediment samples. Both a two end-member model and a three-component fractional contribution model were used to identify possible Pb sources and their percentage contributions in the study area. The isotopic data and modeling indicate a mixed natural and gasoline-derived background in the region. Specifically, the $^{206}Pb/^{207}Pb$ ratio decreases from north to south for the North location and increases from north to south for the Middle and South locations tracking the impact of legacy gasoline-derived lead in the modern background distribution. Enriched locations in the region, dominantly in the Middle and South locations, show the two- component background distribution as well as a third unknown anthropogenic source of contamination. The unknown source is clearly shown to control elevated contamination and its isotopic signature is reported. The consequence of this research serves as benchmark data and useful historical documentation of environmental Pb pollution in the Saudi Arabian coastal areas of the Red Sea.

3.2 Introduction

It is an essential matter in environmental research to recognize the source of pollution and determine the transport history of pollutants. Given the broad range of uses and transport mechanisms, determining the sources of lead in the environment can be difficult. Pb can be found naturally, via rock weathering and aerosol deposition (Monastra et al., 2004; Choi et al., 2007; Monna et al., 2000). Pb is very flexible and soft and has a low melting point (328 C^{o}) (Lessler, 1988; Chen and Hu, 2010). Also, it is recognized as one of the seven metals of antiquity (gold, silver, copper, tin, lead, iron, and zinc) (Lessler, 1988). The common Pb minerals in nature are galena (PbS), cerussite ($PbCO_3$), and anglesite ($PbSO_4$) (Faure, 1977). Additionally, Pb is extracted as a co-product from the ores of copper, zinc, and silver (Chen and Hu, 2010). Because of its unique physical and chemical characteristics, lead has been extensively used in different industries such as in construction, batteries, bullets, paint and fusible alloys (Wani et al., 2015; Al-Saleh et al., 1993; Barbosa et al., 2005; Kim and Kang, 2015; Lee et al., 2019). Anthropogenic contamination of Pb is likely produced in urban areas from industrial sources, exhaust from gasoline vehicles, paint, pesticides, thus complicating the identification of lead pollution sources (Cheng and Hu, 2010; Komárek et al., 2008; Chen et al., 2016 b).

Pb is recognized to be toxic to humans and typically enters the human body via ingestion and/or inhalation and affects most of the functions of the human body (Yu et al., 2016). A variety of diseases such as anemia, central nervous system disorders, and immune system disorders are directly attributed to lead exposure (Kosnett, 2007; Wani et al., 2015; Needleman et al., 1990). Moreover, sleeplessness, tiredness, loss of memory, weight loss, increased blood pressure, and cardiovascular diseases are linked to high Pb concentrations

human blood (Yap et al., 2016). The World Health Organization (WHO) set 10 µg/l (0.01 mg/l) as a limit for Pb in drinking water, and the board on contaminants in the natural way of life at the European Food Safety Authority (EFSA) set 25 µg/week/kg body weight as a maximum total weekly ingestion of Pb (WHO 2011; EFSA 2010). World associations, including the United Nations Environment Program (UNEP) and the World Health Organization (WHO), are supporting the worldwide elimination of Pb paint by 2020 because of the documented severe danger of lead to humans (O'Connor et al., 2018).

Lead is also well documented as a toxin to fauna. Fish are one of the most abundant marine animals and impact humans directly through the food chain. Most of the research on lead toxicity to marine animals has been carried out in fish (Lee et al., 2019; Vinodhini and Narayanan, 2008; Cheng and Hu, 2010). Pb is known as one of the extremely toxic metals to fish due, in part, to its bioaccumulation in tissues, influence on physiological and biochemical functions, and neurotoxicity (Taylor and Maher, 2014; Lee et al., 2019). The liver, kidney, and spleen are the most common tissues in fish for accumulation due to long-term Pb exposure (Vinodhini and Narayanan, 2008; Javed, 2012; Kim and Kang, 2015). Even low concentrations of lead in the marine environment have been shown to cause adverse effects on gills of fishes (Sures and Siddall, 1999; Hwang et al., 2016; Macirella et al., 2019). Additionally, lead exposure to marine algae negatively affects photosynthetic activities and net total chlorophyll concentrations (Gan et al., 2019).

Stable lead isotopes are valuable for discerning Pb source including if it is significantly derived from anthropogenic sources. Utilizing isotopic ratios of components is frequently a superior tracking method to utilizing their concentrations alone to recognize sources of Pb pollution (Alyazichi et al., 2016; Chen et al., 2015). The four known stable

lead isotopes are ^{204}Pb, ^{206}Pb, ^{207}Pb, and ^{208}Pb, with the first one being non-radiogenic. The other three are radiogenic isotopes and produced by the radioactive decay of ^{238}U, ^{235}U, and ^{232}Th (Faure 1977). Various studies have evaluated the adequacy of their ratios, $^{208}Pb/^{206}Pb$ and $^{206}Pb/^{207}Pb$, as indicators of different pollution sources of Pb; they include studies in Scotland (Bacon et al., 1995), France (Monna et al., 2000), East Antarctica (Townsend and Snapeb., 2002), the Czech Republic (Komárek et al., 2008), China (Cheng and Hu, 2010; Yu et al., 2016 ;Liu et al., 2019), Australia (Alyazichi et al., 2016) and Singapore (Chen et al., 2016 a).

Some geological and mineralogical studies have analyzed Pb concentrations and isotopic ratios in the Red Sea deep basins and brine pools (Dupré et al., 1988; Baumann 1994; Altherr et al., 1990; Pierret et al., 2010; Laurila et al., 2014). Pierret et al., (2010) consider Atlantis II Deep as a reference location for the most metal-rich sediments, which assembled through chemical deposition from overlying, mineralized, salt-rich hydrothermal brines.

There is strong recent interest to study lead in marine sediments from the countries bordering the Red Sea due to the rapid development and lack of prior research in the area. This recent body of literature shows lead concentrations were high in some marine sediment locations along the coastal areas of Saudi Arabia (Ruiz-Compean et al., 2017; Karuppasamy et al., 2017; Kahal et al., 2018), Egypt (Mansour et al., 2011; Salem et al., 2014; El-Taher et al., 2018; Badawy et al., 2018;), Sudan (Idris et al., 2007), Jordan (Al-Najjar et al., 2011) and the Jeddah region (Badr et al., 2009; Pan et al., 2011; Abu-Zied et al., 2013; Al-Mur et al., 2017). Despite these recent studies, there remains a serious lack of data and doubt concerning the distribution and sourcing of Pb. The aims of this study is 1)

to evaluate the spatial distribution of Pb isotopic ratios to identify sources of Pb pollution, and 2) to set natural Pb isotopic ratio background values for the study area.

3.3 Materials and Methods

3.3.1 Study Area and Sample Collection

To measure Pb isotopes in Red Sea sediments along Jeddah shoreline, Saudi Arabia, three locations were selected to cover the entirety of the study area (Figure 3.1). Forty total surface sediment samples were collected. The first ten samples collected from the Northern location of Jeddah were taken from an area remote from heavy human activities. Twenty samples were collected from the Middle location near the fish market and the main seaport of the city. The other ten samples were taken near Jeddah Industrial City and refinery plant from the South location. All the samples were collected by stainless steel soil scoop, stored in polyethylene clear flat zipper bags, and held at 4° C until transport to the laboratory.

3.3.2 Samples Preparation

Surface sediment samples were analyzed for total Pb concentration and Pb isotopes following an adapted US EPA Method 3050B (USAEPA, 1996). The method was modified by utilizing approximately 0.20 g of sediment. Prior to analysis, samples were placed in 50 mL tubes, and 5 mL 5% HNO_3 was added to remove significant carbonate. Then, 20 mL of 70% HNO_3 was added to the samples inside a fume hood and digested at 85° C on a hot block until dryness. Samples were resolubilized in a known mass of 5% HNO_3 for analysis. Analyses were run in collision cell technology with kinetic energy discrimination mode (CCT-KED) using an, X-Series 2 Inductively Coupled Plasma-Mass Spectrometer (ICP-MS) made by Thermo Scientific. To establish calibration curves for Pb concentrations and isotopes ratios (^{206}Pb, ^{207}Pb, and ^{208}Pb), multi-element standards (CLMS-2A, from SPEX-

Certi Prep, Metuchen, NJ, USA) were used with a range from 0.1 to 10 ppb. The ICP ran by using 5% HNO_3, mixed from concentrated 70% HNO_3 certified ACS plus (A200C-212) from Fisher Scientific, and 18.2 mΩ nanopure water. To convert the uncorrected values (counts) to the unit of concentration (mg/kg), calibration curves with r^2 values of 0.999 or larger were applied. For quality, each sample was analyzed in triplicate, and a blank sample (5% HNO_3) was measured every twelve samples to verify sufficient washout time between sample runs. All the ICP-MS plasticware used in the analyses were acid washed (5% HCL) for 24 hours and rinsed with nanopure water prior to use.

3.3.3 Enrichment factor (Ef)

The metal enrichment factor (Ef) reflects the status of the environmental contamination by indicating whether the metal is from natural weathering processes or anthropogenic sources. The Ef is calculated using the following equation:

$$\mathrm{Ef} = (C_i/\mathrm{C}_{Rb})_{\mathrm{S}} / (C_i/\mathrm{C}_{Rb})_{\mathrm{B}} \quad (3.1)$$

Where Ef is an enrichment factor for a particular metal, $C_i/\mathrm{C}_{Rb})\mathrm{S}$ is the metal concentration to rubidium ratio (both in mg/kg) in the studied sediment samples (Grant and Middleton 1990; Alyazichi et al., 2016) The average background shale values adopted from Turekian and Wedepohl (1961) are given by $(C_i/\mathrm{C}_{Rb})\mathrm{B}$. Amin et al., (2009) differentiated contamination into different categories based on enrichment factor values, with an Ef value less than 1 showing no enrichment, an Ef value less than 3 showing minor enrichment, an Ef value between 3 to 5 showing moderate enrichment, an Ef value equal to 5 to 10 showing moderately severe enrichment, an Ef value of 10 and 25 showing severe enrichment, and an Ef value of 25 to 50 showing extremely severe enrichment.

3.3.4 Pb sources and contributions

It is essential in most Pb studies to estimate and quantify the Pb contributions from different sources (Kersten et al., 1997; Yu et al., 2016; Xu et al., 2019). Numerous potential anthropogenic Pb sources could discharge and reach the Jeddah coastal region and using only total concentration analysis could be misleading. Each Pb source has its preserved isotopic signatures and does not change under common transport processes (Cheng and Hu 2010; Wanget al., 2014; Monna et al., 1997). It is common in environmental studies to plot two isotope ratios, $^{206}Pb/^{207}Pb$ and $^{208}Pb/^{206}Pb$, against each other to relate samples to the isotopic compositions of different potential Pb sources (Carrasco et al., 2018; Yu et al., 2016; Cheng and Hu 2010; Komárek et al., 2008; Flament et al., 2002). Further, various researchers have used mixing models to analyze such isotopic data (Monna et al., 2000; Komárek et al., 2008; Xu et al., 2014). Here, a two member ,or binary, mixing model is used for the low Pb concentration (< 100 mg/kg) samples. A fractional contribution model of three components, or a ternary model, is used for high Pb concentration (> 100 mg/kg) samples. Specific methods for each model and the rational for each is discussed below.

Based on literature, a linear mixing model was used in the current study to calculate the estimated contributions of Pb from natural sources and gasoline by using the $^{206}Pb/^{207}Pb$ ratio (Komárek et al., 2008; Monna et al., 1997). The model equations used were:

$$X_{\%}^{G} = \left[\left(\frac{^{206}Pb}{^{207}Pb}\right)_{S} - \left(\frac{^{206}Pb}{^{207}Pb}\right)_{NS}\right] / \left[\left(\frac{^{206}Pb}{^{207}Pb}\right)_{G} - \left(\frac{^{206}Pb}{^{207}Pb}\right)_{NS}\right] * \mathbf{100} \quad (3.2)$$

$$X_{\%}^{G} + X_{\%}^{NS} = 100 \quad (3.3)$$

Where $X_{\%}^{G}$ and $X_{\%}^{NS}$ are the contributions of gasoline and natural sources in percentage, $(^{206}Pb/^{207}Pb)S$ is the Pb isotopic composition in the sample, $(^{206}Pb/^{207}Pb)_{NS}$ is

the Pb isotopic composition of the natural sources (1.22) (Carrasco et al., 2018; Chen et al., 2016a; Monna et al., 1995; Komárek et al., 2008), and $(^{206}Pb/^{207}Pb)_G$ is the Pb isotopes composition of the gasoline (1.10) (Bollhöfer and Rosman, 2001; Carrasco et al., 2018; Monna et al., 1995).

The fractional contribution of the three-component model was used to quantify the input from three Pb sources to the sediment samples (Gobeil et al., 1995; Chiaradia et al., 1997; Cheng and Hu, 2010). The following three equations were employed in the model:

$$\left(\frac{208\ Pb}{206\ Pb}\right)S = \left(\frac{208\ Pb}{206\ Pb}\right)F1 + \left(\frac{208\ Pb}{206\ Pb}\right)F2 + \left(\frac{208\ Pb}{206\ Pb}\right)F3 \quad (3.4)$$

$$\left(\frac{206Pb}{207Pb}\right)S = \left(\frac{206Pb}{207Pb}\right)F1 + \left(\frac{206Pb}{207Pb}\right)F2 + \left(\frac{206Pb}{207Pb}\right)F3 \quad (3.5)$$

$$F1 + F2 + F3 = 1 \quad (3.6)$$

Where $(^{208}Pb/^{206}Pb)_S$ and $(^{206}Pb/^{207}Pb)_S$ were the measured ratios of the samples, and F_1, F_2, and F_3 were the proportion contributions of Pb from unknown source, natural sources, and gasoline, respectively. The values of $^{208}Pb/^{206}Pb$ and $^{206}Pb/^{207}Pb$ for the unknown source (F1) were calculated as described by Monna et al., 2000 and Gallon et al., 2011, two plots of 1/Pb concentration versus $^{206}Pb/^{207}Pb$ and $^{208}Pb/^{206}Pb$ were providing linear regression (Figure 3.2 A and B). The intercepts of the regression ($^{206}Pb/^{207}Pb = 1.183$; $^{208}Pb/^{206}Pb = 2.068$), provided an estimate of the isotopic ratios of an unknown source of Pb in the area. The values of the $^{206}Pb/^{207}Pb$ for F2 and F3 were same values used in the equation 3.2.The values of $^{208}Pb/^{206}Pb$ for natural and gasoline sources were not available from literature , so they were calculated from the linear regression of the plot of

$^{208}Pb/^{206}Pb$ and $^{206}Pb/^{207}Pb$ in Figure 3.3. The linear equation from the plot (Y= -0.7767X + 2.9681) was applied, with the $^{206}Pb/^{207}Pb$ values of the natural sources (1.22) and of the gasoline (1.10). The calculated values of $^{208}Pb/^{206}Pb$ was (2.01) for natural and (2.11) gasoline.

3.4 Results and Discussion

The data from Table 3.1 shows that the average concentration of the Pb from the North location of the study area was 4.72 mg/kg with range between 3.57 - 6.96 mg/kg, and the average for the Middle location was 80.44 mg/kg with range between 1.70 - 372.71 mg/kg, where the average for the South location was 147.91 mg/kg and the range between 6.36 - 578.47 mg/kg. The calculated Ef values in the collected Red Sea sediments suggest anthropogenic sources for all locations. As seen in Table 3.1, the sediment samples from our study area have Pb enrichment factors ranging from 30.03 to 130.84 with an average of 71.50, 10.18 to 946.31 with an average of 243.99, and 123.74 to 9607.91 with an average 2397.99 for North, Middle, and south location, respectively. The results indicate that more than 80% of the sediment samples were considered extremely severely enriched with Pb (Ef >50).

No previous data on Pb isotopes has been reported in the Jeddah area. Figure 3.3 demonstrates the distribution of Pb isotopes in the study area. The average ratio for $^{206}Pb/^{207}Pb$ was 1.17, with a range between 1.15-1.18 for the North location. The average was 1.16 with a range of 1.12-1.19 for the Middle location. For the South location, the average was 1.179, and the range was between 1.17-1.18 (Table 3.1). From the data in Figure 3.4, it is apparent that the $^{206}Pb/^{207}Pb$ ratio decreases from north to south for the

North location (1-10) and increases from north to south for the Middle and South locations (11-40).

Given the ubiquitous enrichment across the entire region and the $^{206}Pb/^{207}Pb$ ratio data, it is likely that the region has been impacted by an anthropogenic source that has elevated the entire region's background. That background would be composed of two major components, naturally sourced Pb and the widespread anthropogenic source. That latter source is almost certainly gasoline-derived Pb given the environmental history of the region and omnipresence of enrichment. Meanwhile, there are sample stations with excessively enriched Pb values. It is likely that there exists one or more other anthropogenic sources in addition to the new combined natural-gasoline background. Figure (3.4) demonstrates that the samples from the far north and south could originate from natural Pb (the green zone for natural Pb > 50 %) and demonstrated the effect of legacy gasoline-derived Pb in the modern background distribution.

3.4.1 Sourcing of Background Pb in Sediments

The Pb concentrations of the Jeddah near-shore sediment samples showed two groups, one with lower concentration (<100 mg/kg) and another with a higher concentration (>100 mg/kg) (Tables 3.2 and 3.4). By calculating the percentage contribution of the anthropogenic Pb in the two-end- member model (Equations 3.2 and 3.3), we found the Pb relative contribution for gasoline and, thereby, natural source (Figure 3.6 and 3.7) for the low concentration samples (< 100 mg/kg). The average percentage contribution of Pb from natural source was 53.56% in the range between 69.17-19.17%, and the average for the gasoline was 46.44% with range between 80.83-30.83%. There is a significant positive correlation between $^{206}Pb/^{207}Pb$ and $^{208}Pb/^{206}Pb$ (r^2 =0.79) for the sediment samples from the study area that has the lowest Pb concentrations (<100 mg/kg)

(Figure 3.5).

For the North location, the average contribution of Pb from the natural source was 56.33%, and it was 43.66% for gasoline. The points N4, N9, and N10 (Figure 3.6 A) showed the high contribution of Pb gasoline (54.16, 50.83, and 55.83%, respectively) could be due to heavy traffic activities (Figure 3.7 A). In the Middle location, the average contribution of Pb was 46.61 % of the natural sources and 53.39% for the gasoline. Some points, such as M1, M2, M3, M5 and M7, showed the contribution of Pb gasoline more than 50% (Figure 3.6 B). The sources of Pb gasoline in this location could be from the heavy traffic and the desalination plant, also the activities of the ships at Jeddah's Seaport (Figure 3.7 B). The average contribution of Pb from gasoline was 34.86%, and the natural source was 56.13% in the South location. As shown in Figure 3.6 C, the contribution of the natural source was very high, more than 60%, which indicates that natural Pb enriches the area.

The model showed that some points from the North location (N1, N2, N3, N5, N6, N7, and N8), Middle location (M4, M6, M11, M13, M19, and M20), and South location (S4, S5, S6, S8, S9, and S10) showed more than 50% contribution of natural than the gasoline. Additionally, all of these points sample were in the range of the $^{206}Pb/^{207}Pb$ ratio between 1.16 – 1.18. This finding is consistent with that of Zhu et al. (2010) who reported the natural $^{206}Pb/^{207}Pb$ in the sediments from the South China Sea (1.17), Carrasco et al. (2018) who explored sediments and soil from Singapore (1.21 - 1.18), and Xu et al. (2019) who found values in sediments from eastern Beibu Gulf, South China Sea less than 1.17. On the other hand, the model showed some points with a contribution from gasoline greater than 50% from North location (N4, N9, and N10), and Middle location (M1, M2, M3, M5,

M7, M8, M9, M17) (Figure 3.7). These points were in the range between 1.16-1.12 of $^{206}Pb/^{207}Pb$. These results are consistent with data obtained in 2018 by Carrasco et al. who reported the ratio of the $^{206P}b/^{207}Pb$ for leaded gasoline around 1.124, Chen et al (2016b) who reported the ratio in the South China Sea at 1.137, Chen et al. (2016a) who stated the ratio in the Kuala Lumpur, Singapore as less than 1.14.

The two-end-member model confirms that most marine sediment Pb in the region is derived from natural weathering (terrestrial source) and sediment accumulation with gasoline derived sources.

3.4.2 Possible Sources of Pb in Enriched Marine Sediments

The three member mixing model (Equations 3.4, 3.5, and 3.6) was applied to higher concentration samples (>100 mg/kg). Table 3.3 shows the modeled Pb percentage contributions using the fractional contribution of three sources for enriched Jeddah sediment samples with all coming from the Middle and the South locations.

Six points out of twenty points samples showed contributions of the Pb from gasoline, natural backgrounds, and unknown source for Middle location. The average contribution of Pb from the unknown source in the Middle location was 47.05%, from the natural source was 34.72%, and 18.23% was from gasoline. M14 and M18 had the highest contribution of the unknown source (86.08 and 71.93%) (Figure 3.8 A). For the South location, 48.74% was the average Pb contribution from the unknown source, 32.15% from natural source, and 19.10% from the gasoline. S7 showed the highest percentage contribution from unknown sources (57.19%). Figure 3.9 shows maps of Middle (A), and South (B) locations for the percentage contributions of the Pb from gasoline, natural source, and unknown source in the sediment samples with Pb concentration > 100 mg/kg.

The ternary diagram for Jeddah sediment samples (Pb concentration > 100 mg/kg), including 8 out of 10 points, is displayed in Figure 3.10. The points M10 and S10 were out of the range of 0-100%. The diagram is shown trends from natural source and gasoline to an unknown source. Moreover, the positive correlation (r^2=0.76) between the highest 10 Pb concentration and the percentage contribution of the unknown source of the study area refer strong and effect of this source in these points (Figure 3.11).

The unknown source might be industrial and domestic discharge from the surrounding urban area. Some of the highest lead concentration were from the Middle location (Figure 3.9 A), and were located near industrial and sewage wastewater outflow pipes (Abu-Zied and Orif, 2019). Similarly, the other point was from the South location (Figure 3.9 B), which was near the treated and semi-treated sewage pipe outflow discharge from the Al Kumarra municipal treatment plant (Basaham et al., 2009). Also, the industrial city of south Jeddah has an industrial waste treatment plant; the treated discharged from industrial activities are released nearby (Ramadan and Halawani, 2010).

Table 3.4 illustrates the Pearson correlation coefficients between Pb concentrations and the two end-member model as well as between Pb concentrations and the three-component modelled fractions. The low Pb concentrations (Table 3.4 A) have a negative correlation between the percentage contribution of gasoline Pb (-0.45) and positive correlation with the natural source (0.45). The high Pb concentrations have a strong positive correlation with the percentage of the unknown source (0.87) and negative correlation with the gasoline and natural (-0.87, -0.81) sources. Moreover, the negative correlation between the unknown source with the gasoline (-0.94) and natural (-0.98) indicates the unknown source is controlling the pollution status of these points samples.

3.5 Conclusion

The aim of the present research was to evaluate for the first time the sources of the Pb that may affect the environment of the Red Sea near the Jeddah coastal area. The Middle location was the most impacted location by Pb from different sources. The Ef results showed that more than 80% of the sediment samples were considered extremely severely enriched with Pb. A two end-member model and a three-component fractional contribution model were used to identify possible Pb sources and their percentage contributions in the study area. The linear distribution of the two end members to moderately enriched sites clearly identify a baseline for the region that records a heterogeneous blending of a true natural source and gasoline-derived lead. The study further found a strong positive correlation exists between the highest Pb concentration and an additional unknown anthropogenic source, which controls the overall pollution in the study area. Consequently, this research serves as benchmark data and useful documentation of environmental pollution in the Saudi Arabian coastal areas on the Red Sea. Despite these promising results, questions remain. This would be a productive area for additional work. Further samples such as air, soil sediments and sediment cores should be undertaken to investigate the ratio of Pb isotopes in the area from other matrices and how the various sourcing may have changed over time.

Table 3. 1 An overview of Pb concentration (mg/kg), Pb isotopes ratio, and as well as Enrichment factors (Ef), for the surface sediments from Jeddah shoreline.

		mg/kg	$^{208}Pb/^{206}Pb$	$^{206}Pb/^{207}Pb$	Ef
North	Average	4.72	2.06	1.17	71.50
	Min	3.57	2.04	1.15	30.03
	Max	6.96	2.07	1.18	130.84
Middle	Average	80.44	2.07	1.16	243.99
	Min	1.70	2.04	1.12	10.18
	Max	372.71	2.10	1.19	946.31
South	Average	147.91	2.05	1.179	2397.99
	Min	6.36	2.04	1.17	123.74
	Max	578.47	2.07	1.18	9607.91

Table 3. 2 Isotopic ratio values for the samples with concentrations below 100 mg/kg (n=30) and modeled lead source percentage contributions using the two end-member model.

Sample No	mg/kg	Gasoline %	Natural %	$^{208}Pb/^{206}Pb$	$^{206}Pb/^{207}Pb$
N 1	4.02	45.00	55.00	2.061	1.166
N 2	3.57	30.83	69.17	2.041	1.183
N 3	5.57	43.33	56.67	2.073	1.168
N 4	4.40	54.17	45.83	2.073	1.155
N 5	6.96	40.00	60.00	2.050	1.172
N 6	4.48	38.33	61.67	2.044	1.174
N 7	4.51	35.83	64.17	2.056	1.177
N 8	5.21	42.50	57.50	2.045	1.169
N 9	3.86	50.83	49.17	2.073	1.159
N10	4.62	55.83	44.17	2.073	1.153
M 1	1.70	80.83	19.17	2.100	1.123
M 2	6.70	64.17	35.83	2.082	1.143
M 3	5.04	66.67	33.33	2.064	1.140
M 4	37.44	38.33	61.67	2.062	1.174
M 5	21.64	70.83	29.17	2.094	1.135
M 6	39.63	40.00	60.00	2.060	1.172
M 7	4.56	64.17	35.83	2.075	1.143
M 8	2.95	58.33	41.67	2.081	1.150
M 9	8.32	55.00	45.00	2.065	1.154
M11	75.65	33.33	66.67	2.042	1.180
M13	60.39	33.33	66.67	2.050	1.180
M17	8.06	58.33	41.67	2.080	1.150
M19	36.02	46.67	53.33	2.073	1.164
M20	80.49	37.50	62.50	2.056	1.175
S 4	40.37	31.67	68.33	2.048	1.182
S 5	75.81	36.67	63.33	2.055	1.176
S 6	20.30	35.00	65.00	2.046	1.178
S 8	21.43	40.00	60.00	2.059	1.172
S 9	26.38	32.50	67.50	2.038	1.181
S10	6.36	33.33	66.67	2.040	1.180
Average	20.88	46.44	53.56	2.06	1.16
Min	1.70	30.83	19.17	2.04	1.12
Max	80.49	80.83	69.17	2.10	1.18

Table 3. 3 Isotopic ratio values for samples with concentrations above 100 mg/kg (n=10) and modeled Pb fractional contribution from the three source model.

Sample No	mg/kg	Gasoline %	Natural %	Unknown Sources %	$^{208}Pb/^{206}Pb$	$^{206}Pb/^{207}Pb$
M 10	102.22	38.69	62.49	-1.18	2.05	1.17
M12	102.05	27.49	47.75	24.76	2.05	1.18
M14	286.83	5.55	8.36	86.08	2.07	1.18
M15	175.25	24.92	39.11	35.97	2.06	1.18
M16	181.18	23.33	60.17	16.51	2.04	1.19
M18	372.71	9.85	18.22	71.93	2.06	1.18
S 1	578.47	-0.23	-7.67	107.90	2.07	1.18
S 2	252.62	20.81	37.91	41.27	2.06	1.18
S 3	270.71	18.01	34.23	47.76	2.06	1.18
S 7	186.61	18.48	24.32	57.19	2.06	1.18
Average	250.87	18.69	32.49	48.82	2.06	1.18
Min	102.05	-0.23	-7.67	-1.18	2.04	1.17
Max	578.47	38.69	62.49	107.90	2.07	1.19

(M) Middle location samples. (S) South location samples.

Table 3. 4 Pearson correlation coefficients between Pb concentrations and A) two end- member model source fractions, and B) the three-component fractional contributions from modelling in near-shore sediments near Jeddah.

A	Concentration	Gasoline	Natural
Concentration	1		
Gasoline	- 0.45 *	1	
Natural	0.45 *	- 1.00 **	1

B	Concentration	Gasoline	Natural	Unknown Source
Concentration	1			
Gasoline	- 0.87 **	1		
Natural	- 0.81 **	0.84 **	1	
Unknown Source	0.87 **	- 0.94 **	- 0.98 **	1

** Correlation is significant at the 0.01 level.
* Correlation is significant at the 0.05 level.

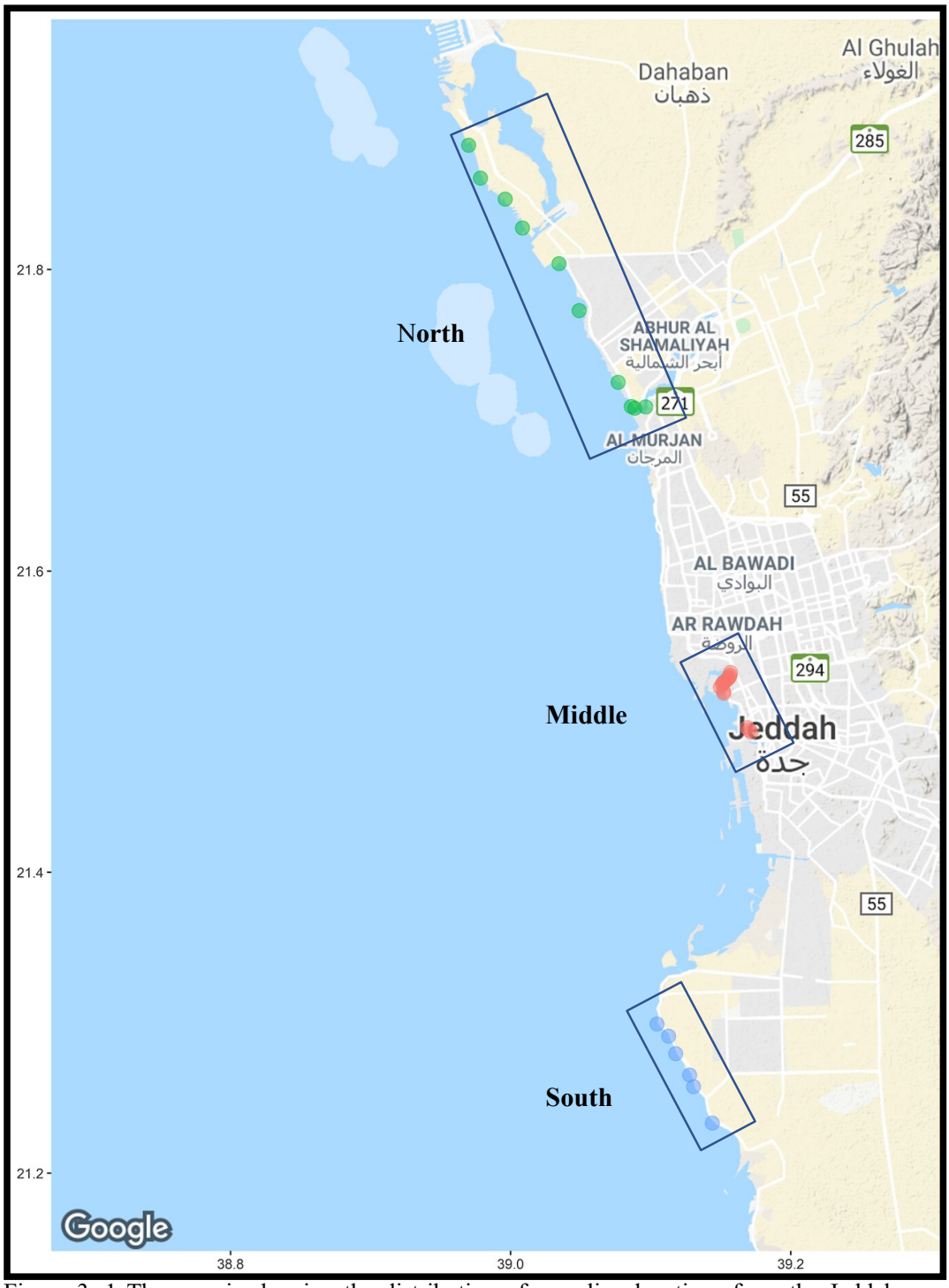

Figure 3. 1 The map is showing the distribution of sampling locations from the Jeddah coast. Approximate boundaries of the three regional locations (North, Middle, and South) are outlined with blue rectangles. The green dots show sample stations for the North location, the red for the Middle location, and the blue dots for the South location.

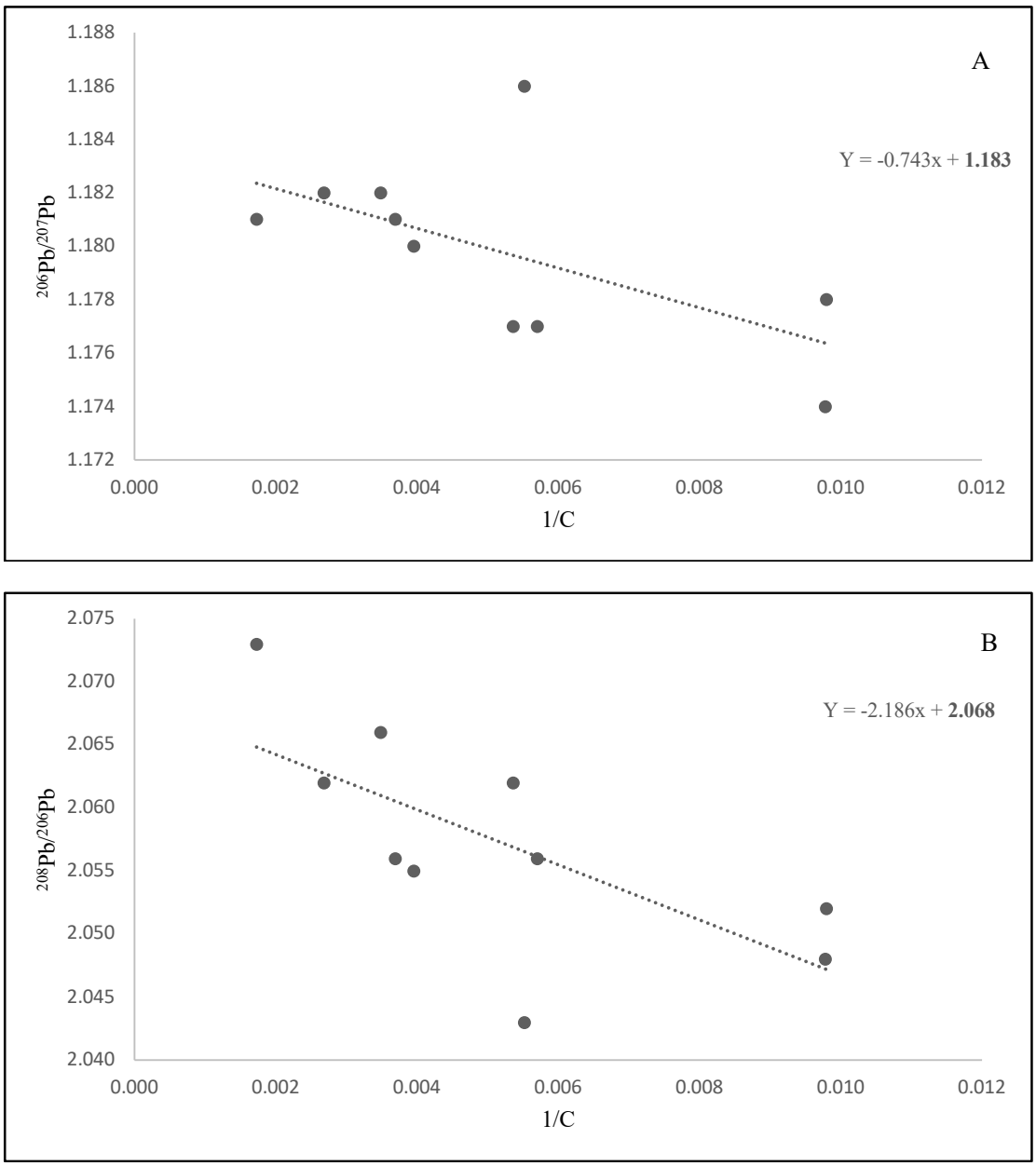

Figure 3. 2 1/ Pb concentration versus $^{206}Pb/^{207}Pb$ (A) and $^{208}Pb/^{206}Pb$ (B) in the higher concentration (> 100 mg/kg sediment samples).

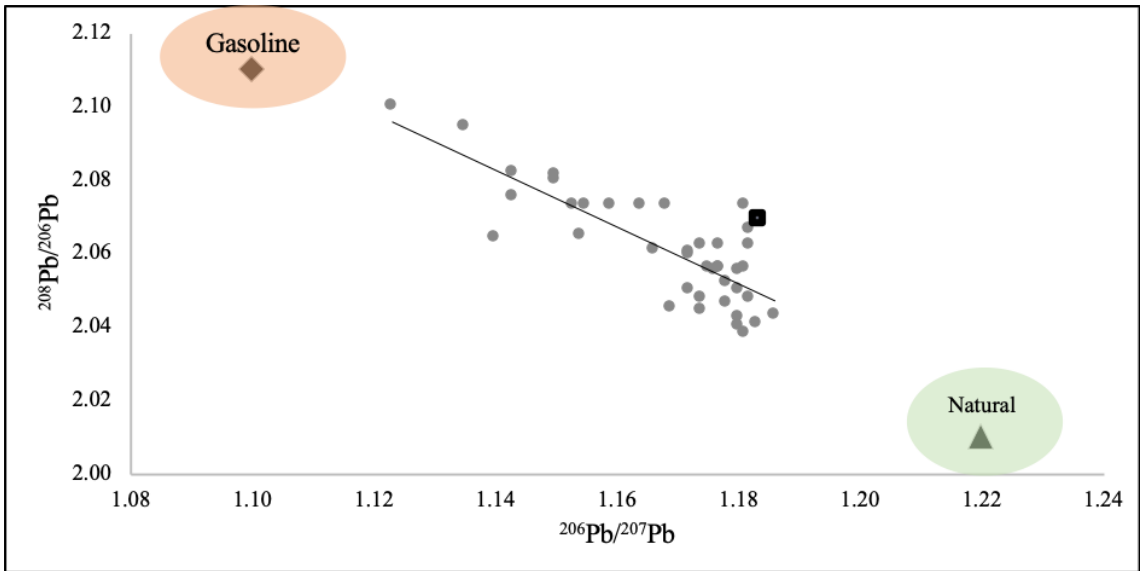

Figure 3. 3 The distribution of Pb isotopic ratios ^{206}Pb /^{207}Pb of surface sediments from the Jeddah shoreline with r^2 =0.66. The black square shows the unknown source from Pb, the triangle displays the natural source, and diamond displays the gasoline source from literature.

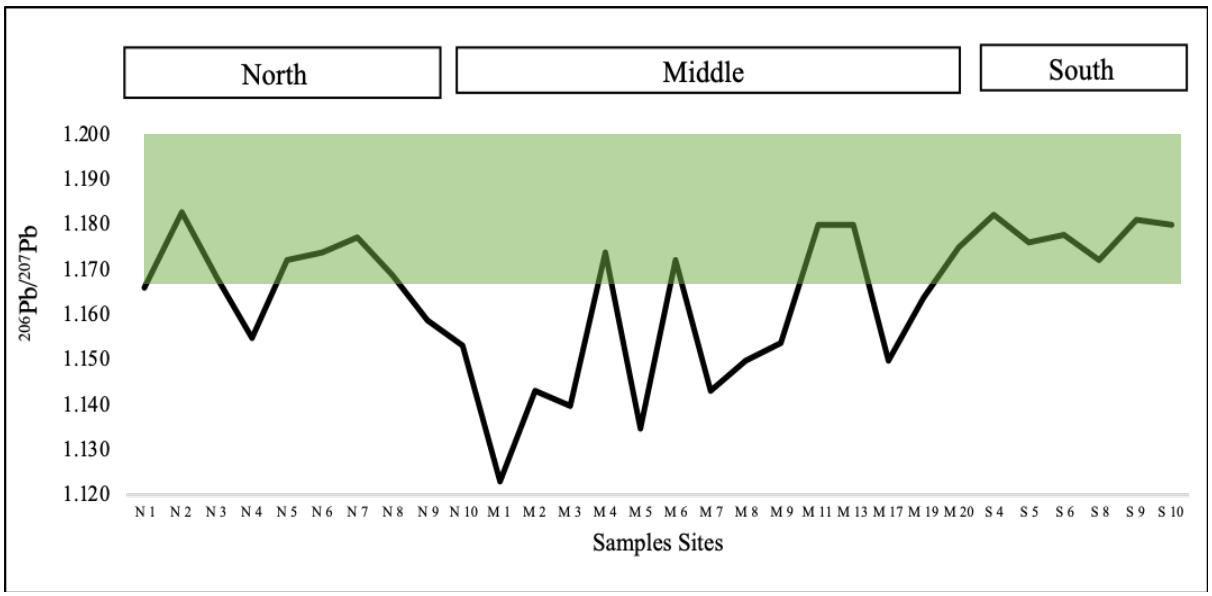

Figure 3. 4 The north to south distribution of ^{206}Pb /^{207}Pb for the low Pb concentration (<100mg/kg) near-shore sediments. The green zone demarcates greater than 50% natural source of Pb.

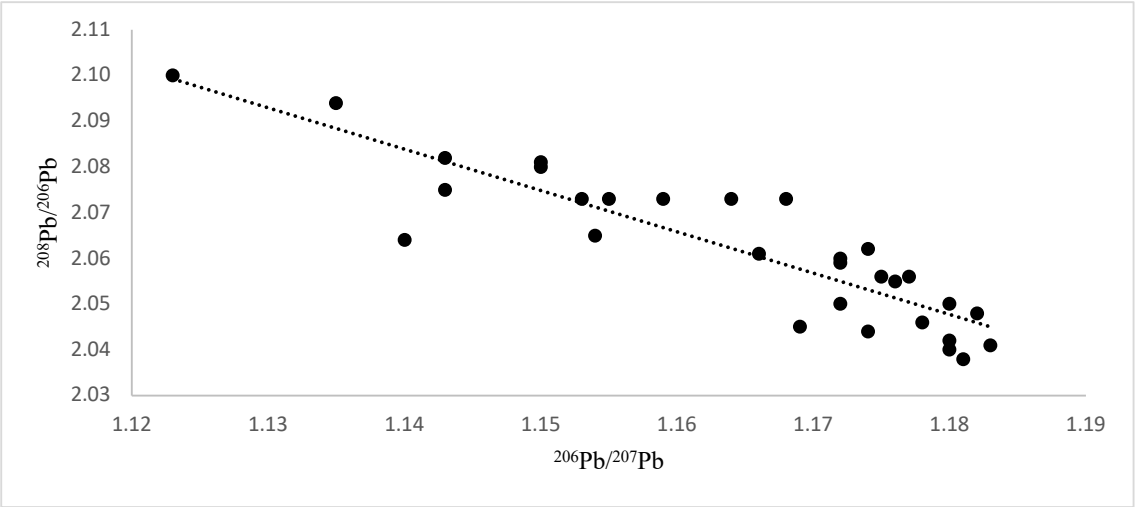

Figure 3. 5 $^{206}Pb/^{207}Pb$ and $^{208}Pb/^{206}Pb$ from low concentration (< 100 mg/kg) sediment samples of this study showing significant positive correlation (r^2=0.79).

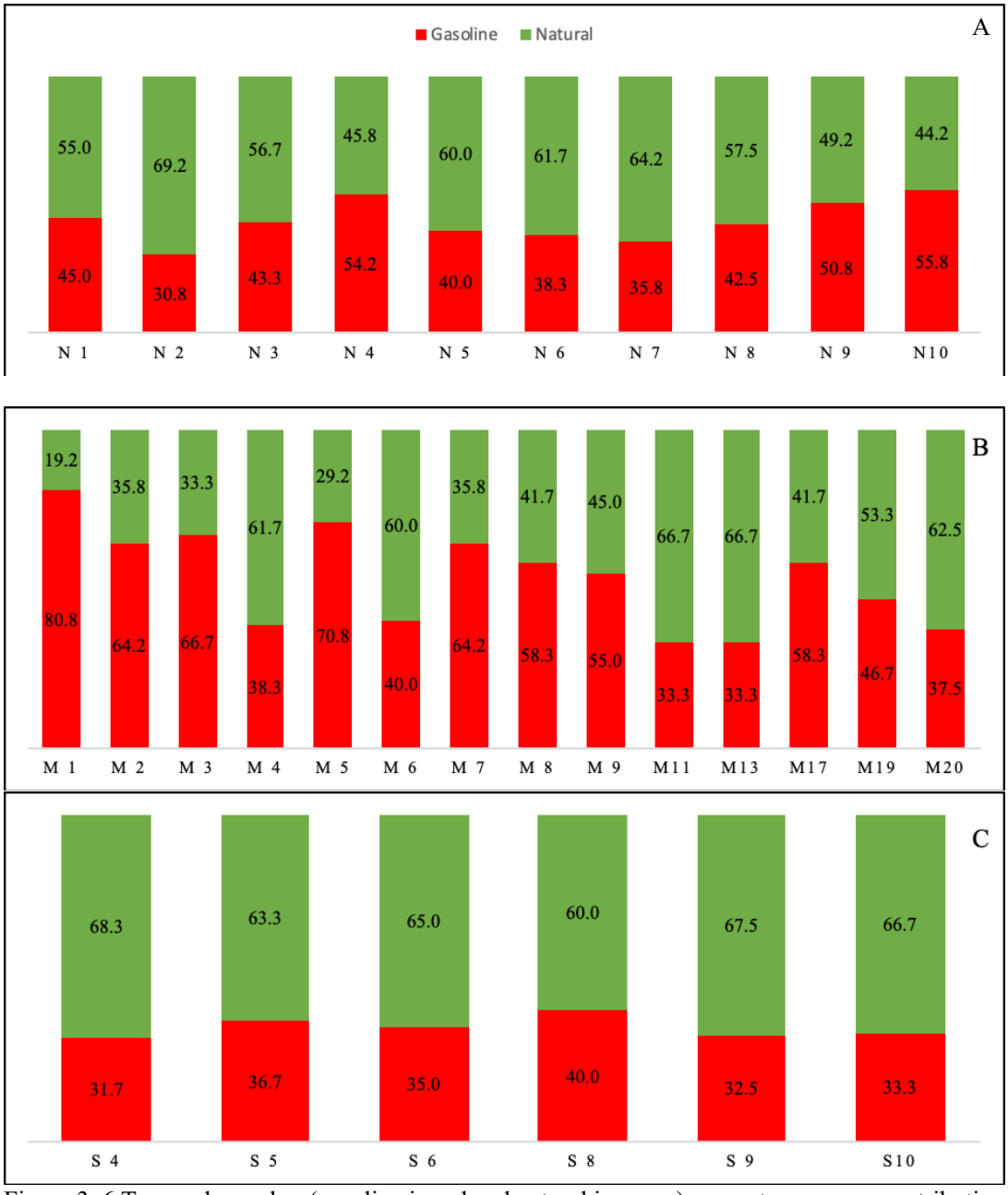

Figure 3. 6 Two end-member (gasoline in red and natural in green) percentage source contribution for North (A), Middle (B) and South (C) locations in the sediment samples with low concentration (< 100 mg/kg).

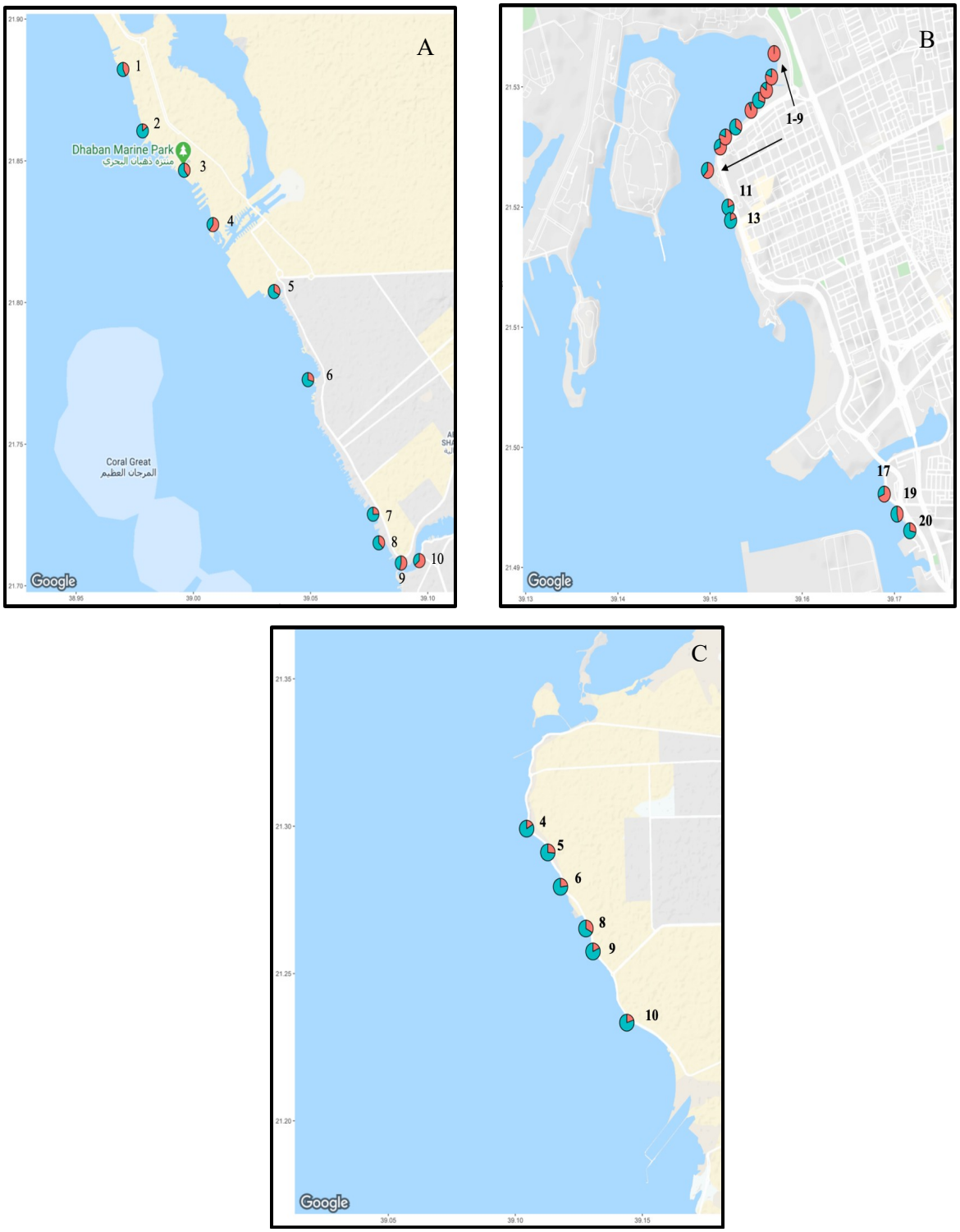

Figure 3. 7 The percentage contributions of the Pb gasoline (red) and natural source of Pb (green) for North (A), Middle (B), and South (C) locations in sediment samples with Pb concentration < 100 mg/kg (n=30).

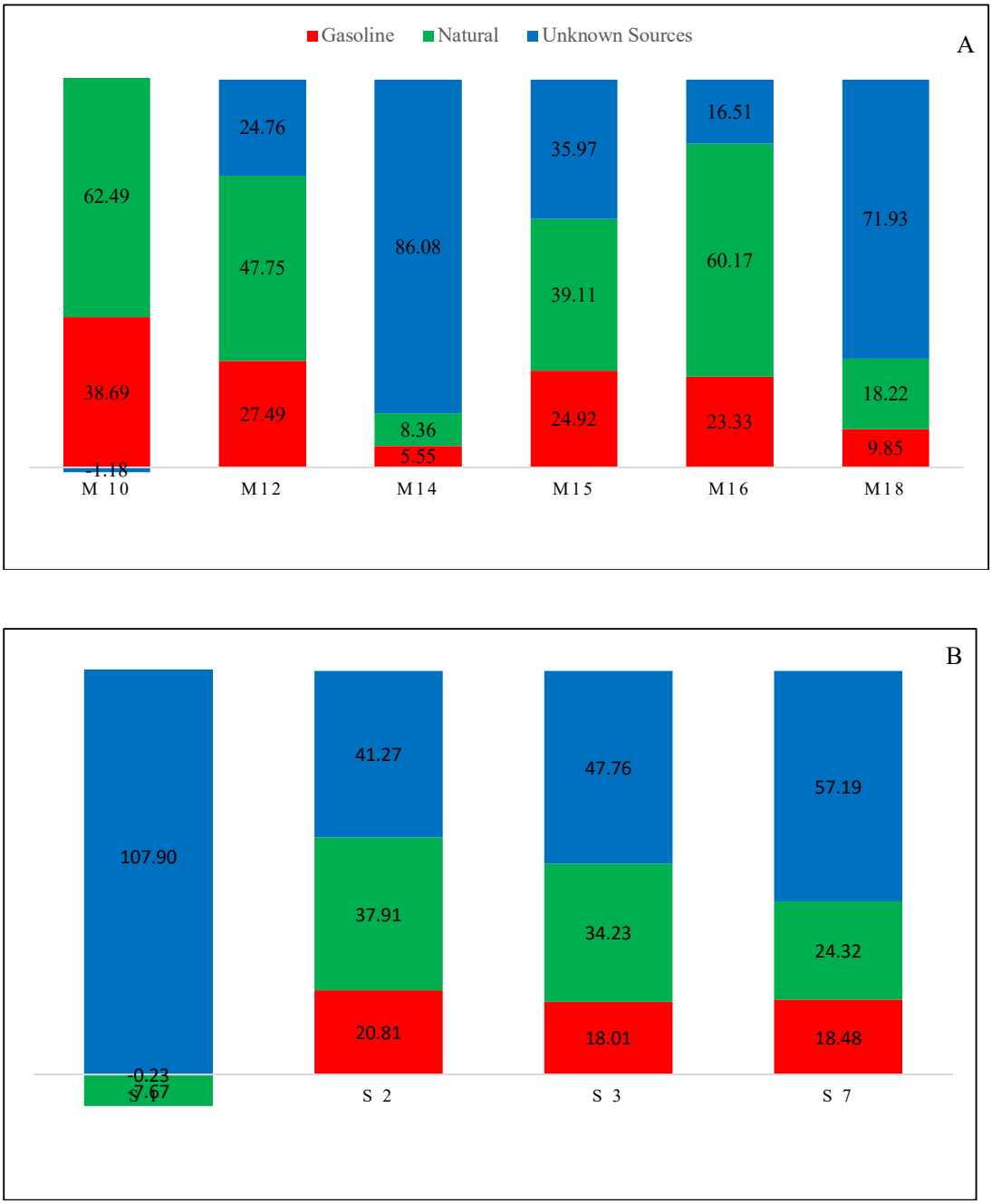

Figure 3. 8 The three-component model (gasoline in red, natural in green, and unknown source in blue) fractional contributions for Middle (A) and South (B) locations in sediment samples with concentrations >100 mg/kg (n=10).

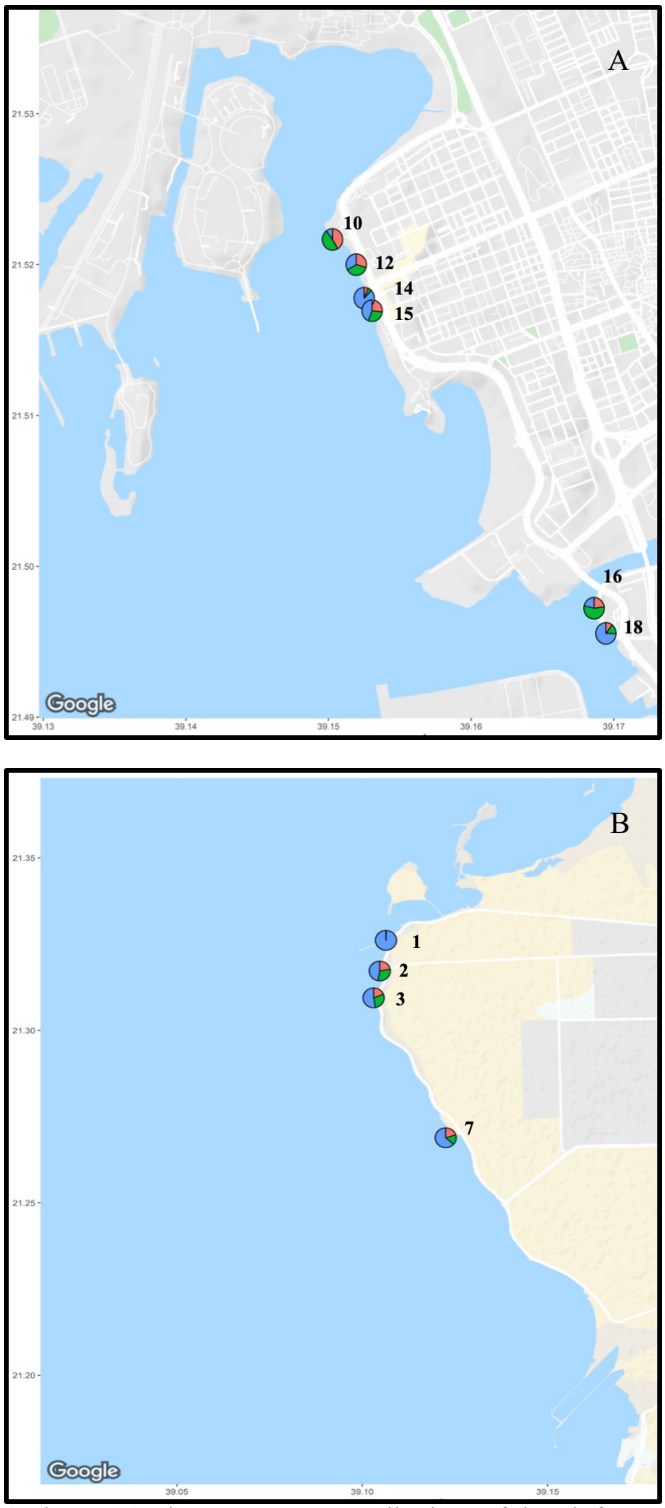

Figure 3. 9 Figure 3.9 The percentage contributions of the Pb from gasoline (red), natural source (green), and unknown source (blue) for Middle (A), and South (B) locations in sediment samples with Pb concentrations > 100 mg/kg (n=10).

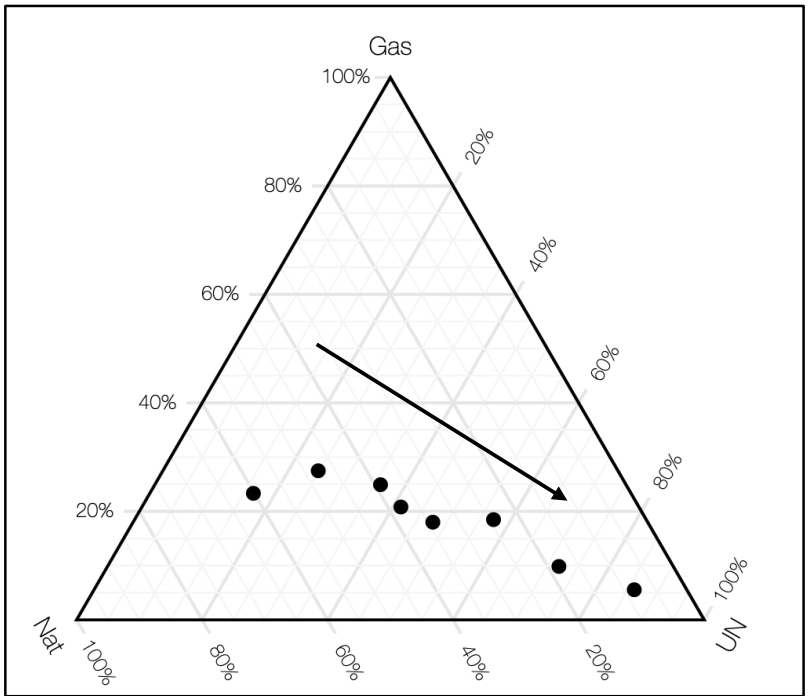

Figure 3. 10 Ternary diagram for the fractional contribution of the three modelled sources: gasoline (Gas), natural (Nat), and unknown source (UN). Sediment samples with Pb concentration > 100 mg/kg with positive fractional components are plotted (n=8).

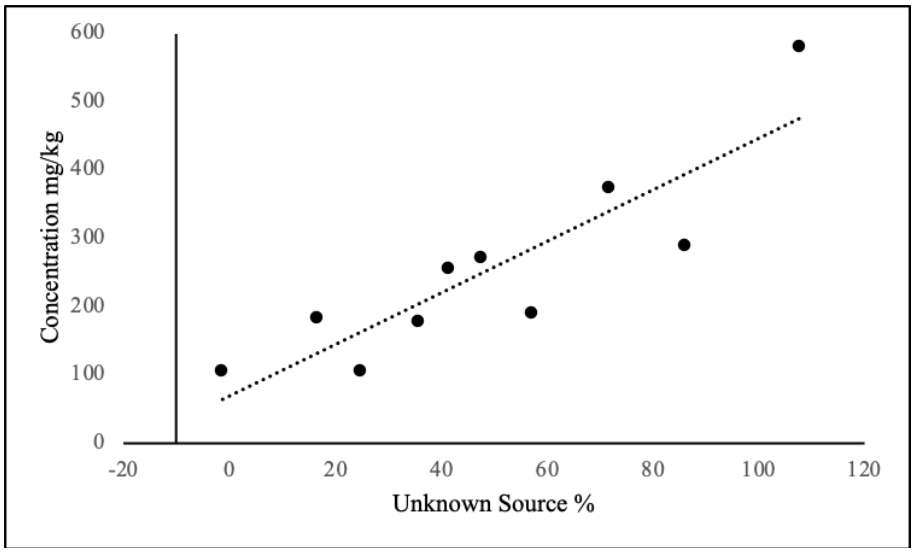

Figure 3. 11 The concentration of Pb in all elevated Pb samples (> 100mg/kg, n=10) versus modelled unknown source fraction shows a significant positive correlation (r^2 =0.76).

.

References

Abu-Zied, R. H., & Orif, M. I. (2019). Recent environmental changes of Al-Salam Lagoon as inferred from core sediment geochemistry and benthic foraminifera, Jeddah City, Saudi Arabia. *Environmental Earth Sciences*, *78*(3), 60. https://doi.org/10.1007/s12665-019-8057- y

Abu-Zied, R. H., Basaham, A. S., & El Sayed, M. A. (2013). Effect of municipal wastewaters on bottom sediment geochemistry and benthic foraminifera of two Red Sea coastal inlets, Jeddah, Saudi Arabia. *Environmental earth sciences*, 68(2), 451-469. https://doi.org/10.1007/s12665- 012-1751-7

Al-Mur, B. A., Quicksall, A. N., & Al-Ansari, A. M. (2017). Spatial and temporal distribution of heavy metals in coastal core sediments from the Red Sea, Saudi Arabia. *Oceanologia*, 59(3), 262-270. https://doi.org/10.1016/j.oceano.2017.03.003

Al-Najjar, T., Rasheed, M., Ababneh, Z., Ababneh, A., & Al-Omarey, H. (2011). Heavy metals pollution in sediment cores from the Gulf of Aqaba, Red Sea. *Natural science*, 3(09), 775. http://dx.doi.org/10.4236/ns.2011.39102

Al-Saleh, I. A., Fellows, C., Delves, T., & Taylor, A. (1993). Identification of sources of lead exposure among children in Arar, Saudi Arabia. *Annals of clinical biochemistry*, 30(2), 142-145. https://doi.org/10.1177/000456329303000205

Alyazichi, Y. M., Jones, B. G., & McLean, E. (2016). Lead isotope fingerprinting used as a tracer of lead pollution in marine sediments from Botany Bay and Port Hacking estuaries, southern Sydney, Australia. *Regional Studies in Marine Science*, 7, 136-141. https://doi.org/10.1016/j.rsma.2016.06.006

Amin, B., Ismail, A., Arshad, A., Yap, C. K., & Kamarudin, M. S. (2009). Anthropogenic

impacts on heavy metal concentrations in the coastal sediments of Dumai, Indonesia. *Environmental Monitoring and Assessment*, *148*(1-4), 291-305. https://doi.org/10.1007/s10661-008-0159-z

Bacon, J. R., Beffow, M. L., & Shand, C. A. (1995). The use of isotopic composition in field studies of lead in upland Scottish soils (UK). *Chemical geology*, 124(1-2), 125-134. https://doi.org/10.1016/0009-2541(95)00030-P

Badawy, W. M., El-Taher, A., Frontasyeva, M. V., Madkour, H. A., & Khater, A. E. (2018). Assessment of anthropogenic and geogenic impacts on marine sediments along the coastal areas of Egyptian Red Sea. *Applied Radiation and Isotopes*, 140, 314-326. https://doi.org/10.1016/j.apradiso.2018.07.034

Badr, N. B., El-Fiky, A. A., Mostafa, A. R., & Al-Mur, B. A. (2009). Metal pollution records incore sediments of some Red Sea coastal areas, Kingdom of Saudi Arabia. Environmental monitoring and assessment, 155(1-4), 509-526.

Barbosa Jr, F., Tanus-Santos, J. E., Gerlach, R. F., & Parsons, P. J. (2005). A critical review of biomarkers used for monitoring human exposure to lead: advantages, limitations, and future needs. *Environmental health perspectives*,113(12), 1669-1674.https://doi.org/10.1289/ehp.7917

Basaham, A. S., Rifaat, A. E., El-Mamoney, M. H., & El Sayed, M. A. (2009). Re-evaluation of the impact of sewage disposal on coastal sediments of the southern Corniche, Jeddah, Saudi Arabia. *Journal of King Abdulaziz University, Marine Sciences*, 20, 109-126. https://www.kau.edu.sa/Files/320/Researches/54566_24891.pdf

Baumann, A. (1994). Lead and strontium isotopes in metalliferous and calcareous pelitic sediments of the Red Sea axial trough. *Mineralium Deposita*, 29(1),81-93.

https://doi.org/10.1007/BF03326398

Bollhöfer, A., & Rosman, K. J. R. (2001). Isotopic source signatures for atmospheric lead: the NorthernHemisphere.Acta,65(11),1727-1740.https://10.1016/S0016-7037(00)00630-X

Carrasco, G., Chen, M., Boyle, E. A., Tanzil, J., Zhou, K., & Goodkin, N. F. (2018). An update of the Pb isotope inventory in post leaded-petrol Singapore environments. *Environmental pollution*, 233, 925-932. https://doi.org/10.1016/j.envpol.2017.09.025

Chen, M., Boyle, E. A., Switzer, A. D., & Gouramanis, C. (2016 a). A century long sedimentary record of anthropogenic lead (Pb), Pb isotopes and other trace metals in Singapore. *Environmental pollution*, 213, 446-459. https://doi.org/10.1016/j.envpol.2016.02.040

Chen, M., Goodkin, N. F., Boyle, E. A., Switzer, A. D., & Bolton, A. (2016 b). Lead in the western South China Sea: Evidence of atmospheric deposition and upwelling. *Geophysical Research Letters*, 43(9), 4490-4499. https://doi.org/10.1002/2016GL068697

Chen, M., Lee, J. M., Nurhati, I. S., Switzer, A. D., & Boyle, E. A. (2015). Isotopic record of lead in Singapore Straits during the last 50 years: spatial and temporal variations. *Marine Chemistry*, 168, 49-59. https://doi.org/10.1016/j.marchem.2014.10.007

Cheng, H., & Hu, Y. (2010). Lead (Pb) isotopic fingerprinting and its applications in lead pollution studies in China: a review. *Environmental Pollution*, *158*(5), 1134-1146. https://doi.org/10.1016/j.envpol.2009.12.028

Chiaradia, M., Chenhall, B. E., Depers, A. M., Gulson, B. L., & Jones, B. G. (1997). Identification of historical lead sources in roof dusts and recent lake sediments from an industrialized area: indications from lead isotopes. *Science of the Total Environment*, 205(2-3), 107-128. https://doi.org/10.1016/S0048-9697(97)00199-X

Choi, M. S., Yi, H. I., Yang, S. Y., Lee, C. B., & Cha, H. J. (2007). Identification of Pb sources

in Yellow Sea sediments using stable Pb isotope ratios. *Marine Chemistry*, 107(2), 255-274. https://doi.org/10.1016/j.marchem.2007.07.008

Dupré, B., Blanc, G., Boulègue, J., & Allègre, C. J. (1988). Metal remobilization at a spreading centre studied using lead isotopes. Nature, 333(6169), 165.

El-Taher, A., Zakaly, H. M., & Elsaman, R. (2018). Environmental implications and spatial distribution of natural radionuclides and heavy metals in sediments from four harbours in the Egyptian Red Sea coast. *Applied Radiation and Isotopes*, 131, 13-22. https://doi.org/10.1016/j.apradiso.2017.09.024

European Food Safety Authority (EFSA). Alexander, J., Benford, D., Boobis, A., Ceccatelli, S., Cravedi, J. P., Di Domenico, A., ... & Filipi9c, M. (2010). Efsa panel on contaminants in the food chain; scientific opinion on marine biotoxins in shellfish—Emerging toxins: Ciguatoxin group. EFSA J, 1627, 1-38.

Faure, G. (1977). Principles of isotope geology, Fourth edition.

Flament, P., Bertho, M. L., Deboudt, K., Véron, A., & Puskaric, E. (2002). European isotopic signatures for lead in atmospheric aerosols: a source apportionment based upon 206Pb/207Pb ratios. *Science of the Total Environment*, 296(1-3), 35-57. https://doi.org/10.1016/S0048- 9697(02)00021-9

Gallon, C., Ranville, M. A., Conaway, C. H., Landing, W. M., Buck, C. S., Morton, P. L., & Flegal,R. (2011). Asian Industrial Lead Inputs to the North Pacific Evidenced by Lead Concentrations and Isotopic Compositions in Surface Waters and Aerosols. Environmental Science & Technology, 45(23), 9874-9882. https://10.1021/es2020428

Gan, T., Zhao, N., Yin, G., Chen, M., Wang, X., Liu, J., & Liu, W. (2019). Optimal chlorophyll fluorescence parameter selection for rapid and sensitive detection of lead toxicity to marine

microalgae Nitzschia closterium based on chlorophyll fluorescence technology. *Journal of Photochemistry and Photobiology B: Biology*, 111551. https://doi.org/10.1016/j.jphotobiol.2019.111551

Gobeil, C., Johnson, W. K., Macdonald, R. W., & Wong, C. S. (1995). Sources and burden of lead in St. Lawrence estuary sediments: isotopic evidence. Environmental science & technology, 29(1), 193-201. https://doi.org/10.1021/es00001a025

Grant, A., & Middleton, R. (1990). An assessment of metal contamination of sediments in the Humber Estuary, UK. Estuarine*, Coastal and Shelf Science*, 31(1), 71-85. https://doi.org/10.1016/0272-7714(90)90029-Q

Hwang, I., Kim, K., Kim, J., & Kang, J. (2016). Toxic effects and depuration after the dietary lead(II) exposure on the bioaccumulation and hematological parameters in starry flounder (Platichthys stellatus . Environmental Toxicology and Pharmacology, 45, 328-333. https://10.1016/j.etap.2016.06.017

Idris, A. M., Eltayeb, M. A. H., Potgieter-Vermaak, S. S., Van Grieken, R., & Potgieter, J. H. (2007). Assessment of heavy metals pollution in Sudanese harbours along the Red Sea Coast.*MicrochemicalJournal*,87(2),104-112. ttps://doi.org/10.1016/j.microc.2007.06.004

Javed, M. (2012). Effects of zinc and lead toxicity on the growth and their bioaccumulation in fish. *Pakistan Veterinary Journal*, 32, 357-362. http://www.pvj.com.pk/.../357-362.pdf

Kahal, A. Y., El-Sorogy, A. S., Alfaifi, H. J., Almadani, S., & Ghrefat, H. A. (2018). Spatial distribution and ecological risk assessment of the coastal surface sediments from the Red Sea, northwest Saudi Arabia. *Marine pollution bulletin*, 137, 198-208. https://doi.org/10.1016/j.marpolbul.2018.09.053

Karuppasamy, M. P., Qurban, M. A., Krishnakumar, P. K., Mushir, S. A., & Abuzaid, N. (2017).

Evaluation of toxic elements As, Cd, Cr, Cu, Ni, Pb and Zn in the surficial sediments of the Red Sea (Saudi Arabia). *Marine pollution bulletin*, 119(2), 181-190. https://doi.org/10.1016/j.marpolbul.2017.04.019

Kersten, M., Garbe-Schönberg, C. D., Thomsen, S., Anagnostou, C., & Sioulas, A. (1997). Source apportionment of Pb pollution in the coastal waters of Elefsis Bay, Greece. *Environmental science & technology*, 31(5),1295-1301. https://doi.org/10.1021/es960473z

Kim, J. H., & Kang, J. C. (2015). The lead accumulation and hematological findings in juvenile rock fish Sebastes schlegelii exposed to the dietary lead (II) concentrations. *Ecotoxicology and environmental safety*, 115, 33-39. https://doi.org/10.1016/j.ecoenv.2015.02.009

Komárek, M., Ettler, V., Chrastný, V., & Mihaljevič, M. (2008). Lead isotopes in environmental sciences: A review. *Environment International*, 34(4), 562–577. https://doi.org/10.1016/j.envint.2007.10.005

Kosnett, M. J. (2007). Heavy metal intoxication and chelators. Basic and clinical pharmacology,10th ed, New York: McGraw-Hill, 945-957.

Laurila, T. E., Hannington, M. D., Petersen, S., & Garbe-Schönberg, D. (2014). Trace metal distribution in the Atlantis II Deep (Red Sea) sediments. *Chemical Geology*, 386, 80-100. https://doi.org/10.1016/j.chemgeo.2014.08.009

Lee, J. W., , H., Hwang, U. K., Kang, J. C., Kang, Y. J., Kim, K. I., & Kim, J. H. (2019). Toxic effects of lead exposure on bioaccumulation, oxidative stress, neurotoxicity, and immune responses in fish: A review. *Environmental toxicology and pharmacology*, 68, 101- 108 https://doi.org/10.1016/j.etap.2019.03.010

Lessler, M. A. (1988). Lead and lead poisoning from antiquity to modern times. *Ohio Journal of Science*, 88 (3).http://hdl.handle.net/1811/23252

Liu, J., Yin, M., Luo, X., Xiao, T., Wu, Z., Li, N., ... & Feng, Y. (2019). The mobility of thallium in sediments and source apportionment by lead isotopes. *Chemosphere*, 219, 864-874. https://doi.org/10.1016/j.chemosphere.2018.12.041

Macirella, R., Sesti, S., Bernabò, I., Tripepi, M., Godbert, N., & Brunelli, E. (2019). Lead toxicity in seawater teleosts: A morphofunctional and ultrastructural study on the gills of the Ornate wrasse (ThalassomapavoL.).Aquatictoxicology,211, 193-201. https://doi.org/10.1016/j.aquatox.2019.04.009

Mansour, A. M., Nawar, A. H., & Madkour, H. A. (2011). Metal pollution in marine sediments of selected harbours and industrial areas along the Red Sea coast of Egypt. *Ann Naturhist Mus Wien Serie A*, 113, 225-244. https://www.jstor.org/stable/41701739

Monastra, V., Derry, L. A., & Chadwick, O. A. (2004). Multiple sources of lead in soils from a Hawaiian chronosequence. *Chemical Geology*,209(3-4), 215-231.https://doi.org/10.1016/j.chemgeo.2004.04.027

Monna, F., Ben Othman, D., & Luck, J. M. (1995). Pb isotopes and Pb, Zn and Cd concentrations in the rivers feeding a coastal pond (Thau, southern France): constraints on the origin(s) and flux(es) of metals. Science of the Total Environment, 166(1), 19-34. https://10.1016/0048- 9697(95)04514-2

Monna, F., Clauer, N., Toulkeridis, T., & Lancelot, J. R. (2000). Influence of anthropogenic activity on the lead isotope signature of Thau Lake sediments (southern France): origin and temporal evolution. *Applied Geochemistry*, 15(9), 1291-1305. https://doi.org/10.1016/S0883-2927(99)00117-1

Monna, F., Lancelot, J., Croudace, I. W., Cundy, A. B., & Lewis, J. T. (1997). Pb isotopic

composition of airborne particulate material from France and the southern United Kingdom: implications for Pb pollution sources in urban areas. *Environmental Science & Technology*, 31(8), 2277-2286. https://doi.org/10.1021/es960870+

Mukai, H., Furuta, N., Fujii, T., Ambe, Y., Sakamoto, K., & Hashimoto, Y. (1993). Characterization of sources of lead in the urban air of Asia using ratios of stable lead isotopes. Environmental Science & Technology, 27(7), 1347-1356. https://doi.org/10.1021/es00044a009

Needleman, H. L., Schell, A., Bellinger, D., Leviton, A., & Allred, E. N. (1990). The long-term effects of exposure to low doses of lead in childhood: an 11-year follow-up report. *New England journal of medicine*, 322(2), 83-88. DOI: 10.1056/NEJM199001113220203

O'Connor, D., Hou, D., Ye, J., Zhang, Y., Ok, Y. S., Song, Y., ... & Tian, L. (2018). Lead-based paint remains a major public health concern: a critical review of global production, trade, use, exposure, health risk, and implications. *Environment international*, 121, 85-101. https://doi.org/10.1016/j.envint.2018.08.052

Pan, K., Lee, O. O., Qian, P. Y., & Wang, W. X. (2011). Sponges and sediments as monitoring tools of metal contamination in the eastern coast of the Red Sea, Saudi Arabia. *Marine pollution bulletin*, 62(5), 1140-1146. https://doi.org/10.1016/j.marpolbul.2011.02.043

Pierret, M. C., Clauer, N., Bosch, D., & Blanc, G. (2010). Formation of Thetis Deep metal-rich sediments in the absence of brines, Red Sea. *Journal of Geochemical Exploration*, 104(1-2), 12- 26. https://doi.org/10.1016/j.gexplo.2009.10.001

Ramadan, M. H., & Halawani, R. F. (2010). Study on Wastewater in Paper Recycling Plants Case Study. *Journal of King Abdulaziz University: Meteorology, Environment & Arid Land Agriculture Sciences,* 21(2).

Ruiz-Compean, P., Ellis, J., Cúrdia, J., Payumo, R., Langner, U., Jones, B., & Carvalho, S. (2017). Baseline evaluation of sediment contamination in the shallow coastal areas of Saudi Arabian Red Sea. *Marine pollution bulletin*, 123(1-2), 205-218. https://doi.org/10.1016/j.marpolbul.2017.08.059

Salem, D. M. A., Khaled, A., El Nemr, A., & El-Sikaily, A. (2014). Comprehensive risk assessment of heavy metals in surface sediments along the Egyptian Red Sea coast. *The Egyptian Journal of Aquatic Research*, 40(4), 349-362. https://doi.org/10.1016/j.ejar.2014.11.004

Sures, B., & Siddall, R. (1999). Pomphorhynchus laevis: The Intestinal Acanthocephalan as a Lead Sink for its Fish Host, Chub (Leuciscus cephalus). Experimental Parasitology, 93(2), 66-72. https://10.1006/expr.1999.4437

Taylor, A. M., & Maher, W. A. (2014). Exposure–dose–response of Tellina deltoidalis to metal contaminated estuarine sediments 2. Lead spiked sediments. *Comparative Biochemistry and Physiology Part C: Toxicology & Pharmacology*, 159, 52-61. https://doi.org/10.1016/j.cbpc.2013.09.006

Townsend, A. T., & Snape, I. (2002). The use of Pb isotope ratios determined by magnetic sector ICP-MS for tracing Pb pollution in marine sediments near Casey Station, East Antarctica. *Journal of Analytical Atomic Spectrometry*, 17(8), 922-928. https://doi.org/10.1039/B203449M

Turekian, K. K., & Wedepohl, K. H. (1961). Distribution of the elements in some major units of the earth's crust. *Geological Society of America Bulletin*, 72(2), 175-192. https://doi.org/10.1130/0016-7606(1961)72[175:DOTEIS]2.0.CO;2

US Environmental Protection Agency. (1996). Method 3050B: Acid digestion of sediments,

sludges, and soils. Test methods for evaluating solid waste, physical/chemical methods.

Vinodhini, R., & Narayanan, M. (2008). Bioaccumulation of heavy metals in organs of fresh water fish Cyprinus carpio (Common carp). *International Journal of Environmental Science & Technology*, 5(2), 179-182. https://doi.org/10.1007/BF03326011

Wang, D., Zhao, Z., & Dai, M. (2014). Tracing the recently increasing anthropogenic Pb inputs into the East China Sea shelf sediments using Pb isotopic analysis. *Marine pollution bulletin*, 79(1- 2), 333-337. https://doi.org/10.1016/j.marpolbul.2013.11.032

Wani, A. L., Ara, A., & Usmani, J. A. (2015). Lead toxicity: a review. *Interdisciplinary toxicology*, 8(2), 55-64. https://doi.org/10.1515/intox-2015-0009

World Health Organization. Edition, F. (2011). Guidelines for drinking-water quality. *WHO chronicle*, 38(4), 104-8.

Xu, D., Wang, R., Wang, W., Ge, Q., Zhang, W., Chen, L., & Chu, F. (2019). Tracing the source of Pb using stable Pb isotope ratios in sediments of eastern Beibu Gulf, South China Sea. *Marine pollution bulletin*, 141, 127-136. https://doi.org/10.1016/j.marpolbul.2019.02.028

Yap, C. K., Cheng, W. H., Karami, A., & Ismail, A. (2016). Health risk assessments of heavy metal exposure via consumption of marine mussels collected from anthropogenic sites. *Science of the Total Environment*, 553, 285-296. https://doi.org/10.1016/j.scitotenv.2016.02.092

Yu, R., Hu, G., Yang, Q., He, H., & Lin, C. (2016). Identification of Pb sources using Pb isotopic compositions in the core sediments from Western Xiamen Bay, China. *Marine pollution bulletin*, 113(1-2), 247-252. https://doi.org/10.1016/j.marpolbul.2016.09.027

Zhu, L., Guo, L., Gao, Z., Yin, G., Lee, B., Wang, F., & Xu, J. (2010). Source and distribution of lead in the surface sediments from the South China Sea as derived from Pb isotopes.

Marine pollution bulletin, 60(11), 2144-2153. https://doi.org/10.1016/j.marpolbul.2010.07.026

Chapter 4

CHARACTERIZATIONS OF $PM_{2.5}$ TRACE METALS FROM THE URBAN-COASTAL AREA OF JEDDAH, SAUDI ARABIA

4.1 Abstract

In this paper, ambient air trace metal concentrations in three urban-coastal locations near Jeddah, Saudi Arabia were analyzed. Jeddah, a coastal city and one of Saudi Arabia's important trade centers with a modest-sized industrial city. The city is, therefore, an attractive target for analysis of airborne delivery of contaminants. The collected data have been examined to measure the compositional changes, to define $PM_{2.5}$ sources, and their contributions and to estimate the influence of atmospheric transport of the ambient PM. Enrichment Factor, Backward Trajectories, and Principle Component Analysis (PCA) were used to categorize and apportion $PM_{2.5}$ sources. The total concentration of Al, Ba, Cr, Cu, Mn, Ni, Pb, V, Zn, Fe, Ti, Ca, Mg, K, and Na were measured from three urban-coastal locations (North, Middle, and South) near Jeddah. The mean particulate matter ($PM_{2.5}$) found was 22.2, 18.9, and 14.2 μg m^{-3} for the Abhour (North Jeddah), Alhamraa (Middle Jeddah), a Alkhomra (South Jeddah) locations, respectively. While elevated $PM_{2.5}$ values were of concern, high lead (Pb) concentrations were documented as well. PCA defined four possible principal sources, and the correlation coefficient results for all elements were supported the PCA finding. PCA results suggest mixed components originating from various sources. Backward trajectory analysis demonstrates air quality intricacies in the

differences of $PM_{2.5}$, specifically with chemical compositions, and clarifies the regional as well as domestic contributions regarding the determined fine air PM concentrations. This study has presented a more in-depth insight into using the trace metals as tracers to verify the emissions sources.

4.2 Introduction

The combination of suspended gases and dust particles that surround us together form air. Any change in this combination impacts the air quality as well as human health. Particulate matter (PM) is derived from either natural sources, such as forest fires, sea spray, dust storms, soil, volcanoes activity, plant pollen, and vegetation (Liora et al., 2015; Kim et al., 2015; Després et al., 2012; Tainio et al., 2010), or anthropogenic sources, including fuel combustion, traffic, corrosion of tires and brakes, different industrial and agricultural activities (Kim et al., 2015; Timmers & Achten, 2016; Taiwo et al., 2014; Mimura et al., 2014). For example, the surface of typical PM has countless pores, which can sorb various pollutants, including heavy metals (Bai et al., 2019). Authors generally emphasize trace elements emitted from industrial activities are significant sources anthropogenic of airborne PM, (Sylvestre et al., 2017; Shaltout et al., 2013). According to Mateus and Gioda (2017). PM has numerous sources and heterogeneous compositions and is , therefore, considered a severe environmental challenge.

$PM_{2.5}$ is particulate matter with diameter <2.5 microns (Esworthy, 2013). Particles of the size are of specific concern as they can go deeper into the respiratory system (Mimura et al., 2014). Several epidemiological reports have documented the link between exposure to $PM_{2.5}$ and adverse health effects such as cardiovascular disease (Lee et al., 2014; McGuinn et al., 2019), increase chronic obstructive pulmonary disease (COPD), asthma

(Bernstein et al., 2004; Hopke et al., 2019), and increase mortality (Laden et al., 2000; Pope et al., 2004).

Heavy metals are often elevated in PM relative to background soils and sediments. Also, they are toxic even at low concentrations (Y. Liu et al., 2018). Furthermore, they are known as non- degradable and biodegradation resistant (J. Liu et al., 2018; Li et al., 2019). Heavy metals such as Cd, Pb, As, Ni, Sb, Cr consider as toxic and carcinogens for human (J. Liu et al., 2018; Shaltout et al., 2013). According to Di Palma et al. (2017), PM acts as a vital transport form of heavy metals in the atmosphere. The size of PM is associated with their potential to be suspended in the atmosphere. PM enable to be transported by the atmosphere for long distances up to thousands of kilometers, and be reminded for long periods, week or up to 30 days (Shaltout et al., 2013; Kim et al., 2015; Tian et al ., 2015). After settlement and during the rain, heavy metal compounds have the ability to transfer inside the food chain and accumulate into the environment.

Emission of pollutants from various sources affect the coastal marine atmosphere, thus impacting the local and regional marine ecosystem (Zhang et al., 2007; Choi et al., 2013). Kadi et al. (2014) pointed out that it is indispensable to examine PM of the local environment as elements influencing its concentrations and behavior. Recently, there has been interest in maritime transport emissions as an added significant source of heavy metals and PM mass concentrations in the coastal marina areas (Nakatsubo et al., 2020; Viana et al., 2014; Xu et al., 2018). Moreover, a variety of studies connect PM increased delivery to coastal areas to sandstorms (Choi & Choi, 2008; Tsai & Chen, 2006). Notably, PM will reflect the inputs of different pollution sources either from the distant areas, including the input from local emissions (Liu et al., 2002).

Saudi Arabia, in recent years, has seen rapid urbanization and industrialization expansion linked to an increase in air pollution (Abdulaal, 2012; Nayebare et al., 2018; Khodeir et al., 2012). Jeddah is an actively growing coastal city in the west of Saudi Arabia. What is more, its economy depends on the tourism industry, logistics and transportation, industrial production, fishing, and oil (Abdulaal, 2012). Both seaport and airport are hubs and traditional stop terminals for pilgrims coming for Makkah, the Holy City, for the Hajj and Umrah throughout the year (Harrison et al., 2017). Jeddah city will have a new comprehensive and integrated public transport service under the Jeddah Public Transportation Program in the next five years (Metro Jeddah, 2019).

To date, there are few studies that have investigated the association between chemical characterization and source apportionment of PM and the general state of air pollution in Jeddah (Kadi 2014; Khodeir et al., 2012; Shaltout et al., 2018) However, few studies have investigated the air quality and the health impacts in Jeddah City (Nayebare et al., 2019; Harrison et al., 2017). Moreover, others studies have characterized PM from sandstorms (Alghamdi., 2015). Abulfaraj et al. (1990) and Aburas et al. (2011) measured Pb concentrations in the Jeddah area and they recommended additional investigations to define the sources of atmospheric Pb.

The $PM_{2.5}$ was collected from three locations to cover the study area: the first location was near the southern coast of Jeddah, the second was near the middle coast of Jeddah, and the third location was near the northern coast of Jeddah. The objectives of the current study are to evaluate $PM_{2.5}$ concentrations and compositions across the three sampling sites and define $PM_{2.5}$ sources, and their contributions and to estimate the influence of atmospheric transport of the ambient PM. Principal Components Analysis

(PCA) was utilized as a known and common statistical method in source apportionment PM researches and also understood the association with each heavy metals in PM.

4.2 Materials and Methods

4.2.1 Sample Collection and Preparation

Air filter samples were gathered from three different locations in Jeddah near the sea: North, Middle, and South. Two filters were collected weekly from each location for three months. Glass fiber filter samples, size 8″ x 10″ for suspended PM less than 2.5 µm ($PM_{2.5}$), were collected by using a high volume ambient particulate matter 2.5 air sampler featuring a mass flow controller (Tisch Environmental- TE-6070 - PM 2.5 MFC). Each sample is an aggregate of 24 hours of collection. The filters were placed in clean plastic bags after sampling. Before and after each sampling, a sampler's vacuum pump was checked to compare flow rates.

The sampler was installed in the North location (Abhor) on the rooftop of a Faculty of Marine Science building at King Abdulaziz University, approximately 10 meters above sea level. The location is near a resort area, the gulf (Sharm Abhour), and King Abdulaziz International Airport. The Middle location (Alhamraa) is the city center of Jeddah and the sampler was placed onto the rooftop of a building approximately 7 meters above sea level. The main fish market and the main desalination plant are the highest potential sources of pollution for this location. The South location (Alkhomra) is located south of Jeddah; the sampler was placed onto the rooftop of a short building approximately 5 meters above sea level. This is near the harbor, Jeddah’s Industrial City, and a mangrove area. A map showing the sites under investigation is illustrated in Figure 4.1.

Prior to the sampling, the filters were placed at room temperature for 24 hours in a

desiccator. A microbalance was used to weigh the filters before and after sampling. Blank filters were processed as well to check for processing errors including gravimetric drift (Srimuruganandam & Nagendra, 2012). After sampling and gravimetric analysis, each filter was divided into two halves. The U.S. EPA method IO 3.5, was applied for elemental extraction and analysis (U.S.EPA. 1999). Briefly, the filter samples were transferred to a 50 mL disposable tube and 10 ml of 16% HCl and 6% HNO_3 was added. The tube was placed on a hot block, covered with a watch glass and heated at 95 ± 5°C for at least 30 minutes. The tube was removed from the hot block and left to cool to room temperature. Subsequently, the extracted solution was transferred to a 50 mL volumetric flask, and the final solution was filtered before analysis.

4.2.2 Analytical Procedure and Analysis

The extracted samples were analyzed via Inductively Coupled Plasma-Mass Spectrometry (ICP-MS) for quantification of total element concentrations of Al, Ba, Cr, Cu, Mn, Ni, Pb, V, Zn, Fe, Ti, Ca, Mg, K, and Na. Analyses were run in gravimetric collection mode.

4.2.3. Apportion and identification and of $PM_{2.5}$ sources

Enrichment Factor, Backward Trajectories and Principle Component Analysis (PCA) were used to categorize and apportion of $PM_{2.5}$ sources.

4.2.3.1 Enrichment Factors

Enrichment factors were computed according to the degree of enrichment in $PM_{2.5}$ related to the earth's crust as described below in equation (4.1) (Nayebare et al., 2018; Taylor 1964; Taylor & McLennan, 1985). Due to its high relative abundance in the crust, aluminum was applied as a reference element to compute EF values (Nayebare et al., 2018).

$$EF = (C_X / C_{Al})\ PM_{2.5} / (C_X / C_{Al})\ crust \quad (4.1)$$

where, C_x concentration of metal X; and C_{Al} Al concentration. Klos et al. (2011) used 10 as a baseline to explain the results of the enrichment factors, where EF≤10 is either crustal in character or unclear as to the anthropogenic impact. However, EF > 10 is indicative of a significant anthropogenic impact (Bai et al., 2019; Nayebare et al., 2018).

4.2.3.2 Backward Trajectory

Backward Trajectory was created using hourly output data of the Weather Research and Forecasting (WRF) model. WRF is the most modern and developed atmospheric modeling system designed for both digital weather forecasting and meteorological study (Qin et al., 2020). In the current study, the analysis was done using a hybrid sigma-pressure vertical coordinate introduced in version 3.9 downloaded from the National Center for Atmospheric Research and Mesoscale and Microscale Meteorology website (UCAR & MMM, n.d)

4.2.3.3 Statistical Analysis

SPSS software (IBM SPSS Statistics Subscription) was used to prepare the Principal Component Analysis (PCA) and the other statistical correlation analysis. PCA was applied to the trace element concentration data gathered at the North location (Abhour), the Middle location (Alhamraa), and the South location (Alkhomra). These analyses were run using Varimax rotation principal component analysis toward four components extracted, which represent sets of trace elements among various sources.

4.3 Results and Discussion

4.3.1 $PM_{2.5}$ Levels

A summary of some descriptive statistics of $PM_{2.5}$ and number of violations of the

daily mean standard of Saudi Arabia, EPA, and WHO guidelines are presented in Table 4.1 (Munir et al., 2016; U.S EPA, 2014; WHO, 2006). The mean $PM_{2.5}$ value was 22.2 μg m^{-3} for the North location (Abhour), 18.9 μg m^{-3} for the Middle location (Alhamraa), and 14.2 μg m^{-3} for the South location (Alkhomra).

The daily Saudi Arabia and EPA standards were exceeded once in both the North and Middle locations. The daily WHO guideline was exceeded three times in the Middle location and twice in the North location. These results show that the South location regularly has lower concentrations than the other two sites, possibly due to the effect of urbanization in Jeddah and the predominant clean marine air influx from the west, despite the industrial activities located in the eastern direction of this location. $PM_{2.5}$ concentrations of this study match results of previous studies carried out in KSA, but not the results of studies carried out in China and Italy (Table 4.2).

4.3.2 Elemental Concentrations

As shown in Table 4.2, the trace metal average concentrations for all locations followed the pattern: Al > Fe > Pb > Cu > Na > V > Zn > Ba > Ti > Mn > Ni > Ca > Cr > Mg > K. Al (781.1 ng m^{-3}) and Fe (413.17 ng m^{-3}) are major elemental components followed by Pb (57.80 ng m^{-3}) and Cu (54.87 ng m^{-3}). Al is considered a crustally-derived element, so the primary source of Al is likely re- suspension of soil-derived particles to the atmosphere (Nayebare et al., 2018; Gao & Anderson, 2001; Marcazzan et al., 2001; Lim et al., 2018). Fe and Cu are enriched in fine PM, attached to both fly ash from heavy oil and coal combustion. (Gordon, 1988; Sylvestre et al., 2017). However, some studies suggest that the earth's crust is the primary source of Fe into PM (Nayebare et al., 2018; Lim et al., 2018). Al and Fe concentrations of this study are in agreement with the results of studies

previously carried out near Jeddah (Al=800 ng m^{-3}, Fe= 590 ng m^{-3}) by Khodeir et al. (2012), and in Italy by Squizzato et al. (2017) (Al=829.5 ng m^{-3}, and Fe=160 ng m^{-3}) , but not with those of a recent Rabigh study, a coastal Red Sea city (Al=1742 ng m^{-3}, Fe=1667 ng m^{-3}) by Nayebare et al. (2016). Nevertheless, the current results exceed those of a recent study from China (Al=117.2 ng m^{-3}, and Fe=86.9 ng m^{-3}) by W. Liu et al. (2018).

The observed depression in Pb concentration in the South location (Alkhomra) (10.2 ng m^{-3}) relative to its values in the other two locations (55 and 108.2 ng m^{-3} for the North and Middle, respectively) suggest that its source is mainly traffic. Aburas et al. (2011) pointed out that the amounts of consumed fuels for the desalination plant and power generation plants for the city contain an estimated Pb amount of around 56 tons/year. Pb average concentration in this study (57.80 ng m^{-3}) was higher than that indicated in Rabigh (7 ng m^{-3}), China (4.8 ng m^{-3}), and Italy (18.4 ng m^{-3}) (Liu et al., 2018; Nayebare et al., 2016; Squizzato et al., 2017) but lower than that obtained in a recent Jeddah study (160 ng m^{-3}) (Khodeir et al., 2012). Cu average concentration in this study was 54.76 ng m^{-3} which was higher than that observed in the studies mentioned in Table 4.2. Anthropogenic emissions are likely the predominant source for Cu.

4.3.3 Identification and apportion of PM2.5 sources.

Enrichment factor, Backward Trajectory and Principle Component Analysis (PCA) were applied to explore $PM_{2.5}$ sources in the area under investigation.

4.3.3.1 Enrichment Factor Analysis (EF)

The current study applied enrichment factor analysis to measured concentration data to define the crustal versus non-crustal sourcing of elements in the PM samples. Weathering or decomposition of earth's crust soil or soil re-suspension activities plus the anthropogenic

processes are considered as the primary sources of trace elements in PM (Khodeir et al., 2012; Nayebare et al., 2016). The distribution of both anthropogenic and natural sources, according to the EF calculation is summarized in Figure 4.2. Anthropogenic sources were clear contributions to enrichment, as shown by EF values >10, for Fe, Pb, and Cu; however, K, Mg, Ca, Cr, Ti, Ni, Mn, Ba, Na, Zn, and V were crustally- derived. Many of the latter exceed EF values of 1 suggesting enrichment but do not exceed the threshold of 10, the baseline used to clearly identify significant anthropogenic contribution (Klos et al., 2011).

Frequently, the sources of the anthropogenic emission in an urban environment are of combustion origins, including emissions from vehicle exhaust, as well as industrial activities (Birmili et al., 2006; Lough et al., 2005; Sternbeck et al., 2002). Both Fe concentration and EF are high in this study (Figure 4.2 and Table 4.2) supporting the interpretation that a portion of the Fe is derived from vehicle exhaust emissions (Amato et al., 2009; Yatkin & Bayram, 2008). Pb, and Cu EF values suggest traffic emissions, tire wear, incineration, fossil fuel combustion, non–ferrous metal industries, and construction activities (Nayebare et al., 2018; Al-Taani et al., 2015; Mateus & Gioda, 2017; Aburas et al., 2011). The relatively considerable EF values for Na may not necessarily be indicative of a significant anthropogenic contribution but rather may be attributable to marine input as sea salt (sea-spray) (Khodeir et al., 2012; Nayebare et al., 2016). Furthermore, the EF values of Zn and V are substantially higher than for other crustal elements. V derives frequently from fuel oil combustion, while Zn regularly comes from vehicular emissions, metal production and combustion in industry (Taiwo et al., 2014; Nayebare et al., 2016; Al-Taani et al., 2015).

4.3.3.2 Backward Trajectory

The wind rose diagrams of the prevailing wind speed and direction are illustrated in Figures A and B during the period from June 15, 2017, to September 15, 2017, where most of the wind was North to West while less of the wind blew from the Southwest to West. The time series data for daily concentrations of $PM_{2.5}$ are shown in Figure 4.4, revealing two events of sudden increase in $PM_{2.5}$ during August 2, and September 13.

Figure 4.5 displays the wind trajectories 72-hrs before sampling for the highest $PM_{2.5}$ values for two days (August 2 and September 13, 2017) followed by eight days of 24-hour periods for forecasted backward trajectory starting at 8 AM each day. The trajectory is labeled from 1 to 8: 1 = the first day, 2 = second day, and 8 is the last day of forecasting. On the fourth day (August 2) as shown in Figure 4.6, and the wind direction was mostly West toward the sampling site. In Figure 4.5 A, the trajectory of the 4^{th} day (August 2, 2017) was from the west which brings air from west of Red Sea where heavy dust storms occur in the Tokar Desert in northeastern Sudan. In Figure 4.5 B, the trajectory of the 4th day (September 13, 2017) was from the northwest Rabigh city. The backward trajectory analysis demonstrated that regional as well as domestic sources contribute to the fine air PM concentrations measured.

Figure 4.7 A and 4.7 B shows that the Moderate Resolution Imaging Spectroradiometer (MODIS) from NASA's Terra satellite captured dust blowing over the Red Sea from August 1 and 2, 2017. The dust plume blew from the Sudan coast and spread out over the Red Sea. Parallel lines into the dust plume vertical to the prevailing wind direction are made by cross-currents of air. Some of the thickest plumes were located near Tokar in northeastern Sudan near the Sudan-Eritrea border. Figure 4.8 A and 4.8 B shows the plume of dust over the Red Sea from North to South, affecting air quality and increasing

the concentrations of $PM_{2.5}$.

4.3.3.3. Factor analysis (FA) and probable source identification

In order to identify conventional sources for trace elements in coastal PM in the Jeddah region. Table 4.3 presents the factor loading results with Varimax rotation and the commonalities. The results explain 84.39% of the total variance and indicate that four factors.

The first factor was densely loaded with Na, Mg, Ca and K, and the presence of Al and Ba; this factor explained most of the total variance (43.75%). These elements help to classify this factor as a combined source of marine aerosol and re-suspension of soil-derived particles. These elements were likely transported from a distal source, during the dust episodes that blew over the city on August 2 and September 13, 2017. The PM can reach the coastal area of Jeddah by strong winds over vast distances. Strong winds blew over Jeddah city from the Tokar region in East Sudan supporting the interpretation of this as a source. Further, similar data was reported by Khodeir et al. (2012). Also, Alghamdi et al. (2015) considered these elements (except for the Ba) as crustal elements, and their concentrations are expected to increase with dust storms.

The second factor explained 18.29% of the total variance. It contained Fe, Ti, and Mn. These elements are typically terrigenous in origin ,but the sourcing of the co-extrusion of these elements can be more complicated than a mono-source. Some PM studies considered Fe as a resuspended dust element; however, other authors suggest it may be emitted from mixed natural and anthropogenic sources (Khodeir et al., 2012; Nayebare et al., 2018; Alghamdi et al., 2015). Similarly, Heal et al. (2005) reported these elements could be emitted from a crustal source besides the local road dust. Indeed, an atmospheric

study for a Chinese coastal site by Gao & Anderson (2001) found enriched Fe in PM attributed into fly ash of coal and heavy oil combustion mixed with natural sources. Ti and Fe frequently originate from regional anthropogenic pollution sources in the Jeddah area (Nayebare et al., 2018). Notably, throughout the sampling, there was major infrastructure development occurring in the city, which involves extensive construction activities and massive transportation. Additionally, these elements are common elements from car tires, brake pads, and cement and concrete industries (Nayebare et al., 2018). In this study, the authors favor the mixed source interpretation given the elevated EF and concentration for Fe.

The third factor explained 14.49% of the total variance and has V, Ni, and Cu likely due to the emissions of oil combustion (Nayebare et al., 2018; Gordon, 1988). Oil refineries, desalination plants, power plants, and industrial and large boilers have been reported as the sources of these elements to Jeddah's atmosphere (Khodeir et al., 2012). The inclusion of Cu in this factor implies that it is of industrial origin (Marcazzan et al., 2001).

Finally, the fourth factor explained only small variance (7.86%) and contained Pb, and Zn. The association of Pb with Zn suggests that pollution emissions of these metals were incineration and fossil fuel combustion (Taiwo et al., 2014; Mateus & Gioda, 2017). According to Aburas et al. (2011), the Saudi government phased out leaded gasoline in 2001. Hjortenkrans et al., (2006) suggest these metals are usually anthropogenic and derived from traffic-related materials, such as brake dust and tire tread .In this study, then, the fourth factor is likely derived from either incineration or transit materials wear.

A correlation matrix for the elements from each of the three locations with r values is presented in Table 4.4. The elements measured of marine and land origin show strong

and statistically significant positive correlations between Na and Al (r = 0.78), Ba (0.76), Ca (0.92), Mg (0.95), and K (0.95). K is also shown to have strong positive correlations with Ba (0.87), Ca (0.90), and Mg (0.97). Ni &V are strongly correlated with each other (0.93) supporting the third factor from PCA. Likewise, Mn shows a strong correlation with Ti (0.99) and Fe (0.99), which is consistent with the PCA findings for the second factor. The weak correlation among other measured elements may indicate that local sources and, therefore, were variable and not likely transported over a long distances.

4.3 Conclusions

This study presents results of ambient $PM_{2.5}$ aerosol collections across three locations in the urban-coastal area of Jeddah, Saudi Arabia, between June 18, 2017, to September 13, 2017. The main aims of the study are to evaluate the impacts of different emissions sources on $PM_{2.5}$ concentrations and composition across the three sampling sites. Data have been examined to assess the differences, to determine $PM_{2.5}$ sources and to evaluate the influence of atmospheric transport of the ambient $PM_{2.5}$. Major outcomes from this study are outlined below:

a) $PM_{2.5}$ average concentrations over the Jeddah Coastal area were 14.2, 18.9, and 22.2 $\mu g\ m^{-3}$ for the South, Middle, and North locations, respectively. These results indicate that the South location has lower concentrations than the other two sites due to the effect of the clean marine air despite relatively close industrial activities that are located downwind.
b) Al and Fe are major elemental components followed by Pb and Cu. The main source of Al and Fe is likely re-suspension of soil-derived particles. Atmospheric Fe and Cu are enriched in PM, attributed to either fly ash from coal and/or heavy oil combustion.

The observed low Pb concentration in the South location (Alkhomra) relative to its values in the other two locations indicate that its source is likely traffic.

c) High EFs for Fe, Pb and Cu, suggest a variety of municipal and industrial sources. The high EF values for Na may be attributed to marine input. The EF values of Zn and V are substantially higher than those for the other crustal elements indicating a clear anthropogenic supply in the urban-coastal area of Jeddah.

d) The daily concentrations of $PM_{2.5}$ showed an increased in two days August 2 and September 13. The trajectory of August 2, 2017 was from the west where a heavy dust storm occurred in the Tokar desert. This is supported by the MODIS images for the same date. The trajectory of September 13, 2017 was from the Northwest. The wind blew over the land and supplied PM to Rabigh and Jeddah.

e) Principle Component Analysis results identified four likely principal sources: particles originating from the marine aerosol and re-suspension of soil-derived particles, particles of mixed natural terrigenous and different sourcing, particles originating from oil combustion and/or heavy industrial emissions, and particles originating from incineration and/or transit materials wear. These interpretations are supported by the elemental correlation matrix from each of the three locations.

The results of this study can both be used as a baseline for future anthropogenic effects of trace metals in the Jeddah coastal area as well as guidance for current remediation strategies and future control policies. These conclusions are consistent with prior research and point to the need for more comprehensive investigation into air pollution in the coastal area to fully understand the significant and major sources of particulate air pollutants in the coastal and neighboring regions. The authors also suggest more measurements of heavy

metals from $PM_{2.5}$ coupled with simultaneous collection of marine water and sediments over long-term sampling to get a clear understanding of aerosol delivery of heavy metals to the regional marine environment in the area, especially Pb. The EF of Pb was high, indicating other anthropogenic sources other than residue remaining of leaded gasoline. Further research is needed to evaluate their contributions to Pb concentrations and distribution to effectively control and manage Pb pollution in the region.

Table 4. 1 Mean, standard deviation (SD), minimum, maximum, and number of violations of the daily mean standard of Saudi Arabia, EPA, and WHO guidelines.

Site Name		North location (Abhour)	Middle location (Alhamraa)	South location (Alkhomra)
Site type		Coastal - Urban - background	Coastal - Urban	Coastal - Suburban - Industrial
Sampling period in 2017		July 30 - Sept. 13	June 18 - Sept. 13	June 18 - July 26
$PM_{2.5}$ ($\mu g\ m^{-3}$)	Mean	22.2	18.9	14.2
	S.D.	11.4	7.5	3.3
	Min.	14.9	10.7	10.1
	Max.	56.5	40.1	20.7
No. of samples		12	21	11
No. of daily mean violations ($\mu g\ m^{-3}$)	S.A. & EPA (35)[1]	1	1	0
	WHO (25)[2]	2	3	0

[1]Daily mean standard of Saudi Arabia and EPA and their value.

[2]WHO daily mean standard and its value.

Table 4. 2 Elemental chemical composition ($PM_{2.5}$ average ± S.D. in µg m^{-3}, Elements average ± S.D. in ng m^{-3}) determined in three sites in this study and other studies.

Reference	Site	$PM_{2.5}$	Al	Ba	Cr	Cu	Mn	Ni	Pb	V	Zn	Fe	Ti	Ca	Mg	K	Na
This study	North location (Abhour)	22.2 ±11.4	780.0 ±170.0	16.0 ±5.9	10.0 ±5.1	75.0 ±34.6	17.0 ±15.0	10.0 ±7.5	55.0 ±101.0	27.0 ±19.1	34.0 ±15.4	727.0 ±760.4	20.0 ±20.2	7.0 ±2.0	3.0 ±0.8	2.0 ±0.5	29.0 ±4.8
	Middle location (Alhamraa)	18.9 ±7.5	887.7 ±251.5	14.7 ±4.8	6.5 ±3.5	28.6 ±9.4	8.3 ±7.6	7.7 ±2.7	108.2 ±288.4	22.8 ±8.7	23.3 ±13.6	308.1 ±357.9	9.1 ±10.9	7.5 ±2.3	2.9 ±0.8	2.1 ±0.6	29.3 ±8.2
	South location (Alkhomra)	14.2 ±3.3	675.6 ±211.9	9.5 ±3.8	4.6 ±2.5	61.0 ±29.6	5.8 ±1.8	10.4 ±3.1	10.2 ±9.8	32.5 ±8.2	23.7 ±11.7	204.4 ±75.6	5.2 ±2.2	6.8 ±2.2	2.5 ±0.8	1.8 ±0.6	25.7 ±7.3
	Average	18.43	781.10	13.40	7.03	54.87	10.37	9.37	57.80	27.43	27.00	413.17	11.43	7.10	2.80	1.97	28.00
Khodeir, et al., 2012	Jeddah (urban - residential), KSA	28.4	800.0 ±1600.0	34.0 ±41.0	2.1 ±3.9	5.6 ±8.8	19.0 ±41.0	6.6 ±3.6	160.0 ±350.0	23.0 ±12.0	41.0 ±69.0	590.0 ±1400.0	55.0 ±160.0	540.0 ±960.0	300.0 ±510.0	190.0 ±230.0	430.0 ±390.0
Nayebare, et al., 2016	Rabigh, Makkah Province, KSA	37.0 ±16.2	1742.0 ±1375.0	--	4.8 ±4.2	5.1 ±3.3	33.7 ±25.6	9.4 ±4.1	7.0 ±6.0	14.5 ±14.6	21.0 ±7.7	1667.0 ±1294.0	168.0 ±130.0	2425.0 ±1942.0	662.0 ±421.0	639.0 ±404.0	1092.0 ±667.0
Liu et al., 2018	Three coastal cities of the Bohai Sea, northern China	116.2 ±64.4	117.2 ±127.1	--	2.0 ±1.4	17.6 ±17.6	26.6 ±18.3	2.4 ±1.6	4.8 ±4.8	9.2 ±5.3	163.7 ±148.0	86.9 ±80.6	--	--	--	--	--
Squizzato et al., 2017	Treviso, Italy	49.5 ±28.5	829.5 ±24.0	--	--	11.0 ±16.7	7.1 ±6.7	5.4 ±5.2	18.4 ±16.6	1.6 ±1.6	54.8 ±31.2	160.5 ±121.5	6.4 ±13.3	423.5 ±137.5	93.0 ±877.0	912.5 ±591.0	--

Table 4. 3 Rotated component matrix for trace elements data from the three sites in Jeddah (principal factors ≥ 0.6 are bold in each column).

Element	Factors				Communalities
	1	2	3	4	
Na	**0.972**	0.098	-0.014	-0.022	0.954
Mg	**0.946**	0.288	-0.003	0.072	0.984
Ca	**0.943**	0.099	0.027	-0.050	0.903
K	**0.936**	0.303	0.094	0.035	0.979
Al	**0.859**	0.059	-0.133	0.217	0.806
Ba	**0.736**	0.567	-0.059	0.242	0.926
Fe	0.200	**0.973**	0.006	0.054	0.989
Ti	0.228	**0.967**	-0.036	0.040	0.989
Mn	0.214	**0.966**	0.037	0.115	0.994
V	-0.009	-0.098	**0.829**	0.397	0.854
Ni	0.017	0.075	**0.813**	0.462	0.880
Cu	-0.026	0.011	**0.812**	-0.177	0.691
Pb	0.067	-0.037	0.003	**0.860**	0.746
Zn	0.010	0.178	0.276	**0.702**	0.601
Cr	0.372	0.207	0.113	0.410	0.362
% of Variance	43.750	18.292	14.494	7.856	
Cumulative %	43.750	62.042	76.536	84.391	

Table 4. 4 Correlation matrix showing r values for trace metals combined from the three study sites (bold correlations are significant at p>0.05).

Element	Al	Ba	Cr	Cu	Mn	Ni	Pb	V	Zn	Fe	Ti	Ca	Mg	K	Na
Al	1.00	**0.75**	0.32	-0.12	0.27	-0.01	0.25	-0.01	0.12	0.24	0.28	**0.75**	**0.83**	**0.78**	**0.78**
Ba		1.00	0.42	-0.09	**0.73**	0.11	0.26	0.00	0.24	**0.70**	**0.72**	**0.69**	**0.88**	**0.87**	**0.76**
Cr			1.00	0.05	0.30	0.34	0.19	0.06	0.35	0.26	0.26	0.27	0.39	0.46	0.39
Cu				1.00	-0.01	0.41	-0.04	0.44	0.20	-0.02	-0.02	-0.04	-0.05	0.05	-0.04
Mn					1.00	0.17	0.09	0.00	0.25	**0.99**	**0.99**	0.30	0.49	0.50	0.30
Ni						1.00	0.35	**0.93**	0.45	0.12	0.06	0.04	0.07	0.13	0.00
Pb							1.00	0.37	0.43	0.05	0.05	0.04	0.14	0.07	0.03
V								1.00	0.37	-0.05	-0.10	0.01	0.01	0.04	-0.06
Zn									1.00	0.18	0.17	0.01	0.11	0.13	0.05
Fe										1.00	**0.99**	0.30	0.48	0.48	0.28
Ti											1.00	0.32	**0.50**	0.49	0.31
Ca												1.00	**0.94**	**0.90**	**0.92**
Mg													1.00	**0.97**	**0.95**
K														1.00	**0.95**
Na															1.00

Figure 4. 1 Regional map showing the three sample sites under investigation.

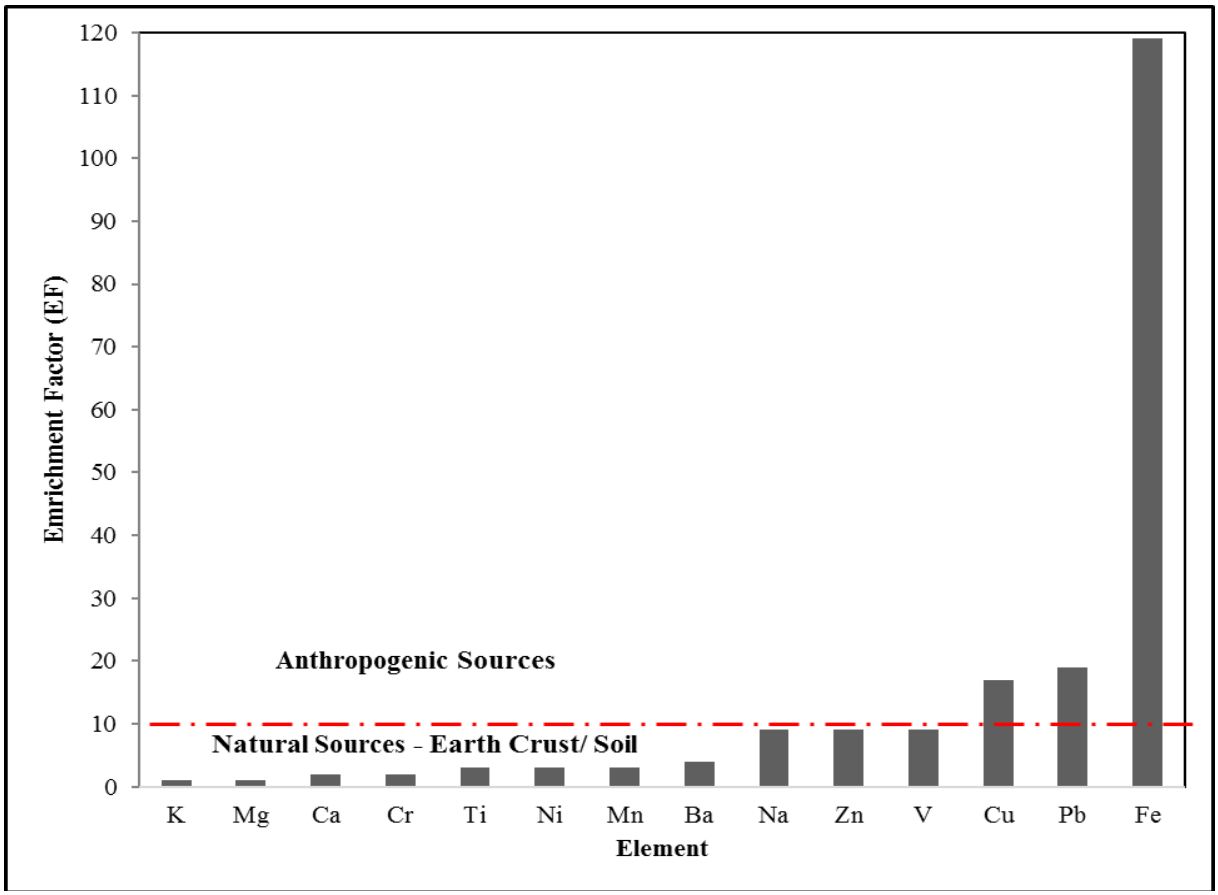

Figure 4. 2 Average elemental Enrichment Factors (EF) for the study region. Red line indicates threshold for clear contamination above natural background.

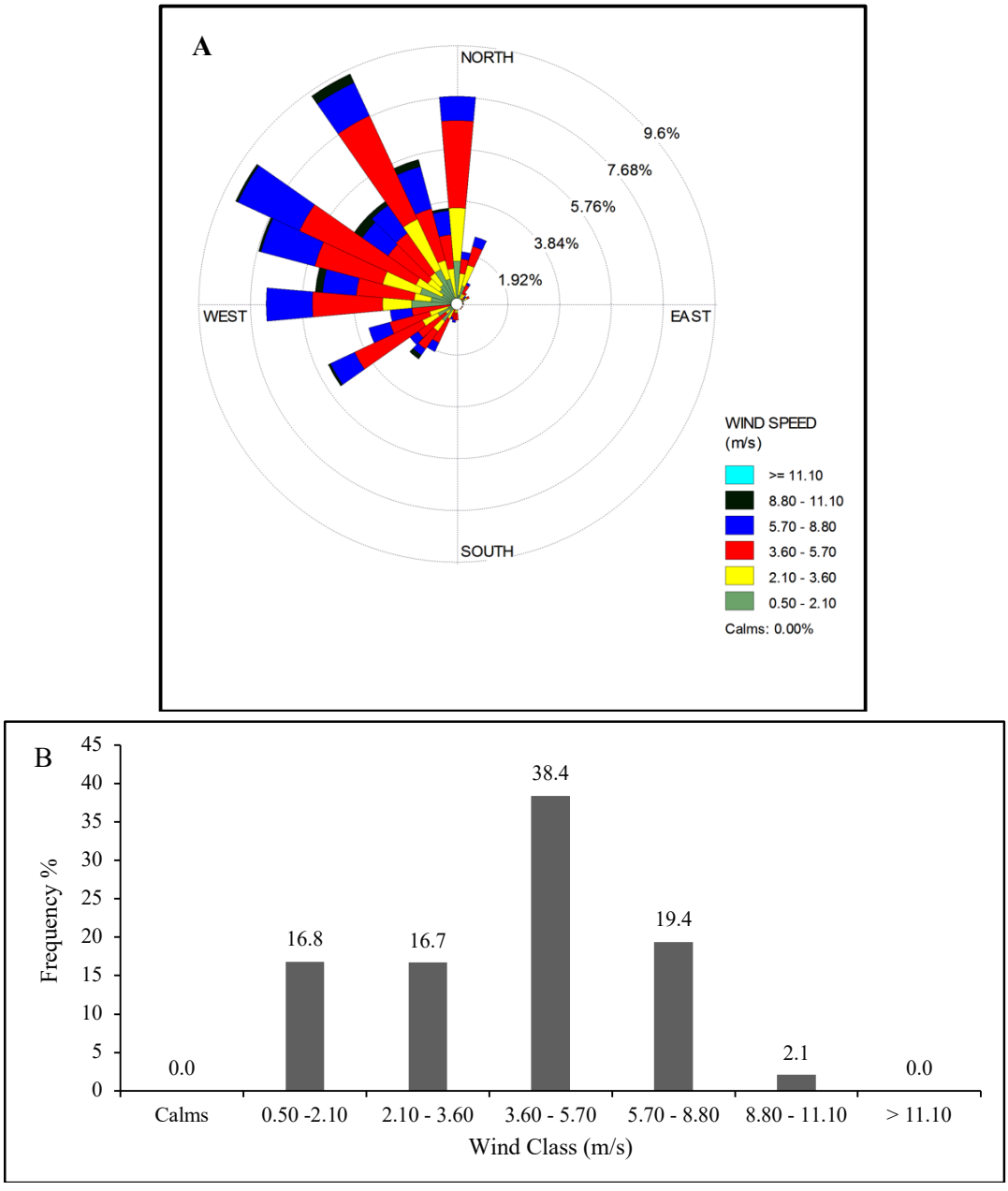

Figure 4. 3 Wind rose for Jeddah, (A) and Wind Class (B)for Jeddah; during the period June 15 to September 15 2017.

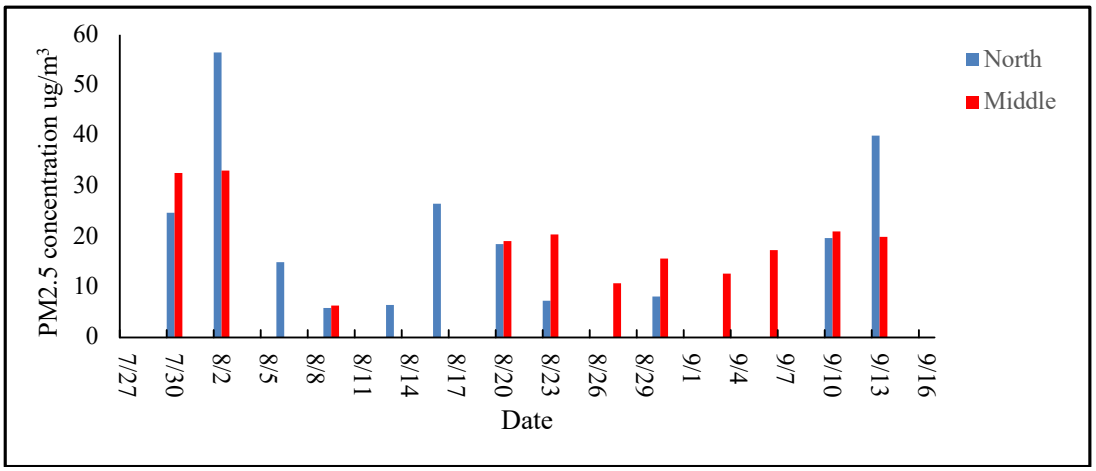

Figure 4. 4 Time series of observed $PM_{2.5}$ from July 27 to September16 2017 for the North and Middle sample locations.

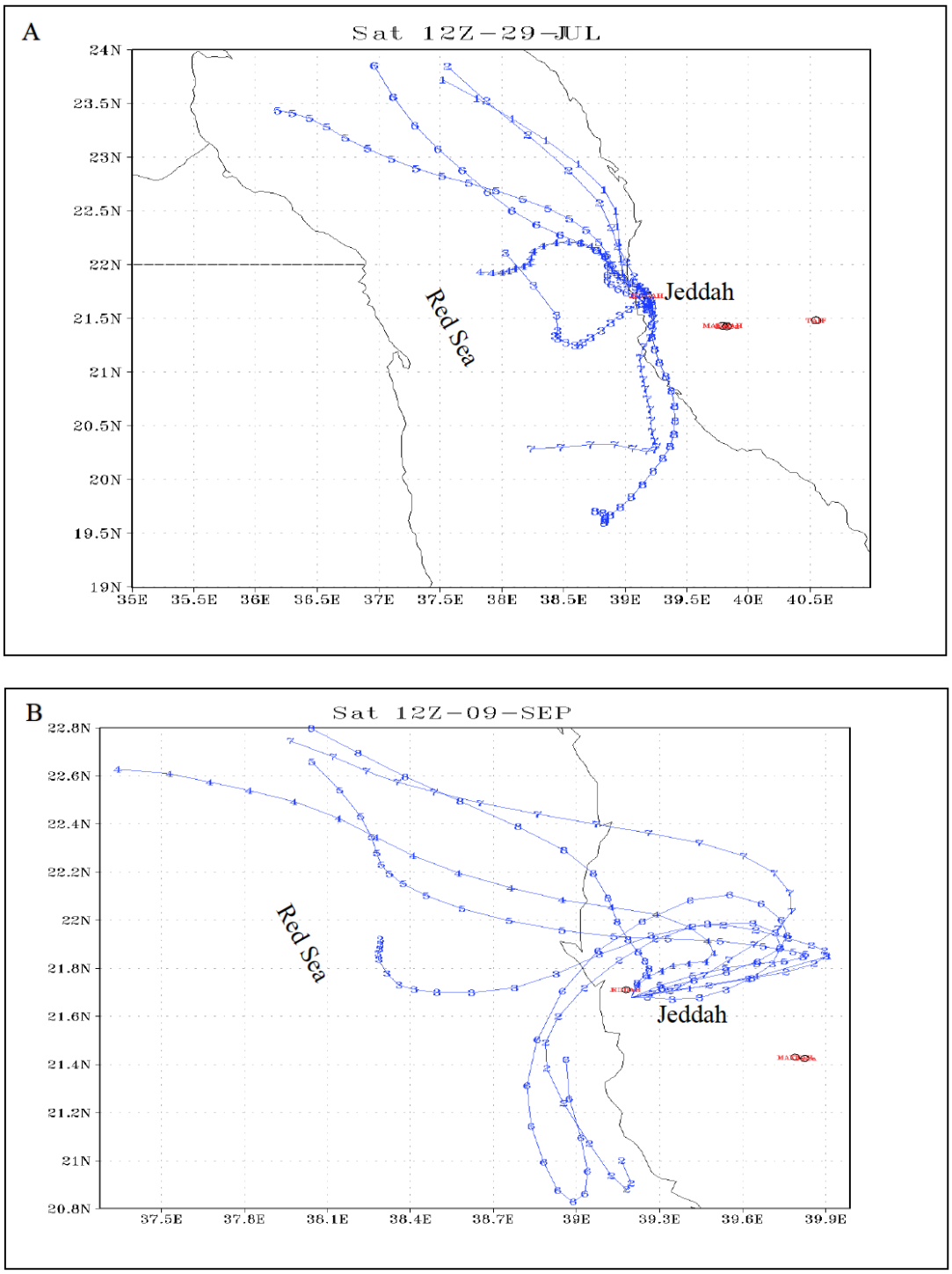

Figure 4. 5 72 Hours forecasted backward trajectory for eight days reach Jeddah at 8 AM. Trajectories labeled from 1 to 8: 1 is the first day, 2 is the second day and 8 is the last day of forecasting (A., 12z29 July 2017 and B., 12z09 September 2017)

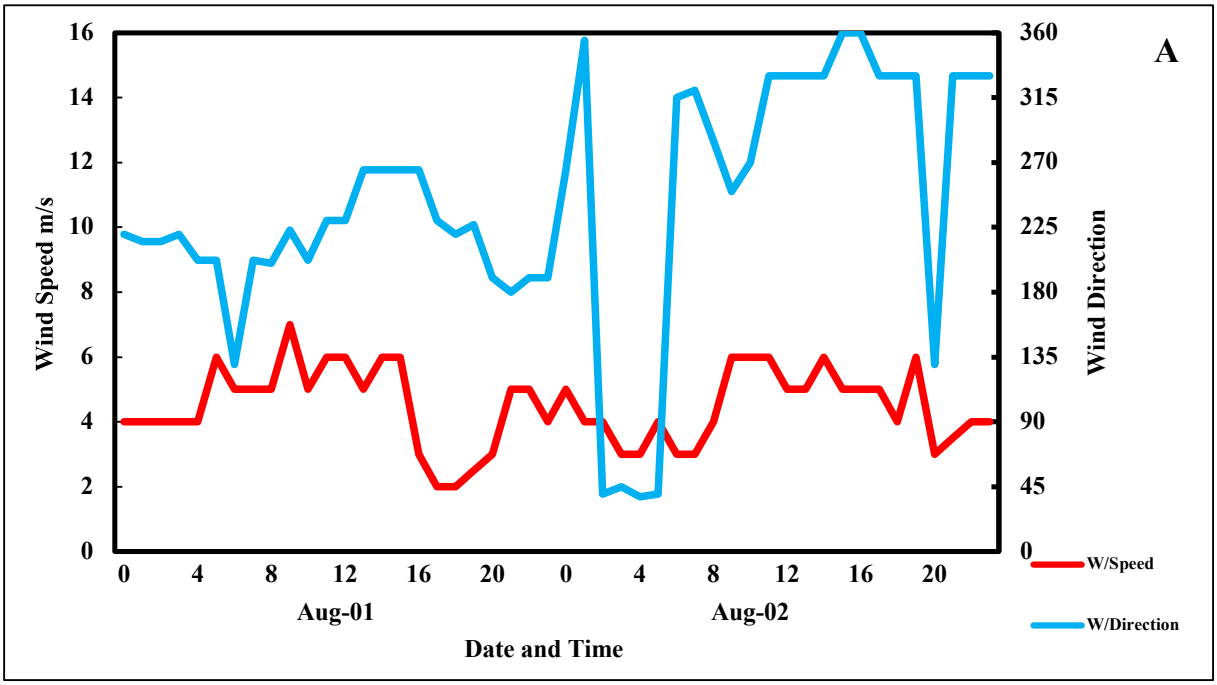

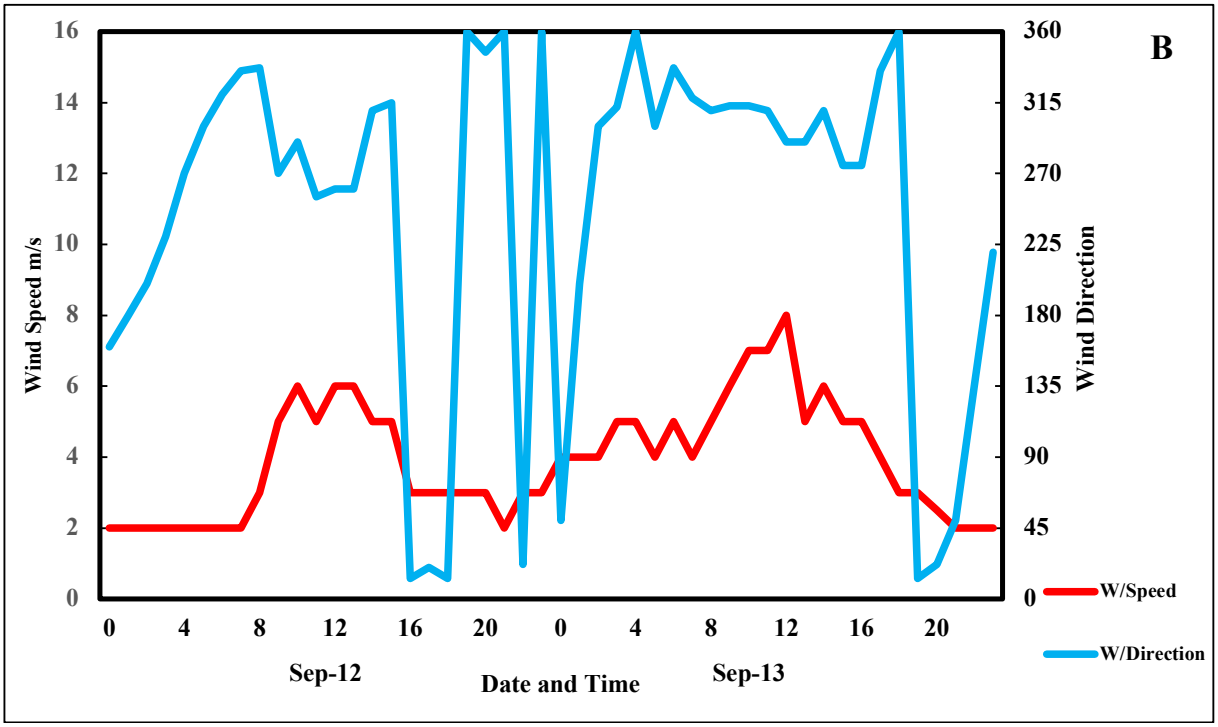

Figure 4. 6 Time series of wind speed and direction (A for August 1-2, 2017 and B for September 12-13, 2017).

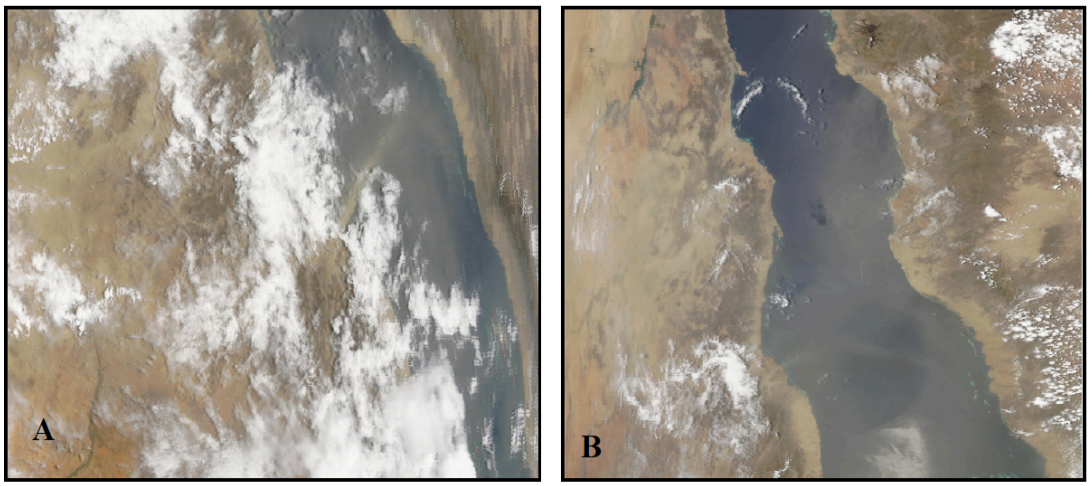

Figure 4. 7 MODIS satellite images on August 1, 2017- 0825 UTC (A) and on August 2, 2017- 1035 UTC (B). (NASA Earth Data).

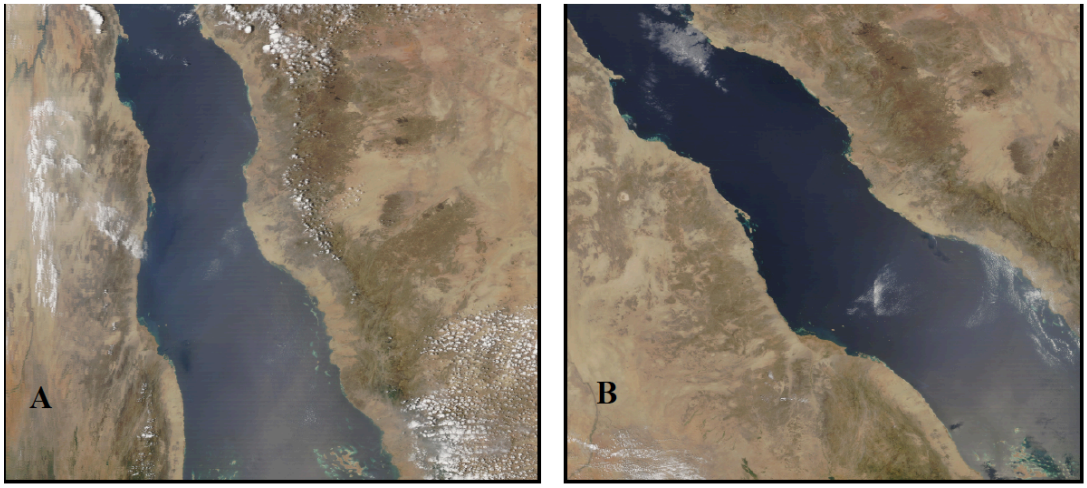

Figure 4. 8 MODIS satellite images for September 12, 2017- 1030 UTC (A) and for September 13, 2017- 0805 UTC (B). (NASA Earth Data).

References

Abdulaal, W. A. (2012). Large urban developments as the new driver for land development in Jeddah. Habitat International, 36(1), 36-46.https://doi.org/10.1016/j.habitatint.2011.05.004

Abulfaraj, W. H., Ahmed, M., Mousli, K. M., & Erturk, F. (1990). Measurement of ambient air lead con-centrations in the city of Jeddah, Saudi Arabia.Environment International, 16(1), 85-88.https://doi-org.sdl.idm.oclc.org/10.1016/0160-4120(90)90208-N

Aburas, H. M., Zytoon, M. A., & Abdulsalam, M. I. (2011). Atmospheric lead in PM 2.5 after leaded gasoline phase-out in Jeddah City, Saudi Arabia. *Clean - Soil, Air, Water, 39*(8), 711–719. https://doi.org/10.1002/clen.201000510

Al-Taani, A. A., Rashdan, M., & Khashashneh, S. (2015). Atmospheric dry deposition of mineral dust to the Gulf of Aqaba, Red Sea: Rate and trace elements. *Marine Pollution Bulletin,* 92(1–2), 252–258. https://doi.org/10.1016/j.marpolbul.2014.11.047

Alghamdi, M. A., Almazroui, M., Shamy, M., Redal, M. A., Alkhalaf, A. K., Hussein, M. A., & Khoder, M. I. (2015). Characterization and elemental composition of atmospheric aerosol loads during springtime dust storm in western Saudi Arabia. *Aerosol and Air Quality Research,* 15(2), 440–453. https://doi.org/10.4209/aaqr.2014.06.0110

Amato, F., Pandolfi, M., Escrig, A., Querol, X., Alastuey, A., Pey, J., Perez, N., & Hopke, P. K. (2009). Quantifying road dust resuspension in urban environment by

Multilinear Engine: A comparison with PMF2. *Atmospheric Environment*, 43(17),2770- 2780.https://doi.org/10.1016/j.atmosenv.2009.02.039

Bai, L., He, Z., Ni, S., Chen, W., Li, N., & Sun, S. (2019). Investigation of PM2.5 absorbed with heavy metal elements, source apportionment and their health impacts in residential houses in the North-east region of China.*Sustainable Cities and Society*, 51, 101690.https://doi.org/10.1016/j.scs.2019.101690

Bernstein, J. A., Alexis, N., Barnes, C., Bernstein, I. L., Bernstein, J. A., Nel, A., Peden, D., Diaz- Sanchez, D., Tarlo, S. M., & Williams, P. B. (2004). Health effects of air pollution. *Journal of Allergy and Clinical Immunology*, *114*(5), 1116–1123. https://doi.org/10.1016/j.jaci.2004.08.030

Birmili, W., Allen, A. G., Bary, F., & Harrison, R. M. (2006). Trace metal concentrations and water solubility in size-fractionated atmospheric particles and influence of road traffic. *Environmental Science and Technology*,*40*(4),1144–1153. https://doi.org/10.1021/es0486925

Choi, H., & Choi, D. S. (2008). Concentrations of PM10, PM2.5, and PM1 influenced by atmospheric circulation and atmospheric boundary layer in the Korean mountainous coast during a duststorm. Atmospheric Research,89(4),330-337 https://doi.org/10.1016/j.atmosres.2008.03.018

Choi, J. kyu, Heo, J. B., Ban, S. J., Yi, S. M., & Zoh, K. D. (2013). Source apportionment of PM2.5 at the coastal area in Korea.Science of the Total Environment, 447, 370-380 https://doi.org/10.1016/j.scitotenv.2012.12.047

Després, V. R., Alex Huffman, J., Burrows, S. M., Hoose, C., Safatov, A. S., Buryak, G., Fröhlich- Nowoisky, J., Elbert, W., Andreae, M. O., Pöschl, U., & Jaenicke, R.

(2012). Primary biological aerosol particles in the atmosphere: A review.*Series B: Chemical and Physical Meteorology*, 64(1), 15598. https://doi.org/10.3402/tellusb.v64i0.15598

Di Palma, A., Capozzi, F., Spagnuolo, V., Giordano, S., & Adamo, P. (2017). Atmospheric particulate matter intercepted by moss-bags: Relations to moss trace element uptake and land use. *Chemosphere*, 176, 361-368. https://doi.org/10.1016/j.chemosphere.2017.02.120

Esworthy, R. (2014). Air quality: EPA'S 2013 changes to the particulate matter (PM) standard. In Air Quality Observation in the U.S.: Systems, Needs, and Standards.

Gao, Y., & Anderson, J. R. (2001). Characteristics of Chinese aerosols determined by individual- particle analysis. *Journal of Geophysical Research Atmospheres*, *106*(D16), 18037–18045. https://doi.org/10.1029/2000JD900725

Gordon, G. E. (1988). Receptor models. *Environmental science & technology*, 22(10), 1132-1142.

Harrison, R. M., Bousiotis, D., Mohorjy, A. M., Alkhalaf, A. K., Shamy, M., Alghamdi, M., Khoder, M., & Costa, M. (2017). Health risk associated with airborne particulate matter and its components in Jeddah, Saudi Arabia. *Science of the Total Environment*, 590, 531- 539 https://doi.org/10.1016/j.scitotenv.2017.02.216 https://doi.org/10.1016/j.atmosenv.2004.11.026

Hjortenkrans, D., Bergbäck, B., & Häggerud, A. (2006). New metal emission patterns in road traffic environments.*Environmental Monitoring and Assessment*, *117*(1–3), 85–98. https://doi.org/10.1007/s10661-006-7706-2

Hopke, P. K., Croft, D., Zhang, W., Lin, S., Masiol, M., Squizzato, S., Thurston, S. W., an

Wijngaarden, E., Utell, M. J., & Rich, D. Q. (2019). Changes in the acute response of respiratory diseases to PM 2.5 in New York State from 2005 to 2016. *Science of the Total Environment*, 677, 328-339. https://doi.org/10.1016/j.scitotenv.2019.04.357

Kadi, M. W. (2014). Elemental spatiotemporal variations of total suspended particles in Jeddah City. *The Scientific World Journal*. https://doi.org/10.1155/2014/325492

Khodeir, M., Shamy, M., Alghamdi, M., Zhong, M., Sun, H., Costa, M., Chen, L. C., & Maciejczyk, P. (2012). Source apportionment and elemental composition of PM2.5 and PM10 in Jeddah City, Saudi Arabia. *Atmospheric Pollution Research*, *3*(3), 331–340. https://doi.org/10.5094/APR.2012.037

Kim, K. H., Kabir, E., & Kabir, S. (2015). A review on the human health impact of airborne particulatematter.*EnvironmentInternational*,74,136-143. https://doi.org/10.1016/j.envint.2014.10.005

Kłos, A., Rajfur, M., Wacławek, M. and Wacławek, M.(2011). Application of enrichment factor (EF) to the interpretation of results from the biomonitoring studies. *Ecol. Chem. Eng*. 18: 171–183.

Laden, F., Neas, L. M., Dockery, D. W., & Schwartz, J. (2000). Association of Fine Particulate Matter from Different Sources with Daily Mortality in Six U.S. Cities. *Environmental Health Perspectives.*108(10),941-947.http://ehpnet1.niehs.nih.gov/docs/2000/108p941- 947laden/abstract.html

Lee, B. J., Kim, B., & Lee, K. (2014). Air pollution exposure and cardiovascular disease. *Toxicological Research*. 30(2), 71-75. https://doi.org/10.5487/TR.2014.30.2.071

Li, P. hui, Yu, J., Bi, C. liang, Yue, J. jie, Li, Q. qian, Wang, L., Liu, J., Xiao, Z., Guo, L.,

& Huang, B. jie. (2019). Health risk assessment for highway toll station workers exposed to PM2.5-boundheavymetals.*AtmosphericPollutioResearch,10(4),1024-1030.* https://doi.org/10.1016/j.apr.2019.01.011

Lim, C. C., Thurston, G. D., Shamy, M., Alghamdi, M., Khoder, M., Mohorjy, A. M., Alkhalaf, K., Brocato, J., Chen, L. C., & Costa, M. (2018). Temporal variations of fine and coarse particulate matter sources in Jeddah, Saudi Arabia. *Journal of the Air and Waste Management, 68(2), 123-138.Association*. https://doi.org/10.1080/10962247.2017.1344158

Liora, N., Markakis, K., Poupkou, A., Giannaros, T. M., & Melas, D. (2015). The natural emissions model (NEMO): Description, application and model evaluation. *Atmospheric Environment*, 122, 493–504. https://doi.org/10.1016/j.atmosenv.2015.10.014

Liu, C. L., Zhang, J., & Shen, Z. B. (2002). Spatial and temporal variability of trace metals in aerosol from the desert region of China and the Yellow Sea. *Journal of Geophysical Research*, 107(D14), ACH-17 https://doi.org/10.1029/2001jd000635

Liu, J., Chen, Y., Chao, S., Cao, H., Zhang, A., & Yang, Y. (2018). Emission control priority of PM2.5-bound heavy metals in different seasons: A comprehensive analysis from health risk perspective.*Science* of the Total Environment. https://doi.org/10.1016/j.scitotenv.2018.06.226

Liu, W. J., Xu, Y. S., Liu, W. X., Liu, Q. Y., Yu, S. Y., Liu, Y., Wang, X., & Tao, S. (2018).Oxidative potential of ambient PM2.5 in the coastal cities of the Bohai Sea, northern China: Seasonal variation and source apportionment. *Environmental Pollution*, *236*, 514–528. https://doi.org/10.1016/j.envpol.2018.01.116

Liu, Y., Xing, J., Wang, S., Fu, X., & Zheng, H. (2018). Source-specific speciation profiles of PM2.5 for heavy metals and their anthropogenic emissions in China. *Environmental Pollution*, 239, 544-553. https://doi.org/10.1016/j.envpol.2018.04.047

Lough, G. C., Schauer, J. J., Park, J. S., Shafer, M. M., Deminter, J. T., & Weinstein, J. P. (2005). Emissions of metals associated with motor vehicle roadways. *Environmental Science and Technology*, *39*(3), 826–836. https://doi.org/10.1021/es048715f

Marcazzan, G. M., Vaccaro, S., Valli, G., & Vecchi, R. (2001). Characterisation of PM10 and PM2.5 particulate matter in the ambient air of Milan (Italy). In *Atmospheric Environment 35(27), 4639-4650*.

Mateus, V. L., & Gioda, A. (2017). A candidate framework for PM2.5 source identification in highly industrialized urban-coastal areas. Atmospheric Environment, 164, 147–164. https://doi.org/10.1016/j.atmosenv.2017.05.025

McGuinn, L. A., Schneider, A., McGarrah, R. W., Ward-Caviness, C., Neas, L. M., Di, Q., Schwartz, J., Hauser, E. R., Kraus, W. E., Cascio, W. E., Diaz-Sanchez, D., & Devlin, R. (2019). Association of long-term PM 2.5 exposure with traditional and novel lipid measures related to cardiovascular disease risk. Environment International. https://doi.org/10.1016/j.envint.2018.11.001

Merto Jeddah,2019. The Jeddah Public Transport Program. http://www.metrojeddah.com.sa/page/JPTP

Mimura, T., Ichinose, T., Yamagami, S., Fujishima, H., Kamei, Y., Goto, M., Takada, S., & Matsubara, M. (2014). Airborne particulate matter (PM2.5) and the prevalence

of allergic conjunctivitis in Japan.Science of the Total Environment. https://doi.org/10.1016/j.scitotenv.2014.04.057

Munir, S., Gabr, S., Habeebullah, T. M., & Janajrah, M. A. (2016). Spatiotemporal analysis of fine particulate matter (PM2.5) in Saudi Arabia using remote sensing data. Egyptian *Journal of Remote Sensing and Space Science*,19(2),195–205. https://doi.org/10.1016/j.ejrs.2016.06.001

Nakatsubo, R., Oshita, Y., Aikawa, M., Takimoto, M., Kubo, T., Matsumura, C., Takaishi, Y., & Hiraki, T. (2020). Influence of marine vessel emissions on the atmospheric PM2.5 in Japan's around the congested sea areas.*Science of the Total Environment*,702,134744 https://doi.org/10.1016/j.scitotenv.2019.134744

NASA Earth Data. https://lance.modaps.eosdis.nasa.gov/realtime

Nayebare, S. R., Aburizaiza, O. S., Khwaja, H. A., Siddique, A., Hussain, M. M., Zeb, J., Khatib, F., Carpenter, D. O., & Blake, D. R. (2016). Chemical characterization and source apportionment of PM2.5 in Rabigh, Saudi Arabia. *Aerosol and Air Quality Research*, *16*(12), 3114–3129. https://doi.org/10.4209/aaqr.2015.11.0658

Nayebare, S. R., Aburizaiza, O. S., Siddique, A., Carpenter, D. O., Hussain, M. M., Zeb, J., Aburiziza, A. J., & Khwaja, H. A. (2018). Ambient air quality in the holy city of Makkah: A source apportionment with elemental enrichment factors (EFs) and factor analysis (PMF). *Environmental Pollution*, 243, 1791–1801. https://doi.org/10.1016/j.envpol.2018.09.086

Nayebare, S. R., Aburizaiza, O. S., Siddique, A., Carpenter, D. O., Arden Pope, C., Mirza, H. M., Zeb, J., Aburiziza, A. J., & Khwaja, H. A. (2019). Fine particles exposure and cardiopulmonary morbidity in Jeddah: A time-series analysis. *Science of the*

Total Environment, 647, 1314–1322. https://doi.org/10.1016/j.scitotenv.2018.08.094

Pope, C. A., Burnett, R. T., Thurston, G. D., Thun, M. J., Calle, E. E., Krewski, D., & Godleski,J. J. (2004). Cardiovascular Mortality and Long-Term Exposure to Particulate Air Pollution: Epidemiological Evidence of General Pathophysiological Pathways of Disease. *Circulation*, 109(1), 71–77. https://doi.org/10.1161/01.CIR.0000108927.80044.7F

Qin, K., Han, X., Li, D., Xu, J., Xue, Y., Loyola, D., Zhou, X., Zhang, K., Li, D., & Yuan, L. (2020). Satellite-based estimation of surface NO2 concentrations over east-central China: A comparison of POMINO and OMNO2d data. *Atmospheric Environment*,224,117322. https://doi.org/10.1016/j.atmosenv.2020.117322

Shaltout, A. A., Boman, J., al Malawi, D. A. R., & Shehadeh, Z. F. (2013). Elemental composition of PM 2.5 particles sampled in industrial and residential areas of Taif, Saudi Arabia. *Aerosol and Air Quality Research*, 13(4), 1356-1364 https://doi.org/10.4209/aaqr.2012.11.0320

Shaltout, A. A., Harfouche, M., Ahmed, S. I., Czyzycki, M., & Karydas, A. G. (2018). Synchrotron radiation total reflection X-ray fluorescence (SR-TXRF) and X-ray absorption near edge structure (XANES) of fractionated air particulates collected from Jeddah, Saudi Arabia. *Microchemical Journal*, 137, 78–84. https://doi.org/10.1016/j.microc.2017.10.001

Squizzato, S., Cazzaro, M., Innocente, E., Visin, F., Hopke, P. K., & Rampazzo, G. (2017). Urban air quality in a mid-size city — PM2.5 composition, sources and identification of impact areas: From local to long range contributions. *Atmospheric*

Research, *186*, 51–62. https://doi.org/10.1016/j.atmosres.2016.11.011

Srimuruganandam, B., & Nagendra, S. S. (2012). Application of positive matrix factorization in characterization of PM10 and PM2. 5 emission sources at urban roadside. *Chemosphere*, 88(1), 120-130. https://doi.org/10.1016/j.chemosphere.2012.02.083

Sternbeck, J., Sj odin, A., & Andr, K. (2002). Metal emissions from road traffic and the influence of resuspension-results from two tunnel studies. In *Atmospheric Environment* .36(30),4735-4744

Sylvestre, A., Mizzi, A., Mathiot, S., Masson, F., Jaffrezo, J. L., Dron, J., Mesbah, B., Wortham, H., & Marchand, N. (2017). Comprehensive chemical characterization of industrial PM2.5 from steel industry activities. Atmospheric Environment,152,180-190 https://doi.org/10.1016/j.atmosenv.2016.12.032

Tainio, M., Tuomisto, J. T., Pekkanen, J., Karvosenoja, N., Kupiainen, K., Porvari, P., Sofiev, M., Karppinen, A., Kangas, L., & Kukkonen, J. (2010). Uncertainty in health risks due to anthropogenic primary fine particulate matter from different source types in Finland. *AtmosphericEnvironment*,44(17),2125-2132 https://doi.org/10.1016/j.atmosenv.2010.02.036

Taiwo, Adewale., Harrison, Roy., & Shi, Zongbo. (2014). A review of receptor modelling of industrially emitted particulate matter. In *Atmospheric Environment,97,109-120* . https://doi.org/10.1016/j.atmosenv.2014.07.051

Taylor, S. R. (1964). Abundance of chemical elements in the continental crust: a new table. *Geochimica et Cosmochimica Acta,28(8),1273-1285.*https://doi.org/10.1016/0016-7037(64)90129-2

Taylor, S. R., & McLennan, S. M. (1985). *The Continental Crust: Its Composition and Evolution*.Blackwell Scientific Publications.

Tian, H. Z., Zhu, C. Y., Gao, J. J., Cheng, K., Hao, J. M., Wang, K., Hua, S. B., Wang, Y., & Zhou, J. R. (2015). Quantitative assessment of atmospheric emissions of toxic heavy metals from anthropogenic sources in China: Historical trend, spatial distribution, uncertainties, and control policies. *Atmospheric Chemistry and Physics*,15(17),10127–10147. https://doi.org/10.5194/acp-15-10127-2015

Timmers, V. R. J. H., & Achten, P. A. J. (2016). Non-exhaust PM emissions from electric vehicles. In *Atmospheric Environment*, 134, 10-17 https://doi.org/10.1016/j.atmosenv.2016.03.017

Tsai, Y. I., & Chen, C. L. (2006). Characterization of Asian dust storm and non-Asian dust storm PM2.5 aerosol in southern Taiwan. *Atmospheric Environment*,40(25),4734-4750 https://doi.org/10.1016/j.atmosenv.2006.04.038

U.S Environmental Protection Agency. (1999). Compendium Method IO-3.5. Determination of Metals in Ambient Particulate Matter using Inductively Coupled Plasma/Mass Spectrometry (ICP/MS). Compendium of Methods for the Determination of Inorganic Compounds in Ambient Air.

U.S. Environmental Protection Agency. (2014). Air Quality Index - A Guide to Air Quality and Your Health. EPA. https://www3.epa.gov/airnow/aqi_brochure_02_14.pdf

UCAR & MMM. (n.d.) https://www2.mmm.ucar.edu/wrf/users/index.html

Viana, M., Hammingh, P., Colette, A., Querol, X., Degraeuwe, B., Vlieger, I. de, & van Aardenne,J. (2014). Impact of maritime transport emissions on coastal air quality in Europe. *Atmospheric Environment*, 90, 96-105

https://doi.org/10.1016/j.atmosenv.2014.03.046

Wei, Y., Zhao, Y., Zhao, X., Gao, X., Zheng, Y., Zuo, H., & Wei, Z. (2020). Roles of different humin and heavy-metal resistant bacteria from composting on heavy metal removal. *Bioresource Technology*, 296, 122375. https://doi.org/10.1016/j.biortech.2019.122375

World Health Organization. (2006). WHO Air quality guidelines for particulate matter, ozone, nitrogen dioxide and sulfur dioxide. World Health Organization,51(6),565573.https://apps.who.int/iris/bitstream/handle/10665/69477/WHO_SDE_PHE_OEH_06.02_eng.pdf;jsessionid=A98CEF8FE6EEB1CEE0DDED66A3DB8279?sequence=1

Xu, L., Jiao, L., Hong, Z., Zhang, Y., Du, W., Wu, X., Chen, Y., Deng, J., Hong, Y., & Chen, J. (2018). Source identification of PM2.5 at a port and an adjacent urban site in a coastal city of China: Impact of ship emissions and port activities. *Science of the Total Environment*, 634, 1205-1213.https://doi.org/10.1016/j.scitotenv.2018.04.087

Yatkin, S., & Bayram, A. (2008). Source apportionment of PM10 and PM2.5 using positive matrix factorization and chemical mass balance in Izmir, Turkey. *Science of the Total Environment*, 390(1),109-123https://doi.org/10.1016/j.scitotenv.2007.08.059

Zhang, X., Zhuang, G., Guo, J., Yin, K., & Zhang, P. (2007). Characterization of aerosol over the Northern South China Sea during two cruises in 2003. *Atmospheric Environment*, 41(36), 7821–7836. https://doi.org/10.1016/j.atmosenv.2007.06.031

Chapter 5

CONCLUSION AND FUTURE WORK

Baseline information fills in the gaps of prior research for future monitoring and development of KSA national regulations for both the Jeddah Coast and the adjacent Red Sea. The research provides a wide spatial array of pollution loading for the region. Further, the work provides a new isotopic baseline post Pb gasoline era which will prove vital to future work. In addition to establishing key data sets the work also pinpoints potential contamination sources and mechanisms. This is seen through establishing a clear set of isotopic Pb ratios for an anthropogenic source in the region as well as determining multiple natural and anthropogenic sources via factor analysis for wind-derived metals.

In chapter two, eighty stations were discussed regarding for the collection of surficial marine sediments from North, Middle, and South locations of the nearshore Jeddah coast. The concentrations of Cr, Mn, Ni, Cu, Zn, and Pb in the collected sediments were determined in order to provide data for tracing the effect of anthropogenic activities on the sediments of the study area. Risk indices show that Pb is the most enriched metal at approximately 88% of the studied stations, which is consistent with an anthropogenic source of Pb. Further, RI values in the South stations — especially the northern end of the South location – indicate high Pb pollution in the area. The Middle location is likely impacted by various sources due to the highest activity in the region. This chapter suggests stringent management needs to be enacted to mitigate pollution in the Middle and South locations and to protect future damage to the North.

Chapter three used stable lead isotopes, ^{206}Pb, ^{207}Pb, and ^{208}Pb, to identify sources

of lead in sediment samples. To date, no previous data on Pb isotopes has been reported for the Jeddah area nor the Red Sea. Indeed, the first lead isotopic data of the Red Sea coastal sediments are presented in this study. The percentage contributions of possible Pb sources in the study area were based on either a two end-member model or a three member fractional contribution model with the low concentration samples modelled by the former and the high concentration samples modelled by the latter. Each model contained gasoline-derived Pb and natural source Pb, both sets of ratios taken from literature. The third component in the three component model was an unknown anthropogenic source constrained in this work by taking end members of 1/C versus ratio plots. The establishment of this anthropogenic source and its isotopic character is a key output of the third chapter. The trend of concentration with the fractional contribution of this unknown source clearly shows it controls elevated concentrations in the region. This is the second key output from the third chapter as it confirms the component as a source of anthropogenic contamination. The conclusions of the study demonstrate that natural and anthropogenic sources such as gasoline and unknown sources contribute to the total Pb load of Jeddah's sediments. The study advises examining the ratio of Pb isotopes in air, soil sediments, and sediment cores for future studies.

Finally, chapter four measures the concentration of the heavy metals in particulate matter ($PM_{2.5}$). The Middle location has the highest Pb concentration. Also, backward trajectory analysis provided interpretation for the sudden increases in PM concentrations for two sampling dates. These examples gave a deeper understanding to the potential sourcing of PM in the region. Principal Component Analysis (PCA) helped define and classify the trace metals into four principal groups. Based on the PCA, we classified Na,

Mg, Ca and K, and the presence of Al and Ba as a combined source of marine aerosol and re-suspension of soil-derived particles. Fe, Ti, and Mn are of terrigenous origin and were transported via wind while V, Ni, and Cu were assigned to emissions of oil combustion. Pb and Zn, were suggested as linked to the emissions of incineration and fossil fuel combustion.

The conclusions of this study have many significant associations for future work. The Red Sea, like a lot of water bodies, is utilized for a diversity of purposes. The current study found that treated and untreated municipal sewage, atmospheric contributions, vehicle exhaust, urban runoff of municipal and industrial discharges, and oil leakage could all be sources of the pollution affecting the Jeddah coastal area. These sources could be controlled by many stakeholders, including the government. Decisions such as these are complicated, however. For example, the desalination plant and maritime traffic are essential and vital for the city; however, they are considered as the primary pollution sources, so while they should be more closely regulated there continued function is imperative.

The area needs more research to collect data about the chemistry and bioavailability of heavy metals. Different kinds of media – such as, water, sediments, and particulate matter from air — should be collected from a wide spatial range of the coastal regions. One of the primary points of future studies should be to set background concentration for each element. Additionally, vital future work for metal speciation analysis of heavy metals will be needed as a necessary tool to pinpoint geochemical phase of heavy metals and create a better comprehension of their mobility and bioavailability.

Due to the availability of lead in the marine environment, future study must include

comprehensive analysis for lead isotopes in the air, water, and sediments to pinpoint primary sources. Also, air pollution monitoring strategies covering the coastal area must be applied in the future to estimate the amount of heavy metals and other compounds which are carried from land-based emission sources to coastal and offshore waters, especially via $PM_{2.5}$. Refinery plant, petroleum tankers, and loading operations in the South location should also receive research attention. More information on polycyclic aromatic hydrocarbons as organic anthropogenic pollutants would further help us to establish environmental contamination concerns in the Jeddah coastal area.

This study provided data of significant elevation of some heavy metals from various sources. Following up on this data requires monitoring. The Jeddah coastal information system already has buoy stations to assess water quality and identify the main sources of contamination near Jeddah. These buoy stations need to be expanded over the coastal area and more sensors need to be added for multiple pollution elements (Mayerle et al. 2016). Here it is suggested that monitoring should be extended with new technology, including satellite images and drone patrols, to monitor pollution point. Satellite images record prior status of the region and examine its change over time. As an example, a more in-depth understanding of the aerosols and the sources of its origin, including associated physical processes, has been shown elsewhere (Ukhov et al., 2020). The next logical step in using remotely sensed data is to combine satellite imagery with Drone patrols to discover any waste discharge points for quick responses. While this is as yet realized it is surely possible given current technology paired with data from studies such as this dissertation. Lastly, we further suggest bioremediation strategies such as increasing mangroves trees, especially in the affected areas, to reduce the avaiability of heavy metals

in the sediments. Mangrove has the ability to tolerate, and even accumulate, heavy metals and sewage nutrients (Mandura 1997; Usman et al., 2013). Combining these strategies guided by the data provided will yield a cleaner, safer Jeddah coast well into the future even under significant development and urbanization.

References

Mayerle, R., Al-Subhi, A., Jaramillo, J. F., Salama, A., Bruss, G., Zubier, K., ... & Ladwig, N. (2016). Development of a coastal information system for the management of Jeddah coastal waters in Saudi Arabia. Computers & geosciences, 89, 71-78. https://doi.org/10.1016/j.cageo.2015.12.006

Ukhov, A., Mostamandi, S., da Silva, A., Flemming, J., Alshehri, Y. M., Shevchenko, I., & Stenchikov, G. L. (2020). Assessment of natural and anthropogenic aerosol air pollution in the Middle East using MERRA-2, CAMS data assimilation products, and high-resolution WRF-Chem model simulations. https://doi.org/10.5194/acp-2020-17

Mandura, A. S. (1997). A mangrove stand under sewage pollution stress: Red Sea. Mangroves and Salt marshes, 1(4), 255-262.

Usman, A. R., Alkredaa, R. S., & Al-Wabel, M. I. (2013). Heavy metal contamination in sediments and mangroves from the coast of Red Sea: Avicennia marina as potential metal bioaccumulator. Ecotoxicology and environmental safety, 97, 263-270. https://doi.org/10.1016/j.ecoenv.2013.08.009